Latest results of the ALICE Collaboration and plans for ALICE 3

A. Marin for the ALICE Collaboration

DPC-SMF

XVIII Mexican Workshop on Particles and Fields 2022
November 21st - 25th,
Puebla - México

GSI ALICE

Outline

- Introduction
- Selected physics highlights
- Status Run 3
- Upgrades:
  - Run 4: ITS3, FoCal
  - Run 5 + 6: ALICE 3

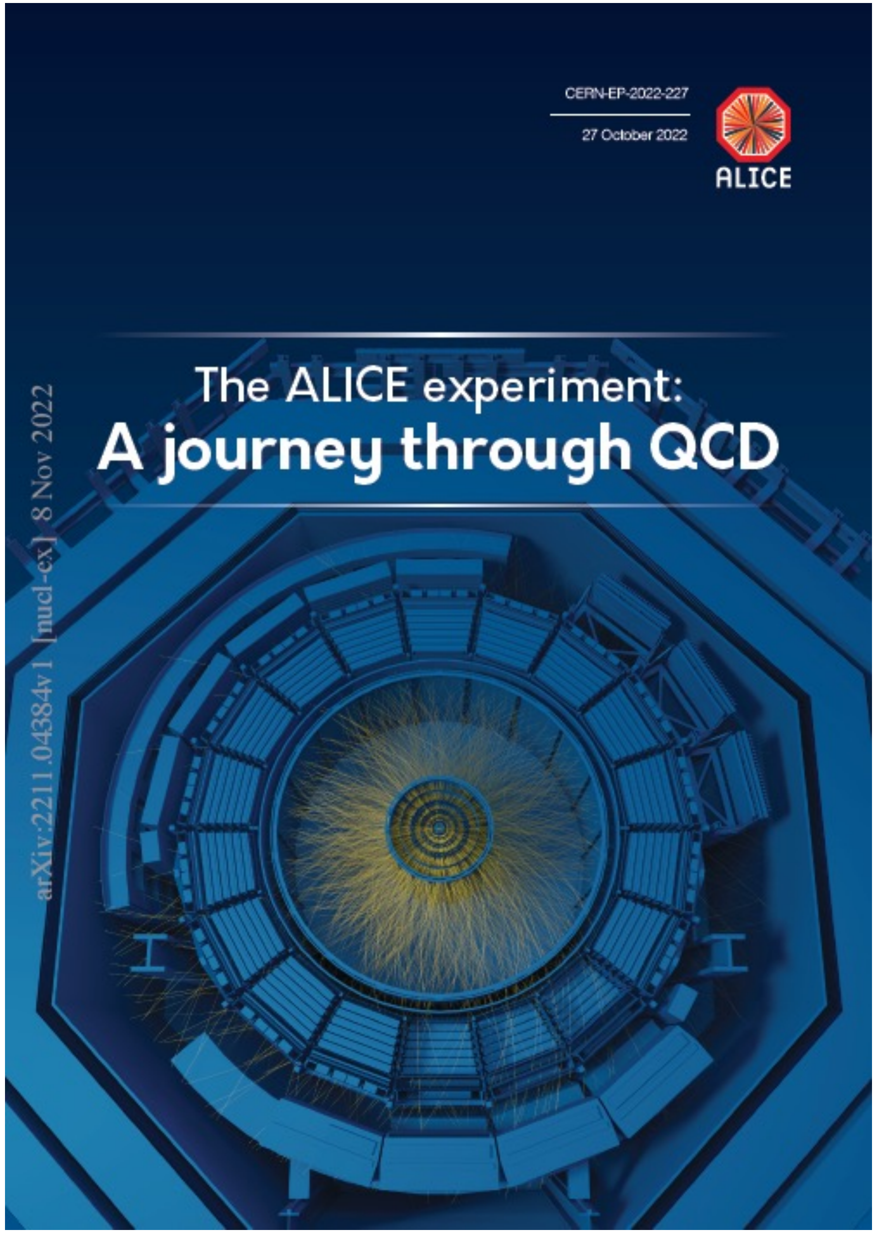

Exploration of the QCD phase diagram

Ann. Rev. Nucl. Part. Sci. 71 (2021) 403

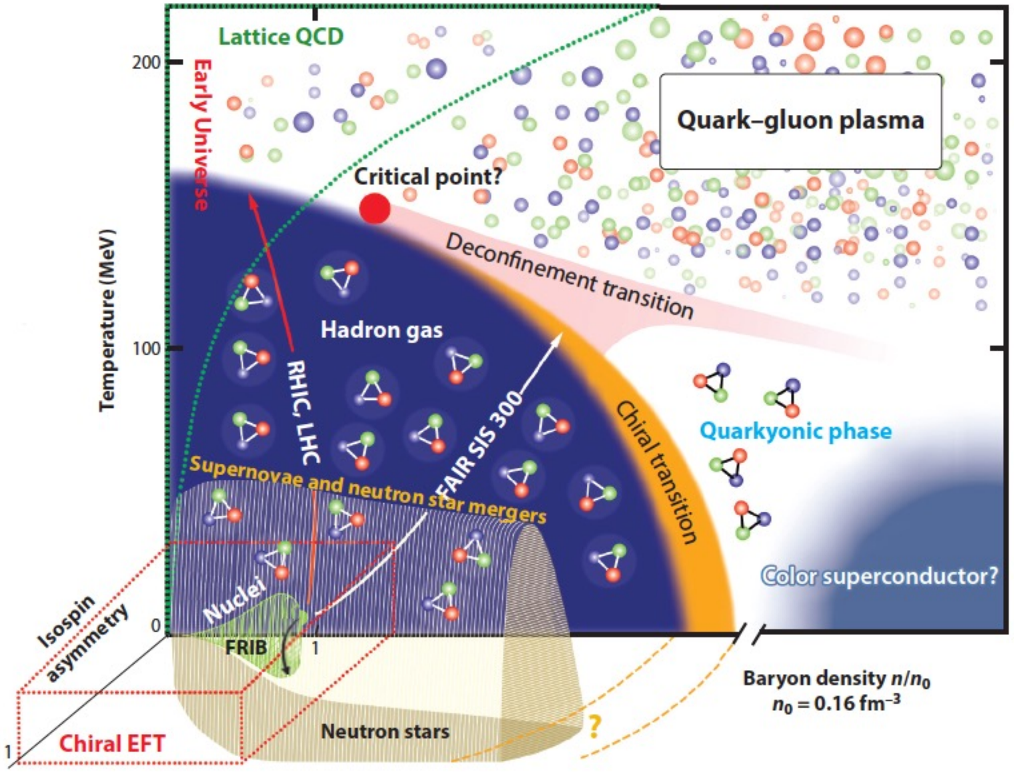

Heavy-ion collisions

Explore and characterize phase diagram of QCD matter

QGP

- quarks and gluons are deconfined
- hot and dense thermalized medium
- strongly interacting
- existed few μs after the Big Bang
- predicted by lattice QCD above a critical energy density

Time evolution of heavy-ion collisions

Courtesy C. Shen

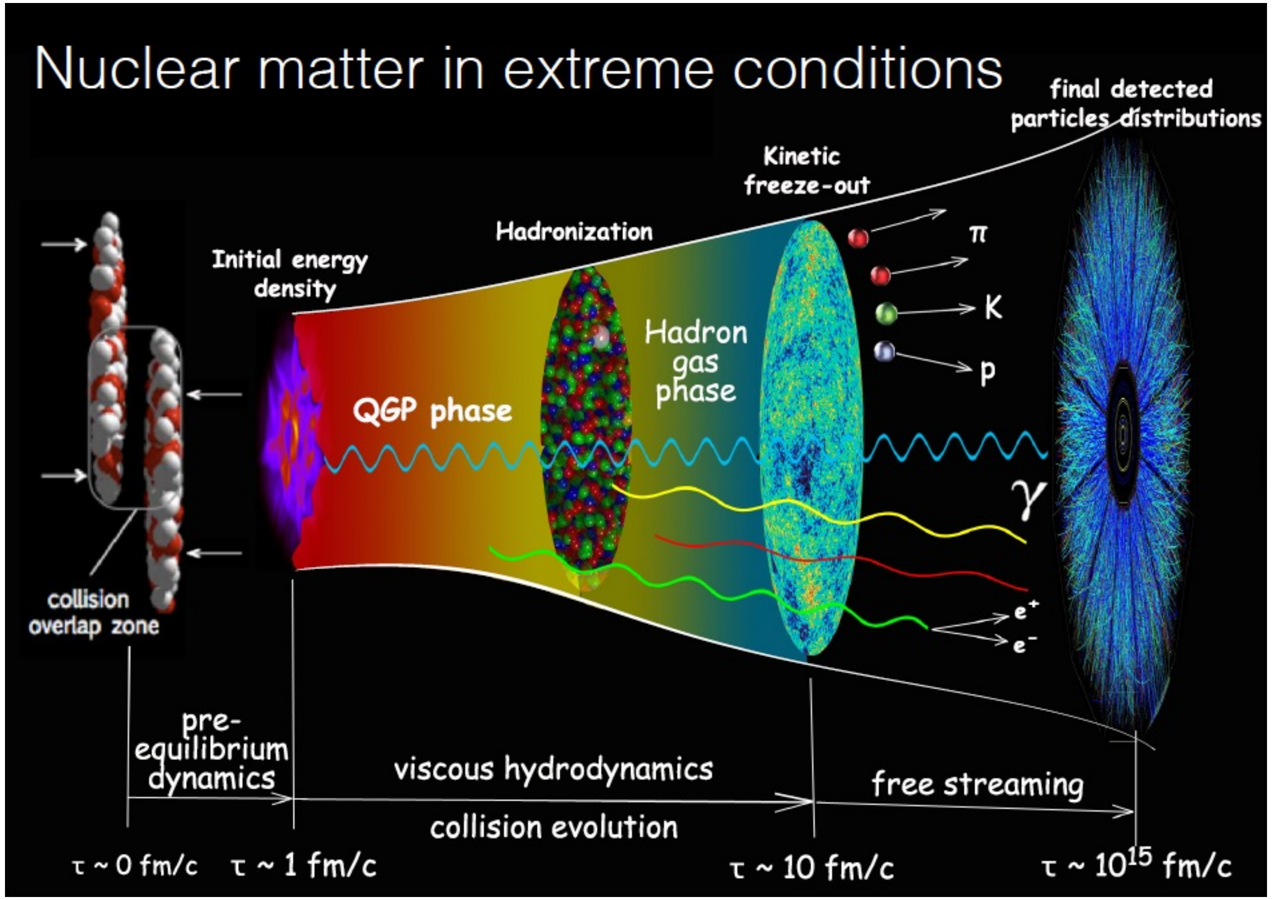

Study different probes

↓

Collect information at each stage

↓

Characterize the QGP and hadron gas phase

AA collisions
pA and pp : control and reference systems

The ALICE Collaboration

40 countries,
172 institutes,
2033 members

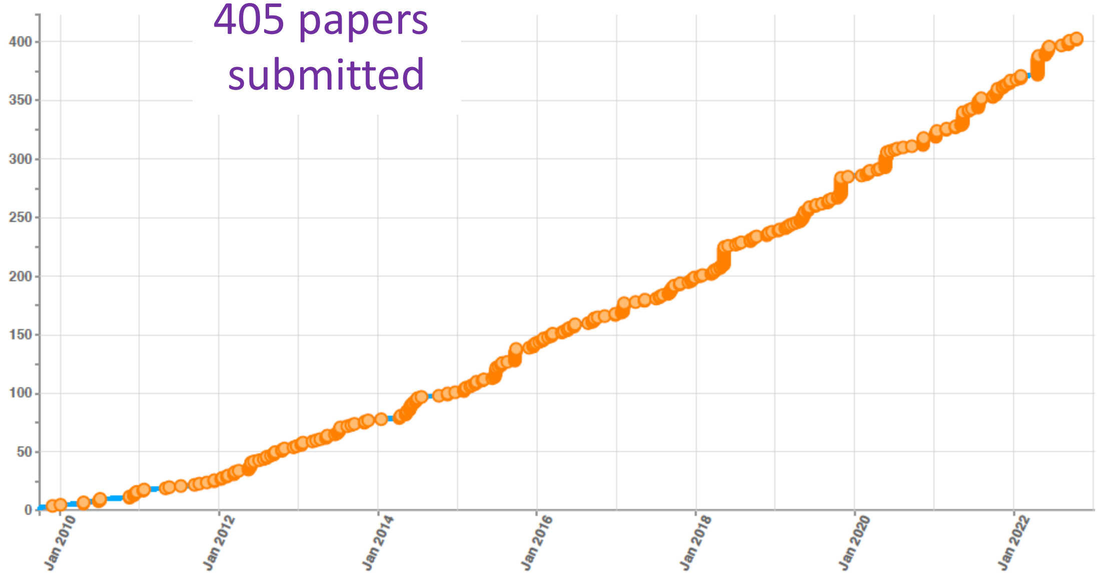

Run 1 Run 2

System	Year(s)	$\sqrt{s_{NN}}$ (TeV)	L_{int}
Pb-Pb	2010,2011 2015,2018	2.76 5.02	75 μb^{-1} 800 μb^{-1}
Xe-Xe	2017	5.44	0.3 μb^{-1}
p-Pb	2013 2016	5.02 5.02, 8.16	15 nb^{-1} 3 nb^{-1}, 25 nb^{-1}
pp	2009-2013 2015,2017 2015-2018	0.9,2.76, 7,8 5.02 13	200 μb^{-1}, 100 mb^{-1} 1.5 pb^{-1},2.5 pb^{-1} 1.3 pb^{-1} 36 pb^{-1}

The ALICE detector (version 1: Run 1 + Run 2)

Central barrel | η | < 0.9
Tracking
PID
Calorimeters

ACORDE (cosmics)

Forwards detectors:
- AD (diffraction selection)
- V0 (trigger, centrality)
- T0 (timing, luminosity)
- ZDC (centrality, ev. sel.)
- FMD (N_{ch})
- PMD (N_{γ}, N_{ch})

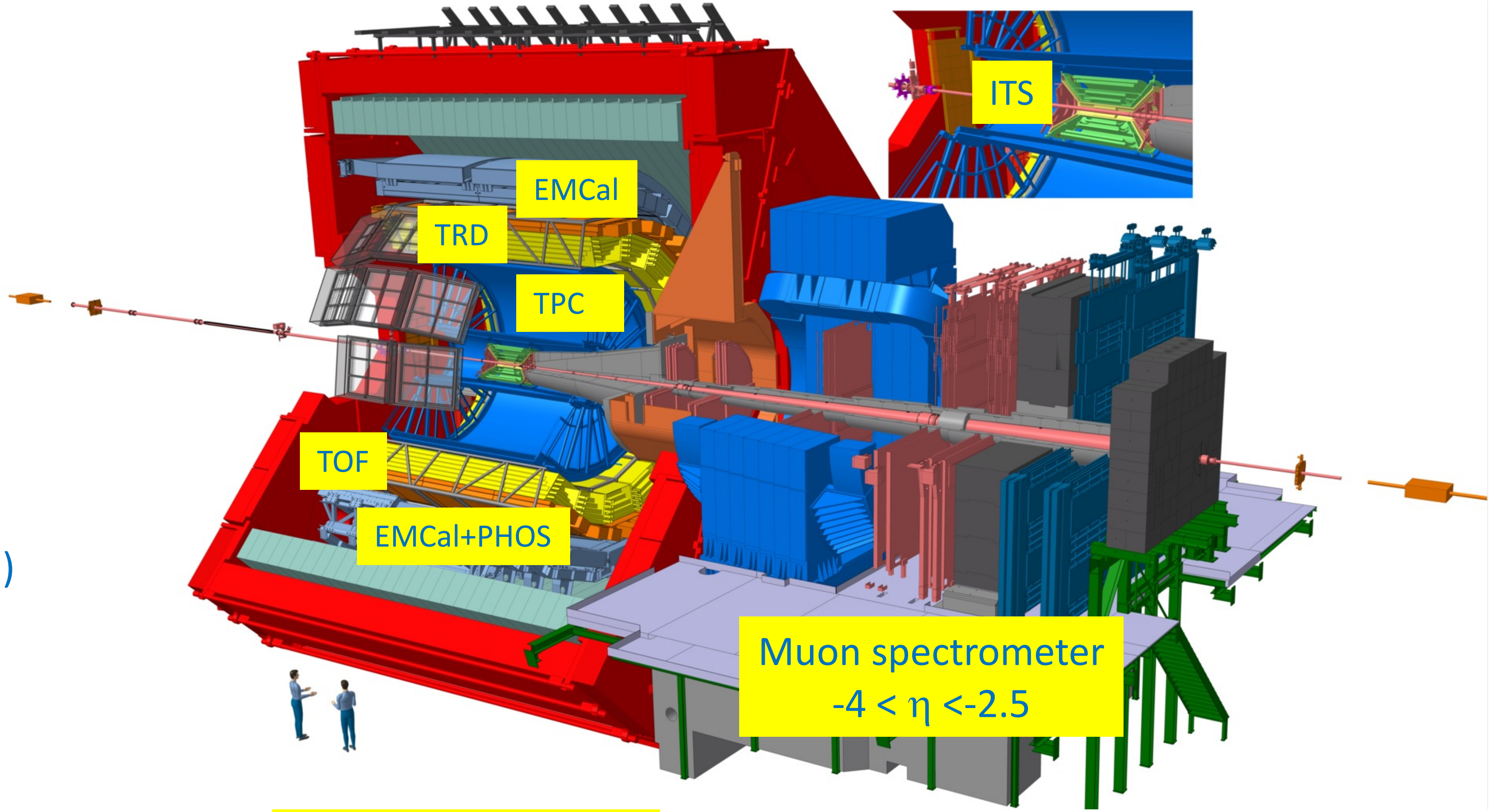

Size: 16 x 26 meters
Weight: 10,000 tons
Detectors: 18

Pb-Pb collision in ALICE

0-2.5%: $dN_{ch}/d\eta = 2035 \pm 52$

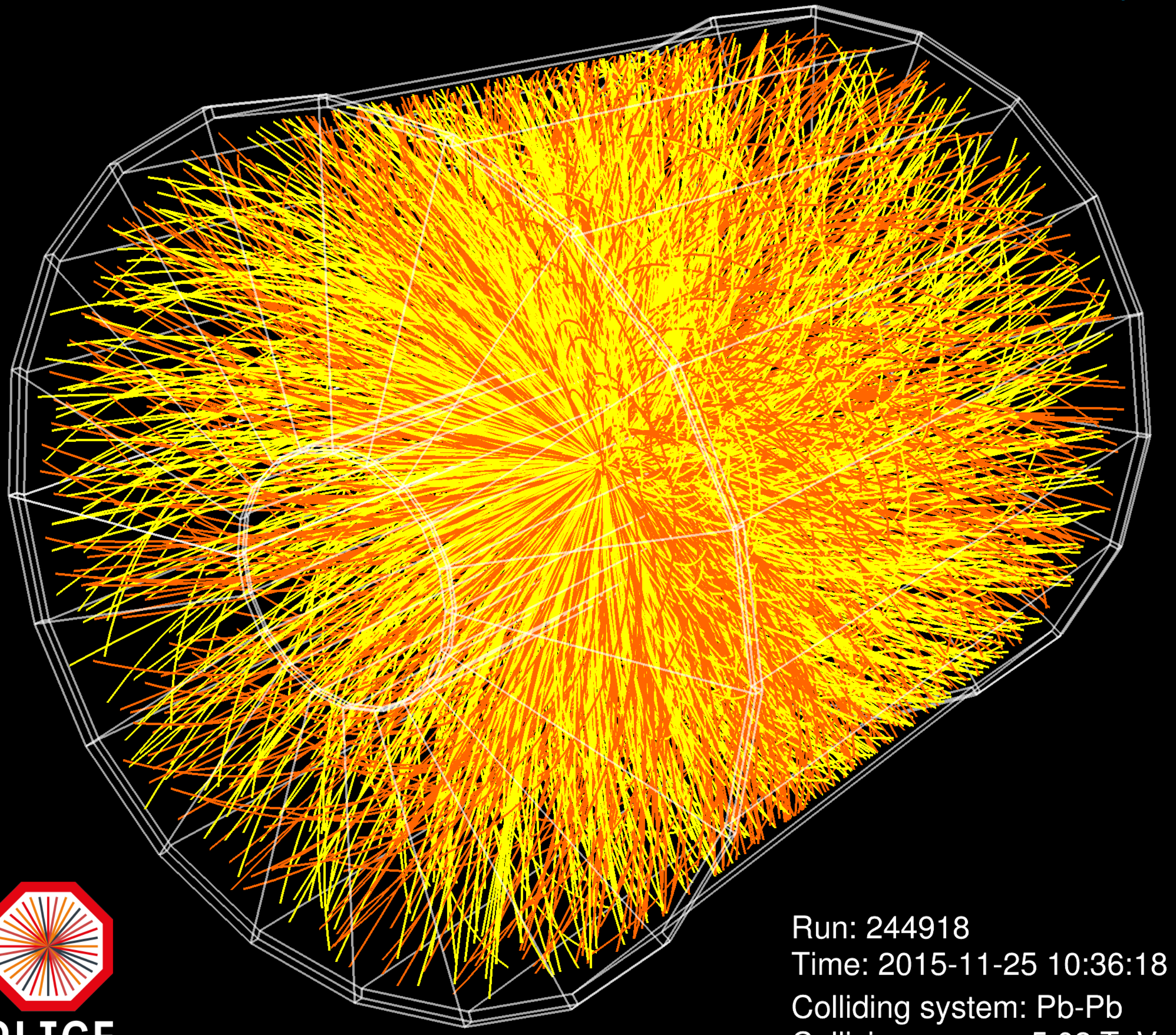

Introducing some observables

ALICE centrality determination

ALICE-PUBLIC-2018-011

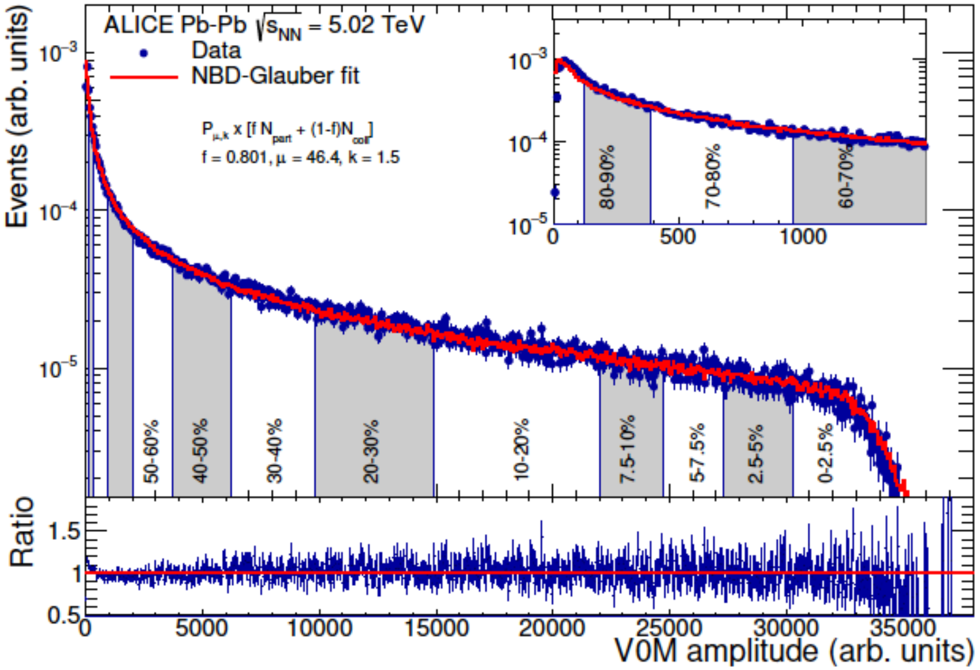

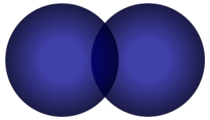

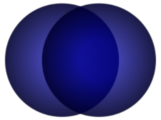

Centrality	$\langle N_{part} \rangle$	RMS	(*sys.*)	$\langle N_{coll} \rangle$	RMS	(*sys.*)	$\langle T_{PbPb} \rangle$ (1/mbarn)	RMS (1/mbarn)	(*sys.*) (1/mbarn)
0-1%	401.9	7.55	0.46	1949	87	21.1	28.83	1.29	0.177
1-2%	393.9	10.2	0.496	1844	81.3	20.1	27.28	1.2	0.171
2-3%	384.4	11.7	0.752	1755	80.8	20.3	25.96	1.19	0.2
3-4%	373.9	12.5	0.762	1673	79.9	18.8	24.75	1.18	0.18
4-5%	362.9	13	0.738	1593	77.6	17.8	23.57	1.15	0.178

Anisotropic flow

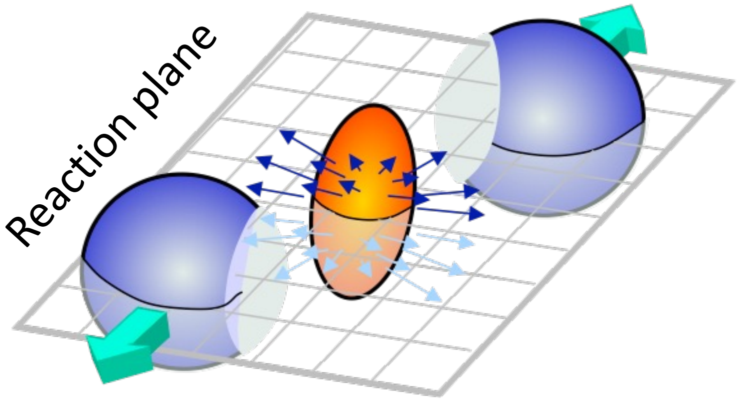

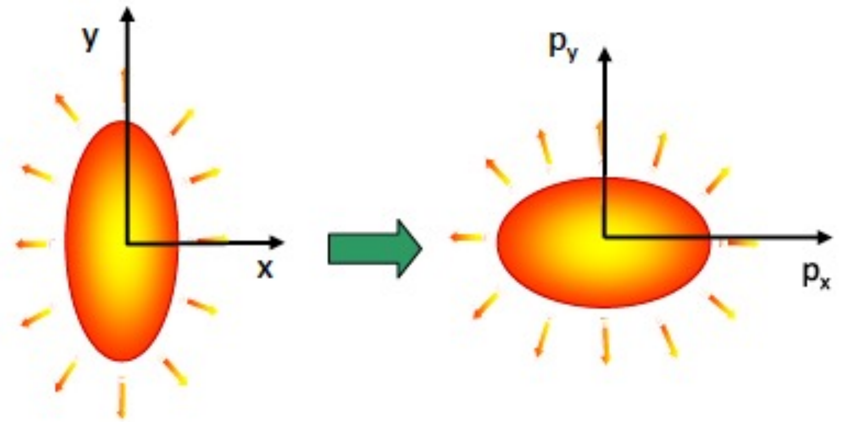

Initial spatial anisotropy → Strong pressure gradients → Anisotropy of produced particles

Fourier analysis of particle distribution:
v_1 : directed flow
v_2 : elliptic flow
v_3 : triangular flow ...

Sensitivity to early expansion

$$\frac{dN}{d\varphi} \propto 1 + 2\sum_{n=1}^{\infty} v_n \left[\cos(n(\varphi - \Psi_n)\right]$$

Medium modifications: R_{AA}

$$R_{AA}(p_t) = \frac{1}{\langle N_{coll} \rangle} \times \frac{dN_{AA}/dp_t}{dN_{pp}/dp_t}$$

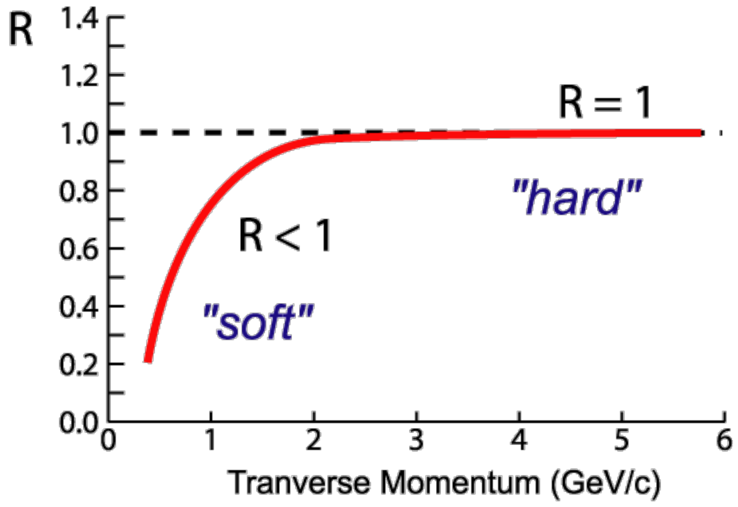

Measurement in pp collisions
is essential/mandatory.

Measurement in p-Pb collisions as
control experiment

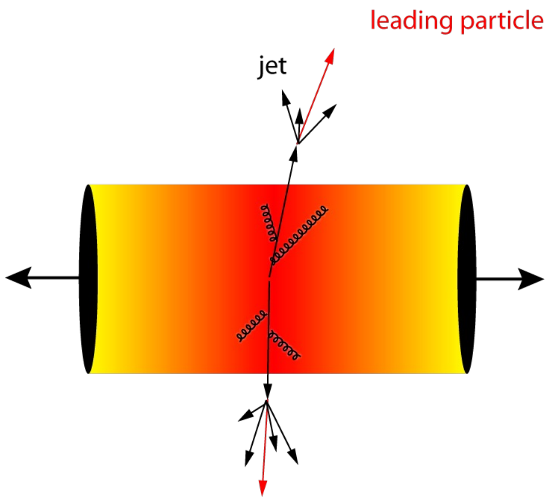

No "Effect":
- R < 1 at small momenta
- R = 1 at higher momenta where hard processes dominate

Suppression:
- R < 1

$$\Delta E(\varepsilon_{QGP}; C_R, m, L)$$

$$\Delta E_g > \Delta E_{c \approx q} > \Delta E_b$$

$$R_{AA}^{\pi} < R_{AA}^{D} < R_{AA}^{B}$$

Goal: Use in-medium energy loss
to measure medium properties

Global properties

Charged-particle production

PRL 116 (2016) 222302

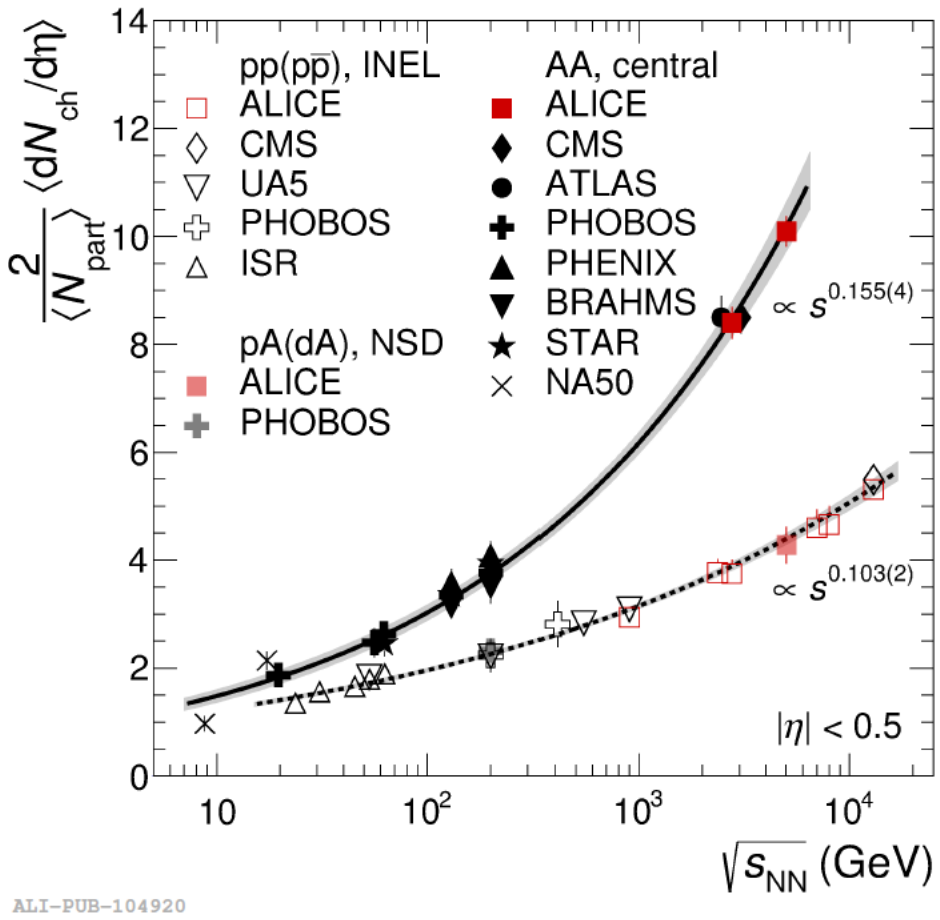

Increase of charged-particle production in nuclear collisions much faster with √s than in pp

More of the available energy used for particle production in heavy-ion collisions

Particle production in Pb-Pb

PRC 101 (2020) 044907

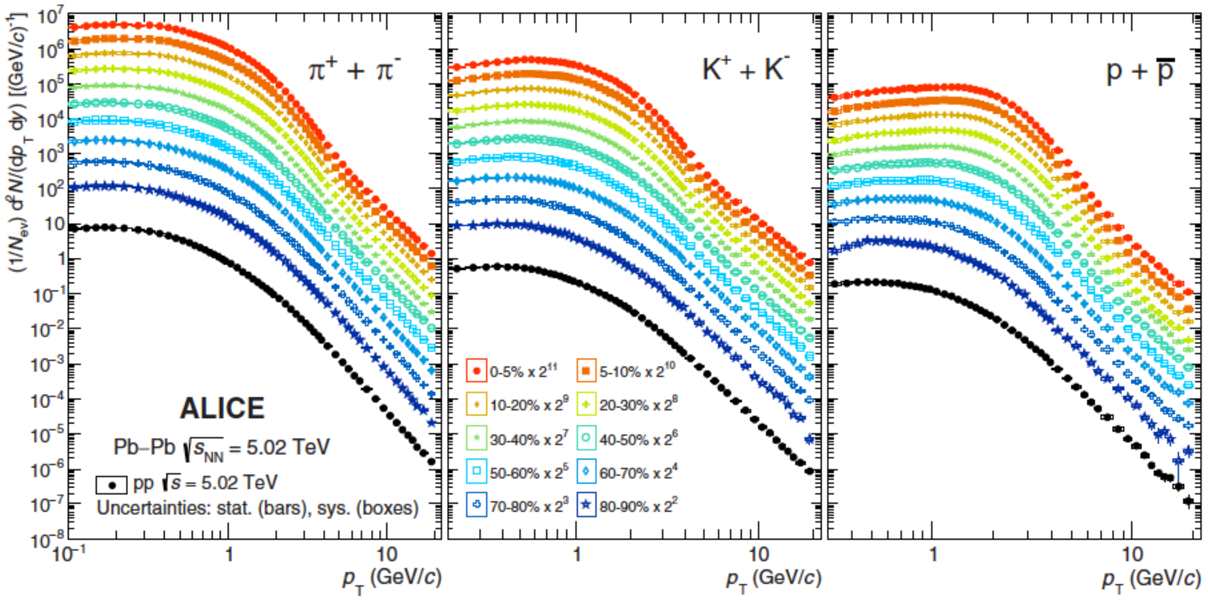

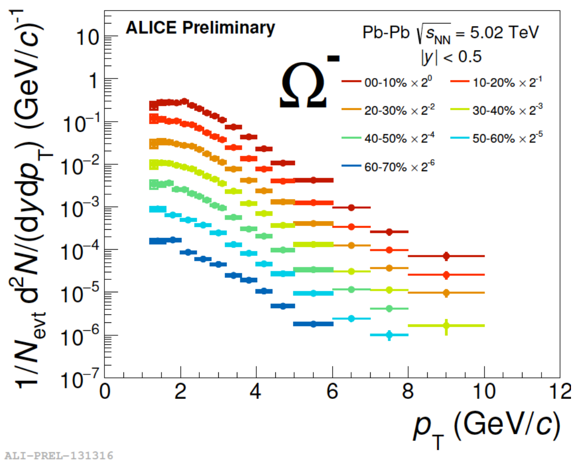

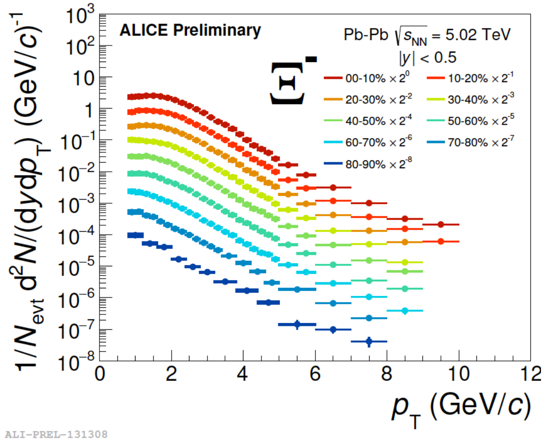

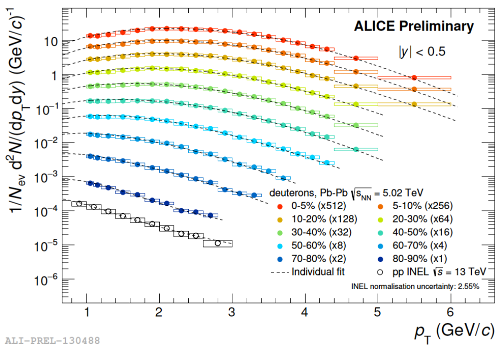

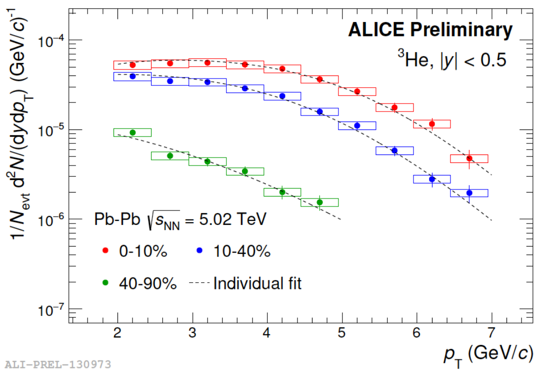

- precise p_T and centrality differential measurements of various light-flavour particle species at highest Pb-Pb collision energy

- large number of multiplicity dependent measurements in pp and p-Pb

Integrated particle yields

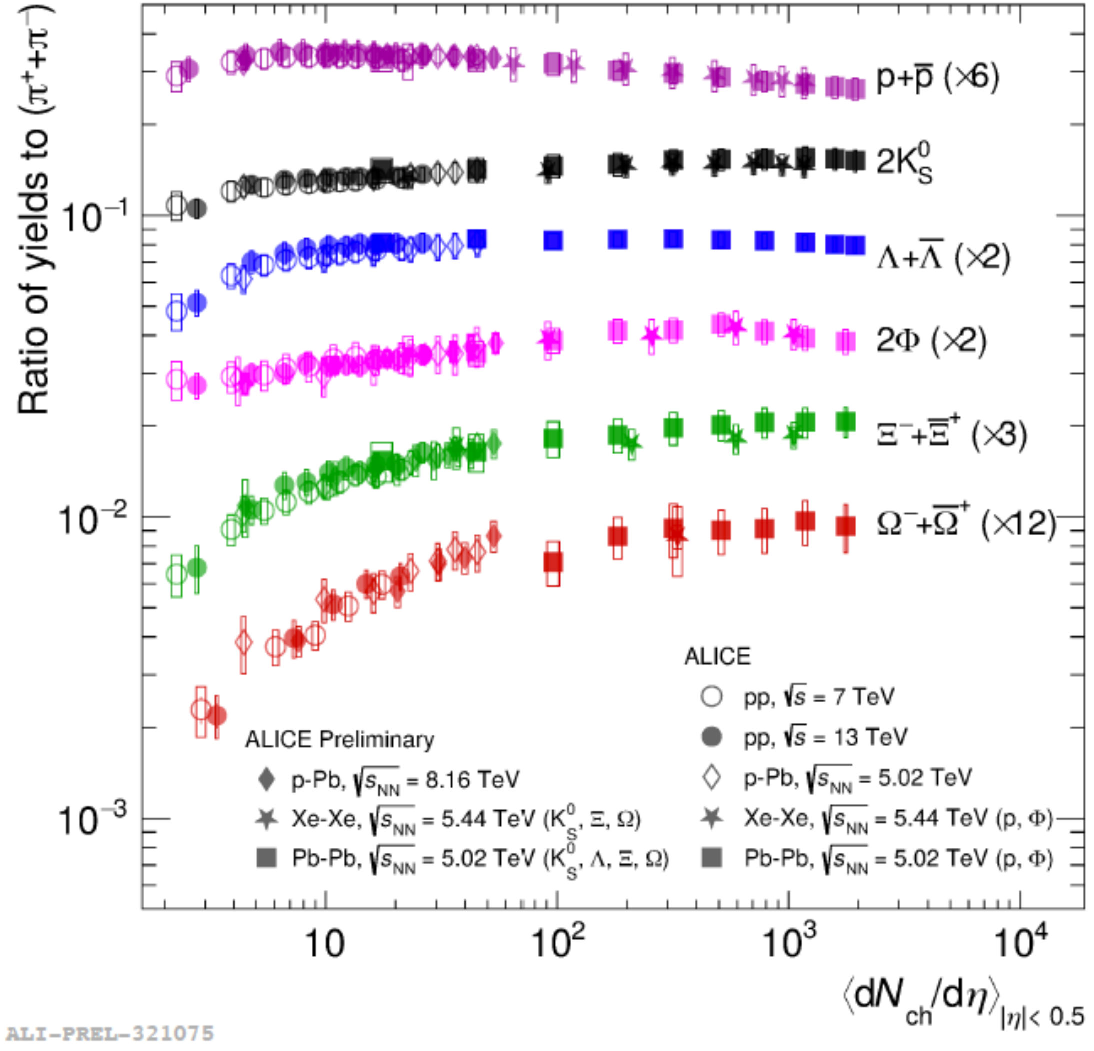

|S| = 0

|S| = 1

|S| = 1

|S| = 0 (hidden)

|S| = 2

|S| = 3

- Continuous evolution of strangeness production between different collision systems and energies

- Hadron chemistry driven by multiplicity

- Magnitude of strangeness enhancement grows with strange quark content:

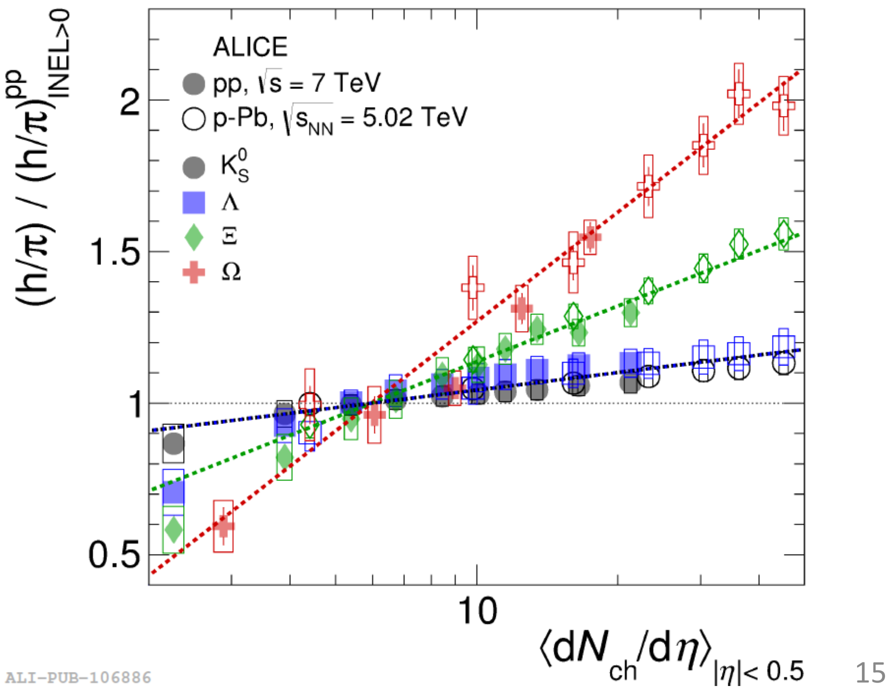

Nature Physics 13 (2017) 535

Elliptic flow in Pb-Pb, and in pp, p-Pb

arXiv: 2206.04587

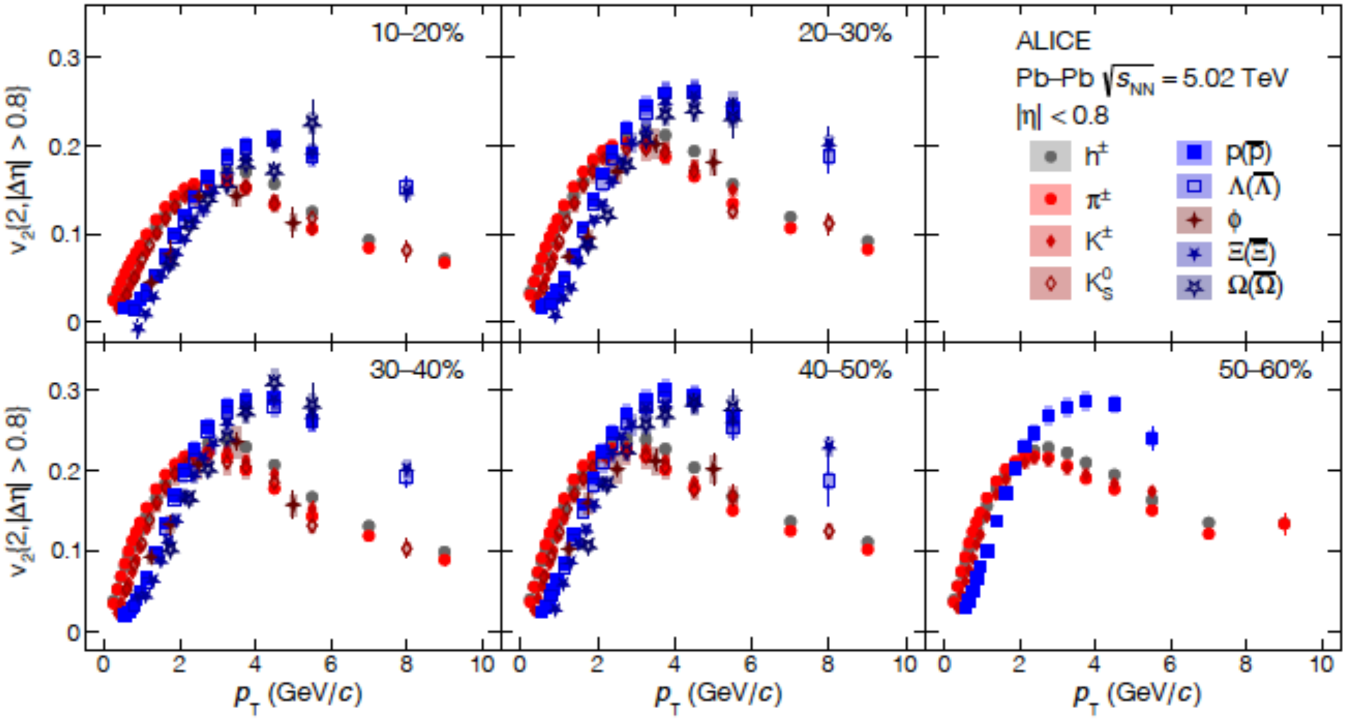

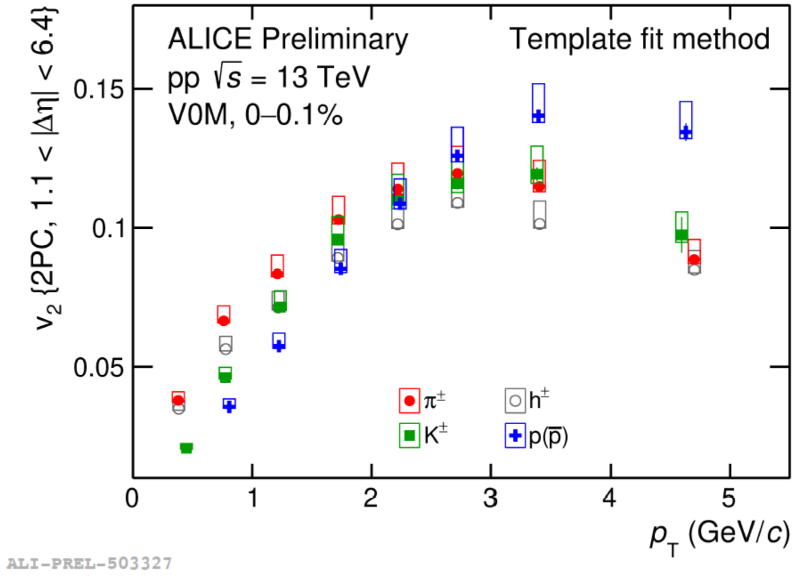

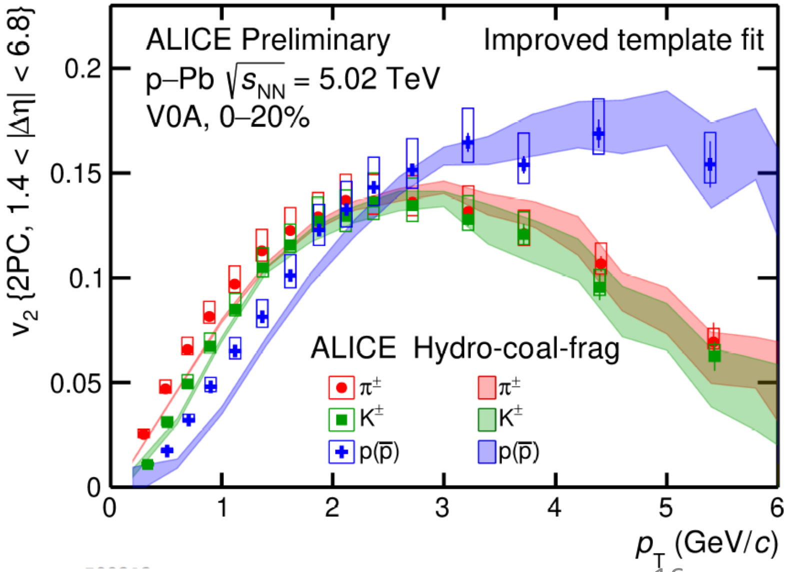

Low p_T:
Mass ordering
→ hydrodynamic flow
Intermediate p_T:
Baryon vs meson grouping : in Pb-Pb, and high multiplicity pp & p-Pb
→ quark-level flow + recombination

Constraining initial condition and QGP medium properties

Nature 15(2019)1113
Phys. Rev. C 101, 024911 (2020)

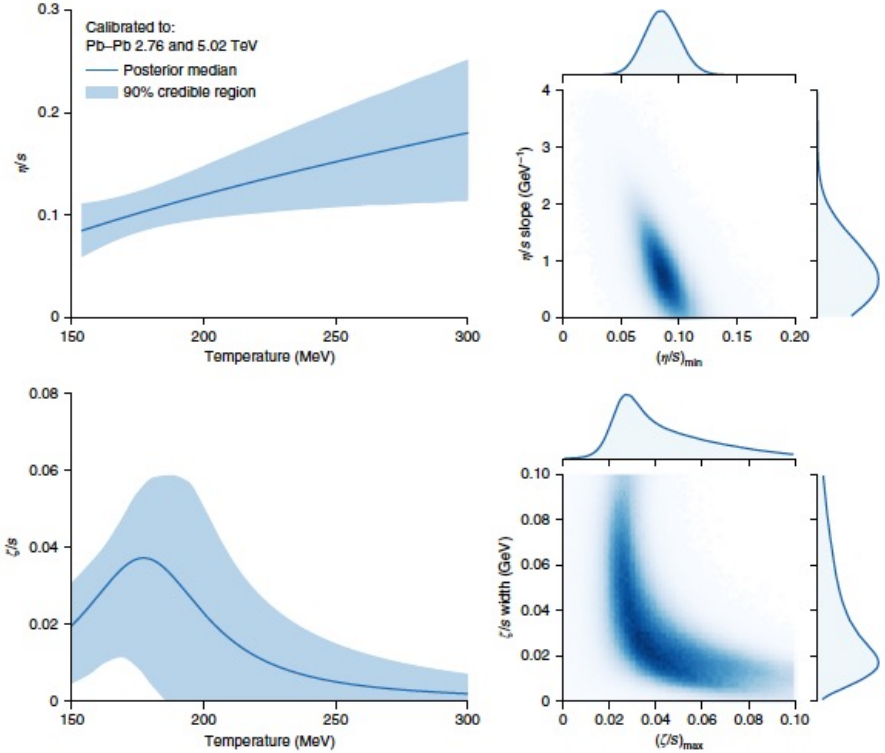

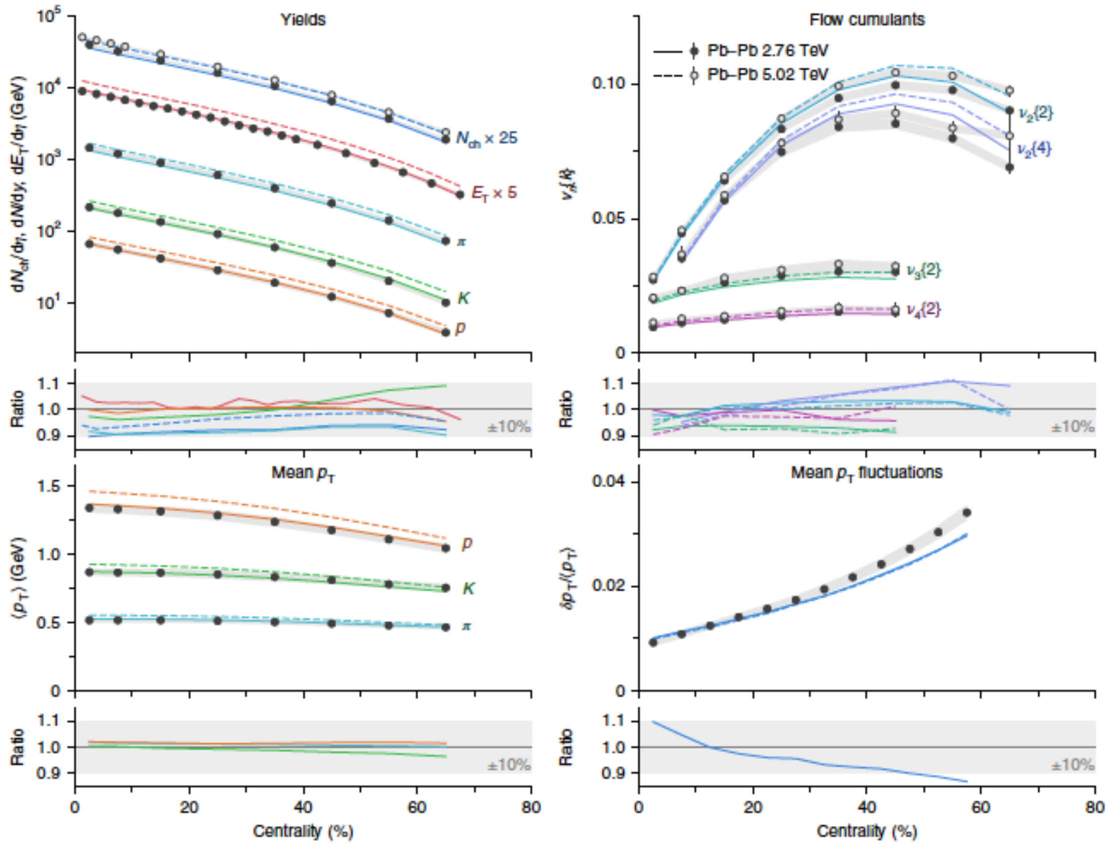

- near T_c, shear viscosity/entropy density close to AdS/CFT lower bound $1/4\pi$ rising with temperature in QGP
- bulk viscosity/entropy density peaks near T_c

Initial-state correlations

Accessing initial conditions: v_2 - $[p_T]$ correlations

PLB 834 (2022) 137393

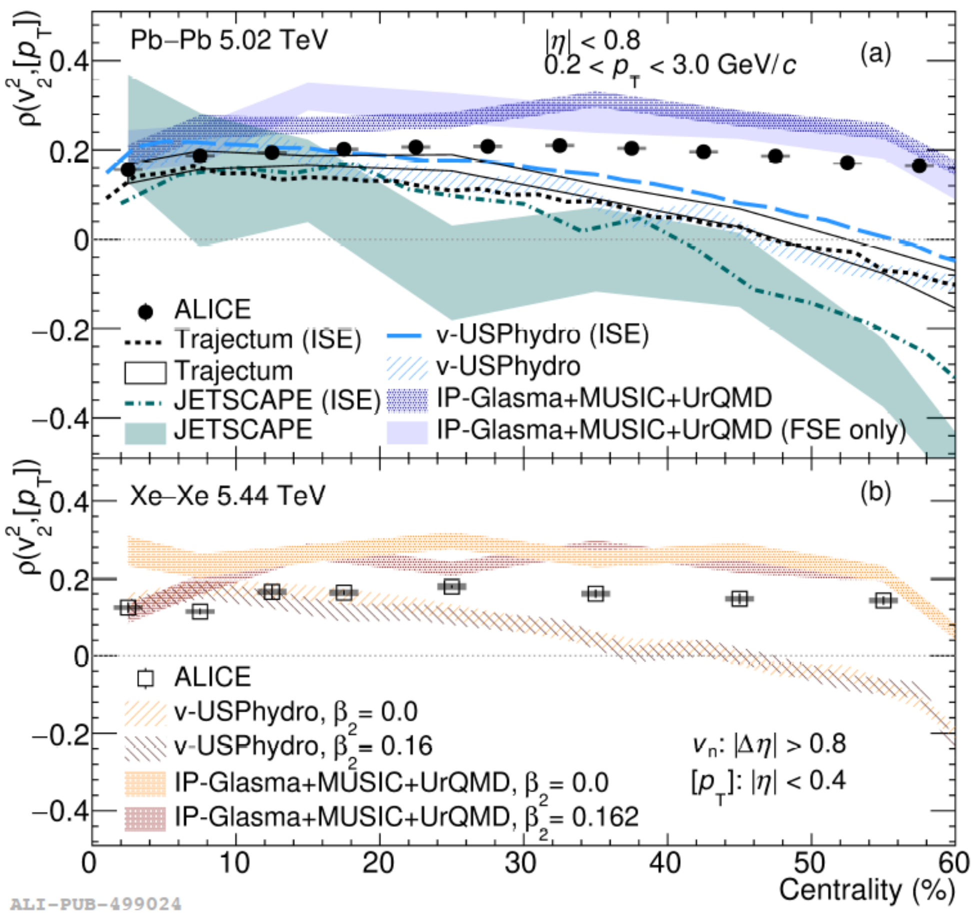

$$\rho(v_n^2,[p_T]) = \frac{\mathrm{Cov}(v_n^2,[p_T])}{\sqrt{\mathrm{Var}(v_n^2)}\sqrt{c_k}},$$

- positive correlation observed
- almost no centrality dependence

Initial conditions:
Trento ↔ IP - Glasma

IP-Glasma closer to data than Trento

including these data in the Bayesian global fitting
→ better constraint on the initial state in nuclear collisions
(Prerequisite for study of QGP transport properties)

Two-particle transverse momentum correlator G_2

PLB 804 (2020) 135375

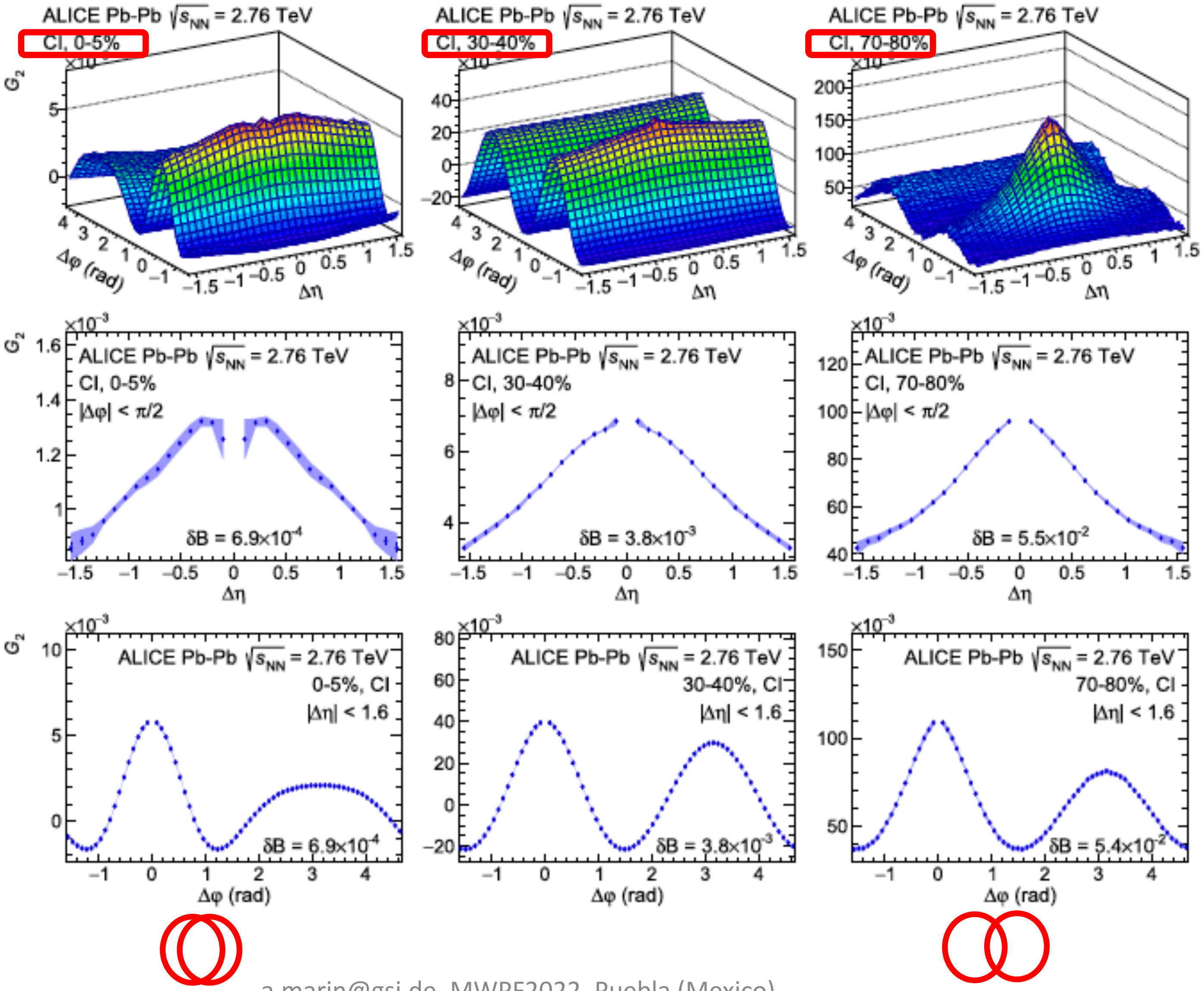

Extraction of QGP transport characteristics

$$G_2(\Delta\eta,\Delta\varphi) = \frac{1}{\langle p_T \rangle^2}\left[\frac{\langle \sum_i^{n_{1,1}} \sum_{j\neq i}^{n_{1,2}} p_{T,i}\, p_{T,j}\rangle}{\langle n_{1,1}\rangle\langle n_{1,2}\rangle} - \langle p_{T,1}\rangle\langle p_{T,2}\rangle\right]$$

- Sensitive to momentum currents transfer
- The longitudinal dimension provides fingerprints of this transfer
- The reach of the transfer ⇒ proxy for the shear viscosity η/s

Longitudinal width evolution with collision centrality ⇒ η/s

$$\sigma_c^2 - \sigma_0^2 = \frac{4}{T_c}\frac{\eta}{s}\left(\tau_0^{-1} - \tau_{c,f}^{-1}\right)$$

Gavin, Abdel-Aziz, PRL 97 162302 (2006)
Sharma, Pruneau, PRC 79 024905 (2009)
STAR, PLB 704, 467–473 (2011)

G_2 widths evolution: Pb-Pb, p-Pb and pp

PLB 804 (2020) 135375

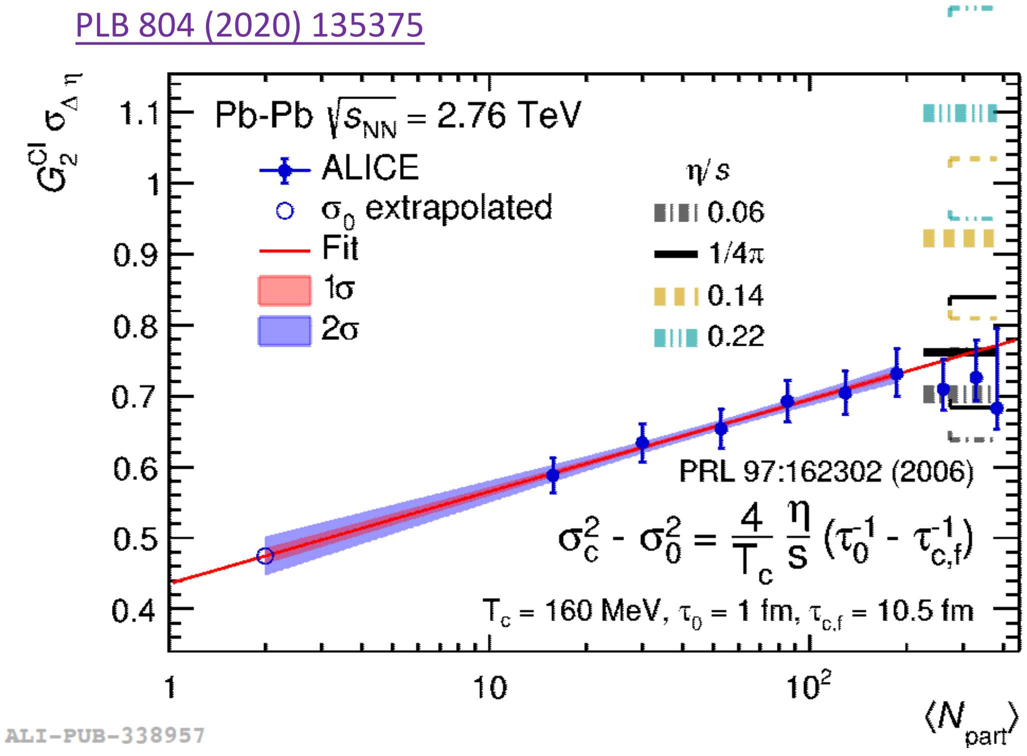

arXiv: 2211.08979

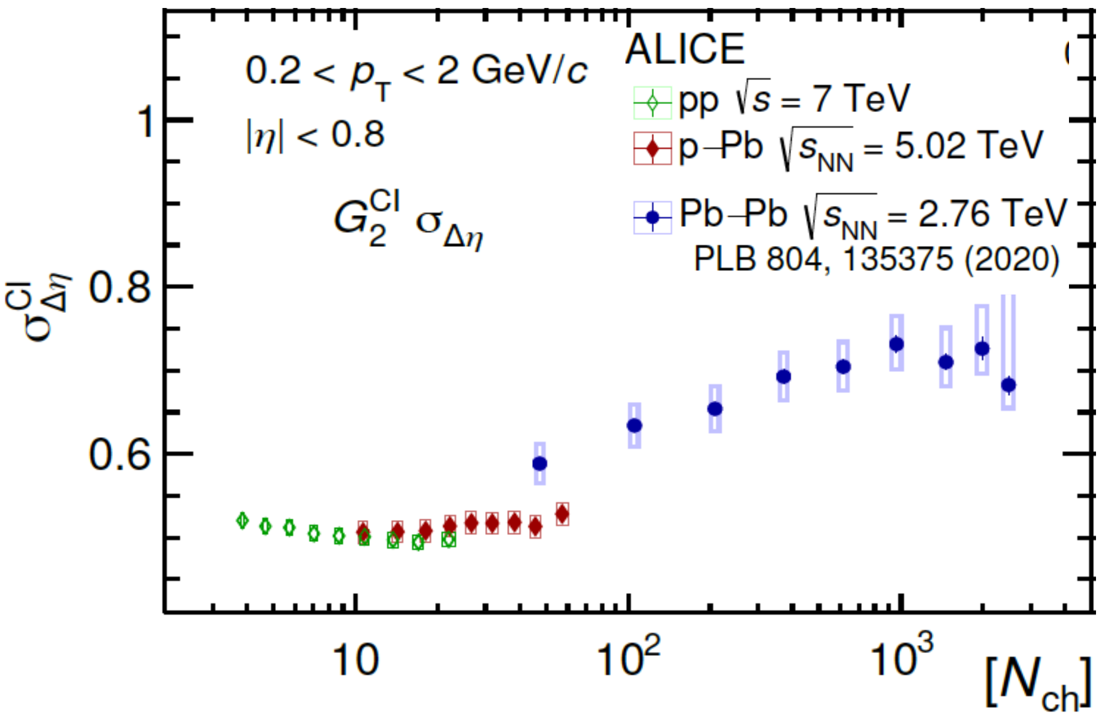

Data seem to favour small η/s values

V. Gonzalez *et al.*
EPJC 81 (2021) 5, 465

No evidence for shear viscous effects in pp & p–Pb based on $G_2^{CI}\sigma_{\Delta\eta}$

- System lifetime too short for viscous forces to play a significant role?

Antideuteron number fluctuations, $\rho_{\bar{p}\bar{d}}$

$$\frac{\kappa_2}{\kappa_1} = \frac{\langle (n - \langle n \rangle)^2 \rangle}{\langle n \rangle}$$

$$\rho_{\bar{p}\bar{d}} = \frac{\langle (n_{\bar{d}} - \langle n_{\bar{d}} \rangle)(n_{\bar{p}} - \langle n_{\bar{p}} \rangle) \rangle}{\sqrt{\kappa_{2\bar{d}} \kappa_{2\bar{p}}}}$$

arXiv: 2204.10166

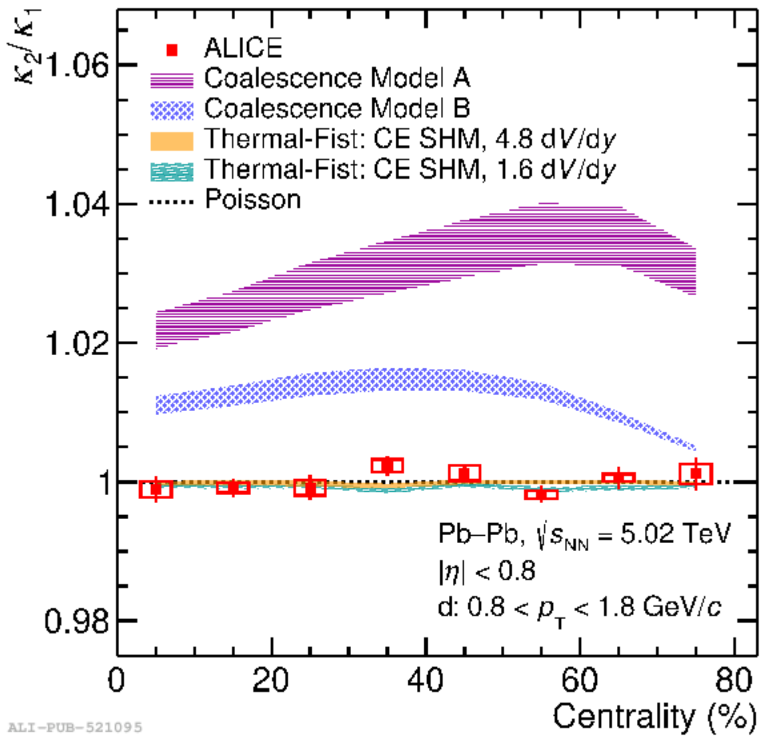

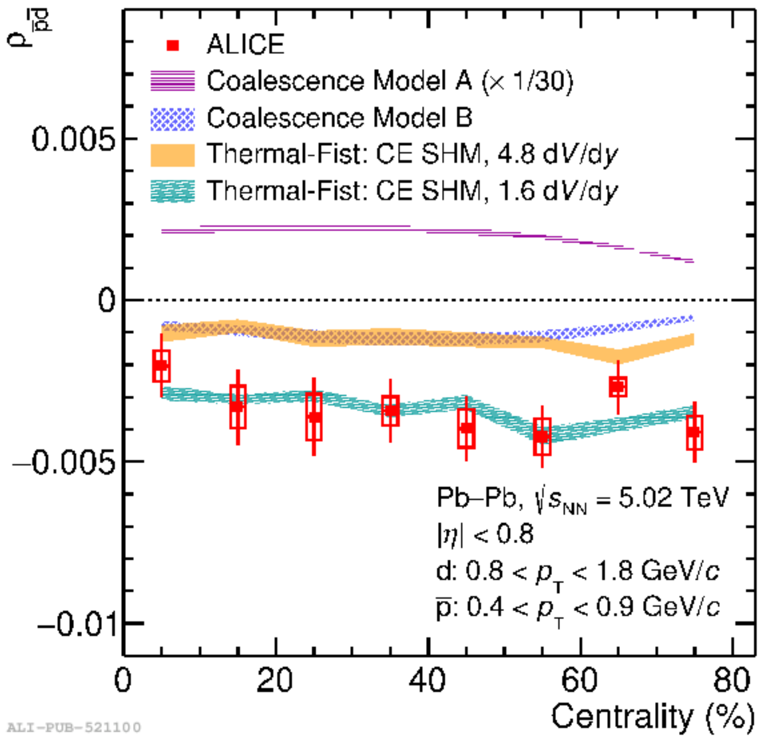

Simple coalescence models are discarded. Data favor SHM

Correlation antiprotons-antideuterons constrains the correlation volume for baryon number conservation

←→ Different from net-proton fluctuation results

arXiv :2204.10879, MUSIC+URQMD+COAL matches the data

Electromagnetic radiation

Dielectron production in central Pb—Pb at $\sqrt{s_{NN}}$ = 5.02 TeV

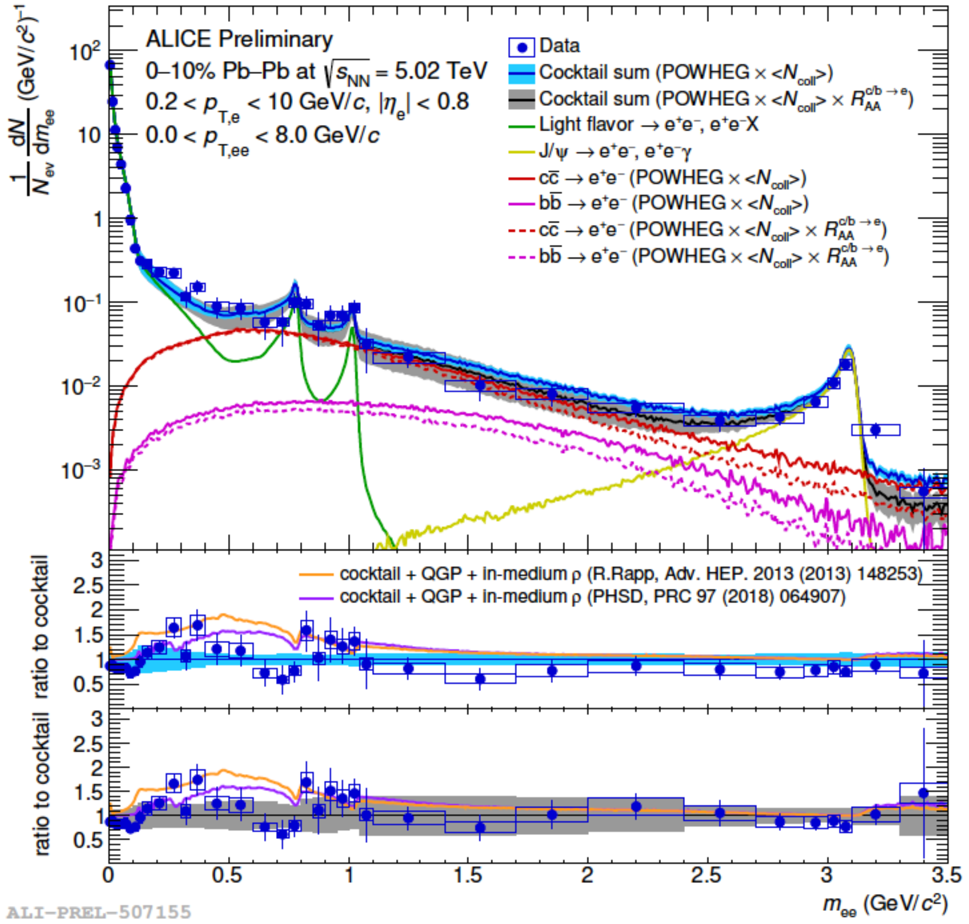

Comparison to hadronic cocktail, including:

- N_{coll} -scaled HF measured in pp at $\sqrt{s}$ = 5.02 TeV

Phys. Rev. C 102 (2020) 055204

⟶ Vacuum baseline

- Include measured R_{AA} of $c/b \longrightarrow e^{\pm}$

Phys. Lett. B 804 (2020) 135377

⟶ Modified-HF cocktail

Intermediate-mass region (IMR) from 1.1 < m_{ee} < 2.7 GeV/c^2

⟶ Consistent with HF suppression & therm. radiation from QGP

Indication for an excess at lower mass

⟶ Compatible with thermal radiation from HG

QGP thermal emission

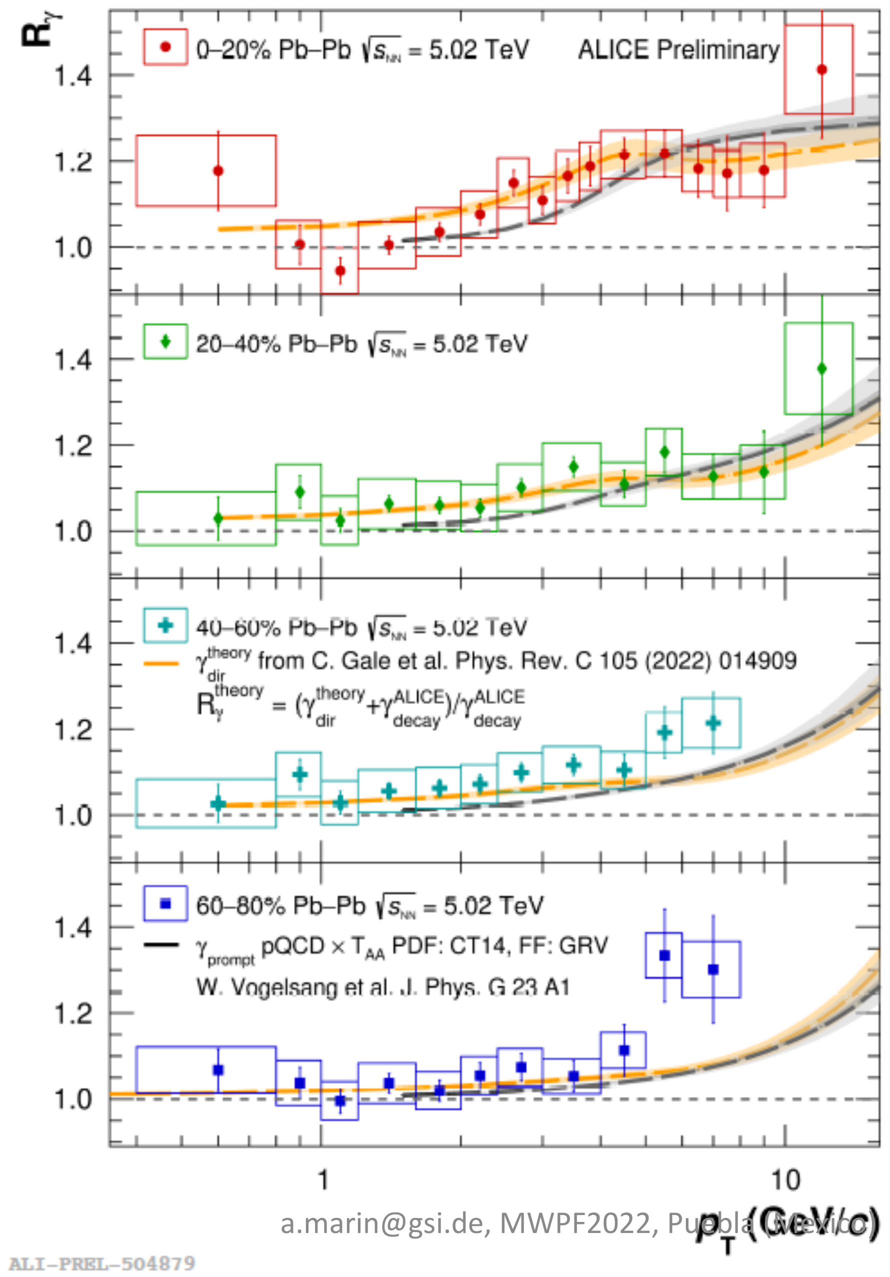

$$R_\gamma = N_{\gamma,\mathrm{inc}}/N_{\gamma,\mathrm{dec}} \approx \left(\frac{N_{\gamma,\mathrm{inc}}}{\pi^0}\right)_{\mathrm{meas}} / \left(\frac{N_{\gamma,\mathrm{dec}}}{\pi^0}\right)_{\mathrm{sim}}$$

$$R_\gamma^{\mathrm{pQCD}} = 1 + N_{coll} \cdot \frac{\gamma_{\mathrm{pQCD}}}{\gamma_{\mathrm{decay}}}$$

At low p_T :

- thermal radiation should dominate
- R_γ is close to 1 → small thermal and pre-equilibrium photon contribution
- Models with thermal and pre-equilibrium photons, can describe the data better than the calculation including only prompt photons

For p_T > 3 GeV/c:

- can be attributed to prompt (hard scattering) photons
- data is consistent with NLO pQCD calculation of prompt photons in pp collisions, scaled with T_{AA}
  Calculation by W. Vogelsang, using PDF: CT14, FF: GRV

QGP thermal emission

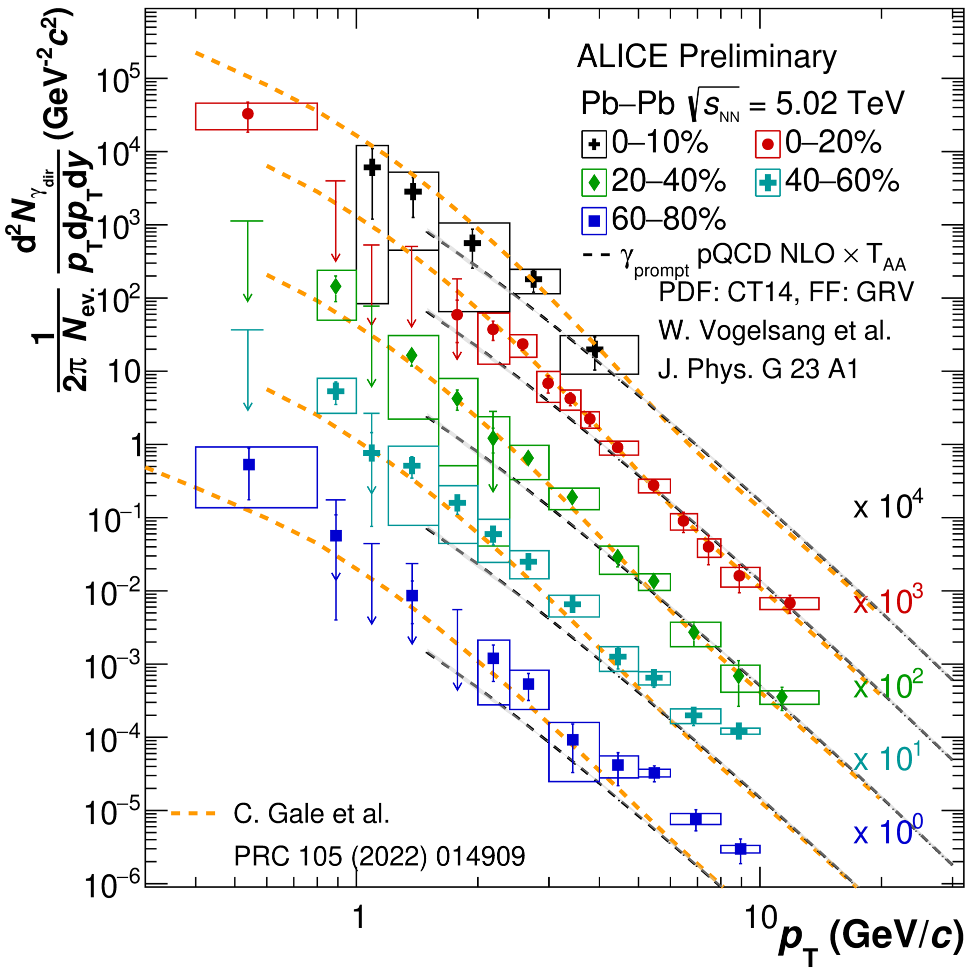

$$N_{\gamma,\mathrm{dir}} = N_{\gamma,\mathrm{inc}} - N_{\gamma,\mathrm{dec}} = \left(1 - \frac{1}{R_\gamma}\right) \cdot N_{\gamma,\mathrm{inc}}$$

$$\gamma_{\mathrm{dir}} = \frac{\gamma^*_{\mathrm{dir}}}{\gamma^*_{\mathrm{incl}}} \cdot (\gamma_{\mathrm{incl}})_{\mathrm{real}}$$

New measurement of direct γ in Pb-Pb at 5.02 TeV

- Virtual γ method, 0-10% centrality
- Real γ (conversion method), other centralities

Low p_T ($p_T \lesssim 3$ GeV/c) – "thermal" photons

- consistent with model with pre-equilibrium and thermal photons

High p_T ($p_T \gtrsim 3$ GeV/c) – prompt photons

- consistent with pQCD expectations

Quarkonia

Charmonium dissociation and regeneration

J/ψ suppression due to color screening in the QGP

reduced at low p_T and central rapidity by $c\bar{c}$ regeneration

~ 100 $c\bar{c}$ pairs per central Pb-Pb

$$R_{AA} = \frac{1}{\langle N_{coll} \rangle} \frac{dN/dp_T|_{PbPb}}{dN/dp_T|_{pp}}$$

P. Braun-Munzinger & J. Stachel, Nature 448 (2007) 302

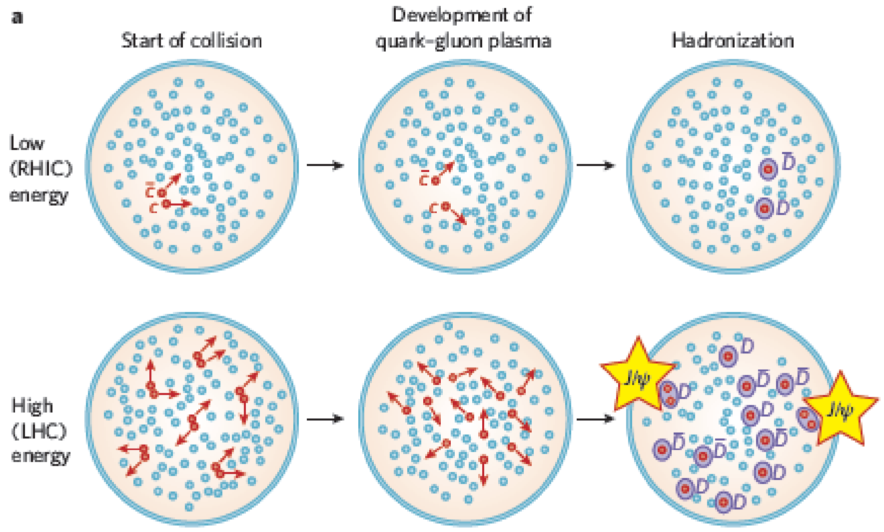

PLB 805 (2020) 135434

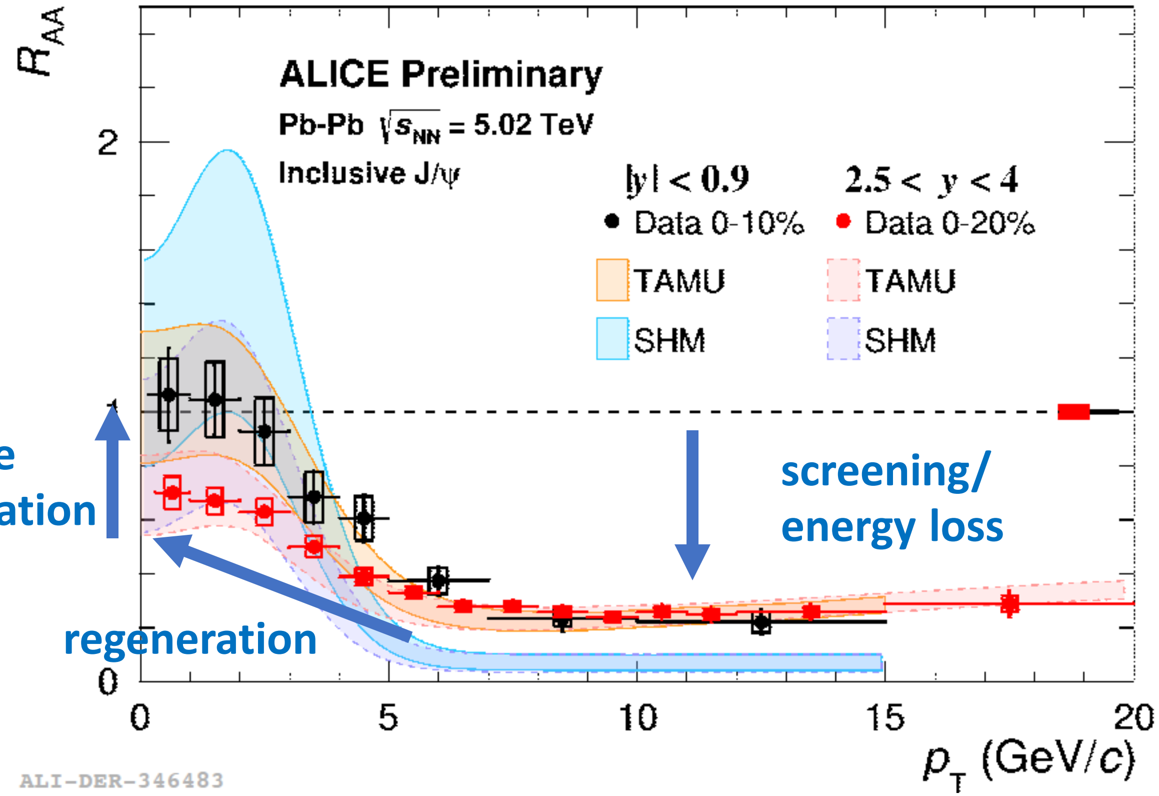

Charmonium dissociation and regeneration

- J/ψ suppression due to color screening in the QGP

Reduced at low p_T and central rapidity by $c\bar{c}$ regeneration

~ 100 $c\bar{c}$ pairs per central Pb-Pb

- New result: measured $\psi(2S)$ ~ x 10 lower binding energy !
- To pin down the role of these two mechanisms

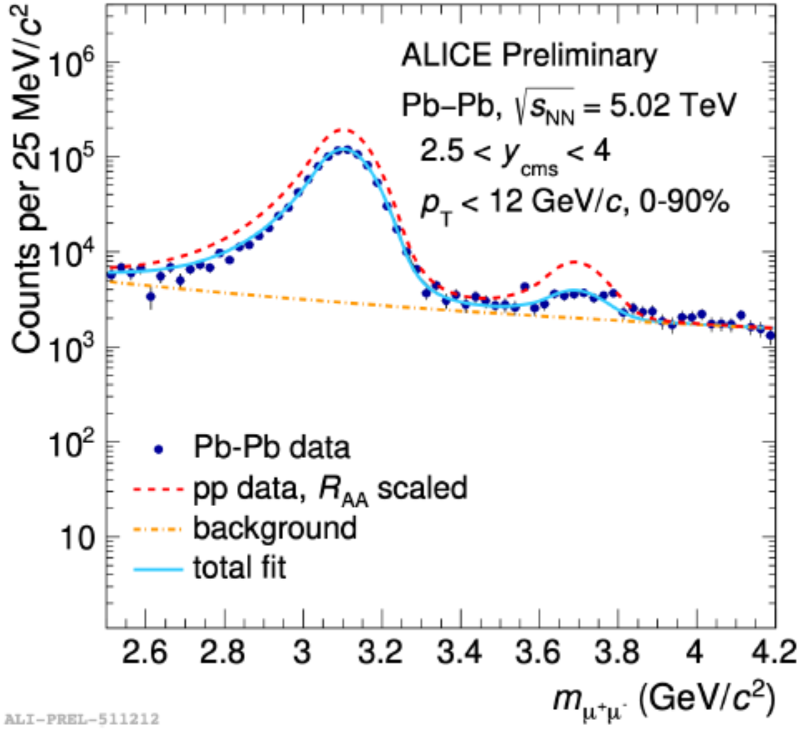

arXiv: 2210.08893

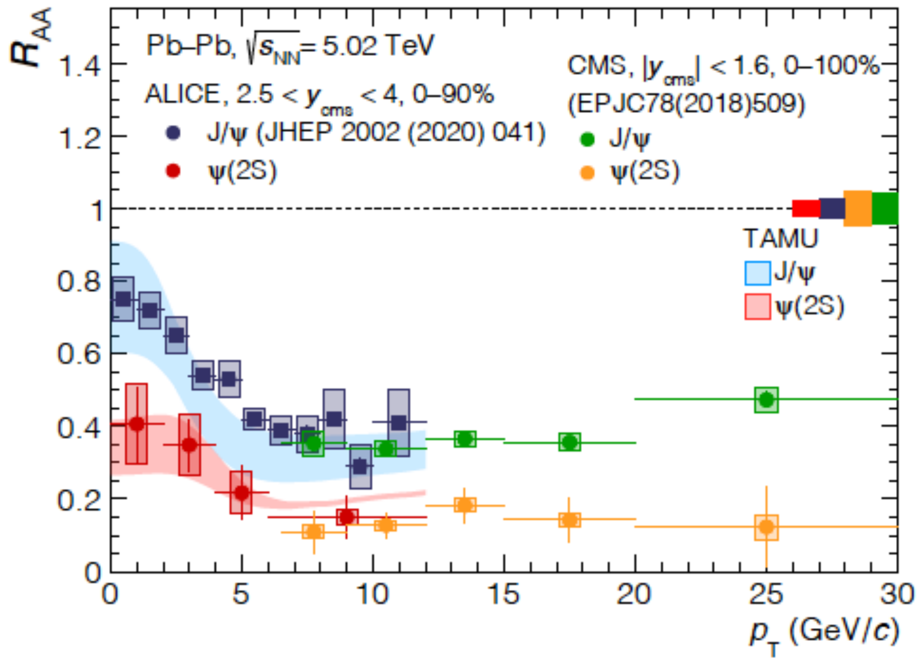

$\psi(2S)$ x2 more suppressed than J/ψ

Hint of regeneration at low p_T

Polarization of J/ψ in Pb-Pb collisions

$$W(\theta) \propto \frac{1}{3+\lambda_\theta}(1+\lambda_\theta \cos^2\theta)$$

Polar angular distribution of dilepton decay

arXiv: 2204.10171

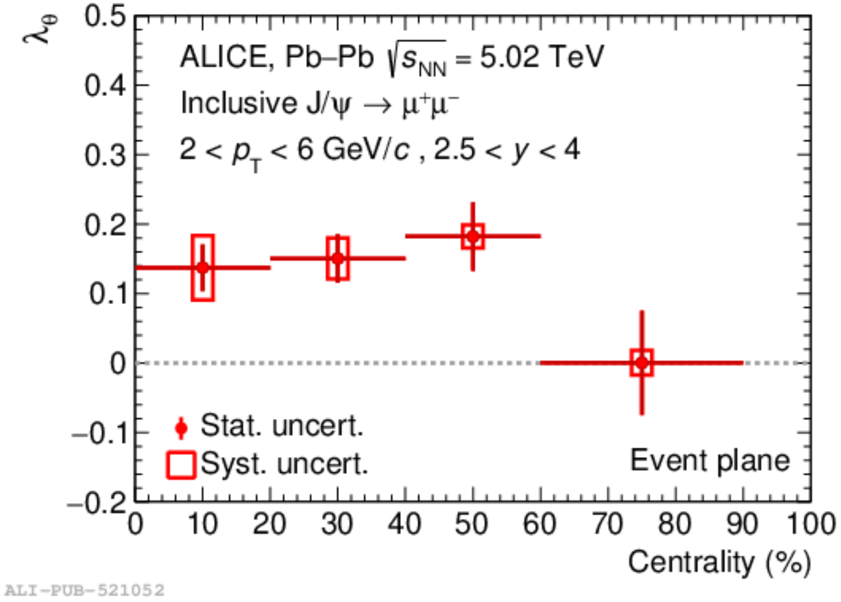

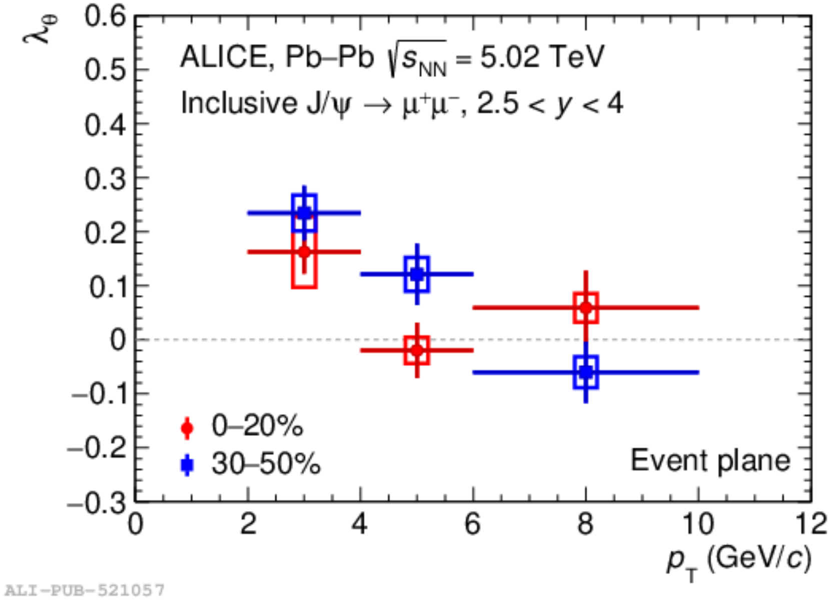

- Clear signal observed by ALICE
- Increase towards lower p_T (reaching **3.9 σ**) disfavours effects due to early ***B***
- Link to QGP vorticity and spin-orbit coupling?

→ Interpretation needs further theory studies

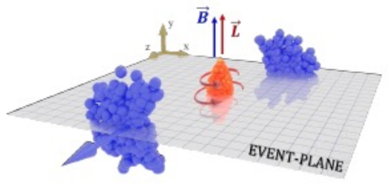

Partonic interactions in matter:
heavy quarks, jets

Open heavy-flavor production: D^0, D^+, D^{*+}

JHEP 01 (2022) 174

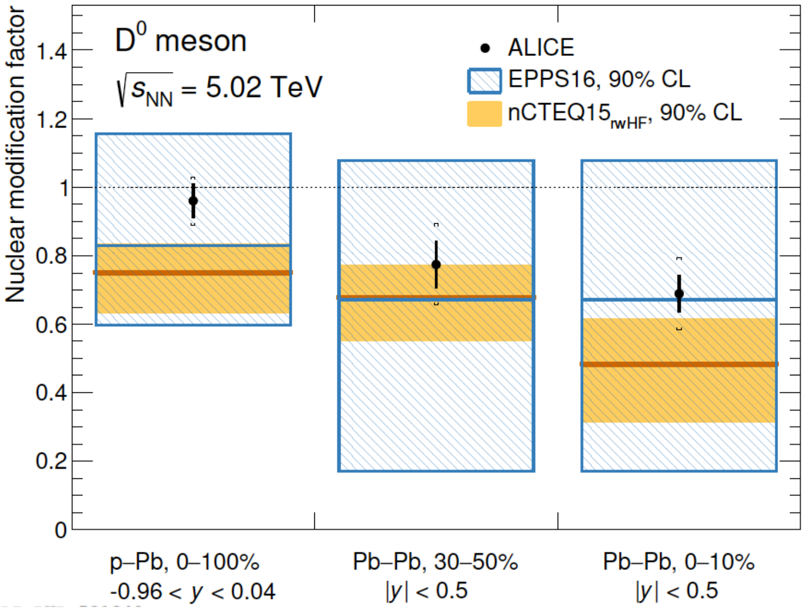

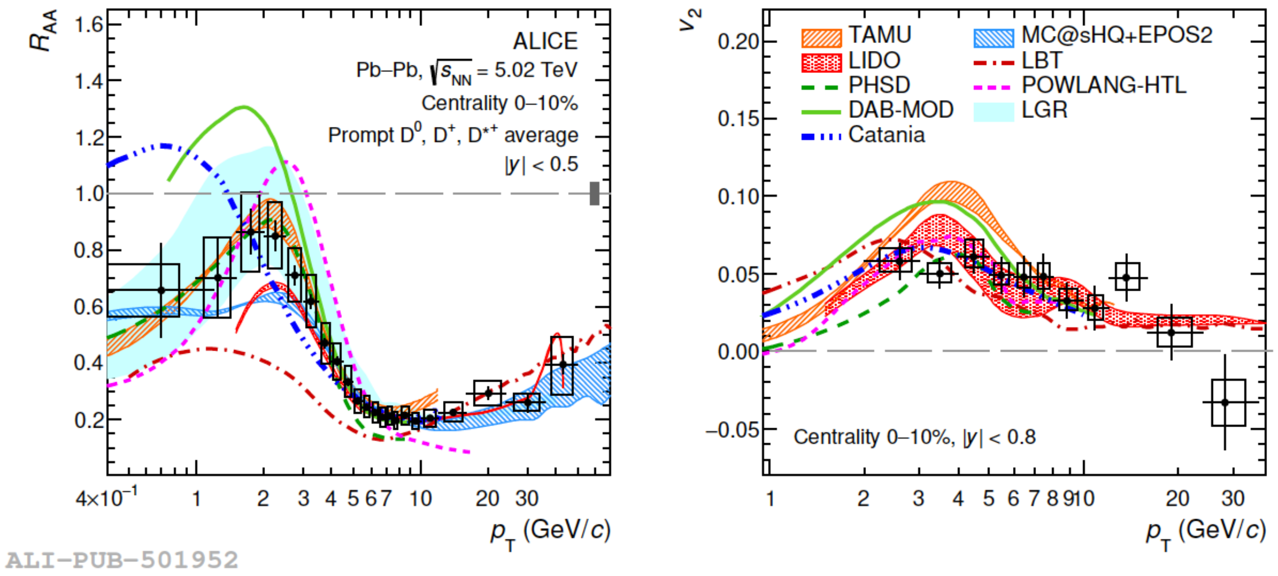

Precise R_{AA} and elliptic flow (v_2 , v_3) non-strange D mesons
→ constraints on to charm quark energy loss models

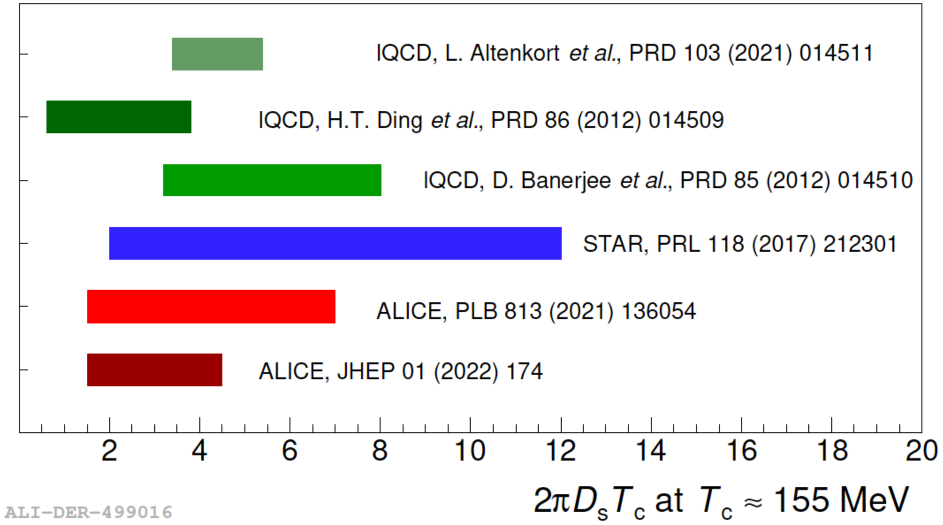

- Intermediate and high p_T :

Radiative energy loss important

- Low/intermediate p_T :

Charm-quark hadronisation via recombination essential

Spatial diffusion coefficients:

$1.5 < 2\pi D_s T_c < 4.5$ → relaxation time of τ_{charm} ~ 3-8 fm/c

Quark-mass dependence of energy loss

Prompt D^0: c→ D^0

Non prompt D^0: b→ c → D^0

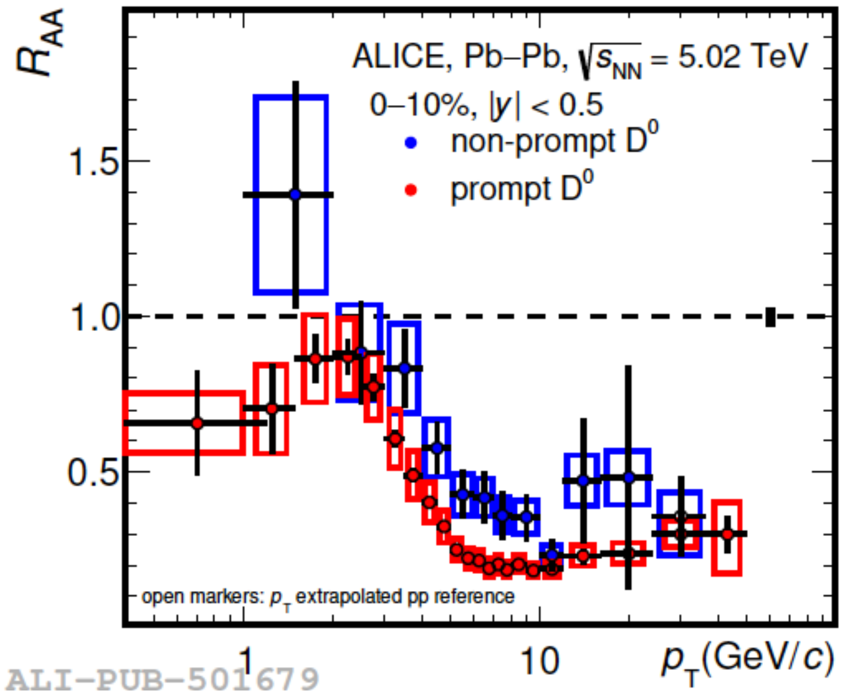

arXiv: 2202.00815

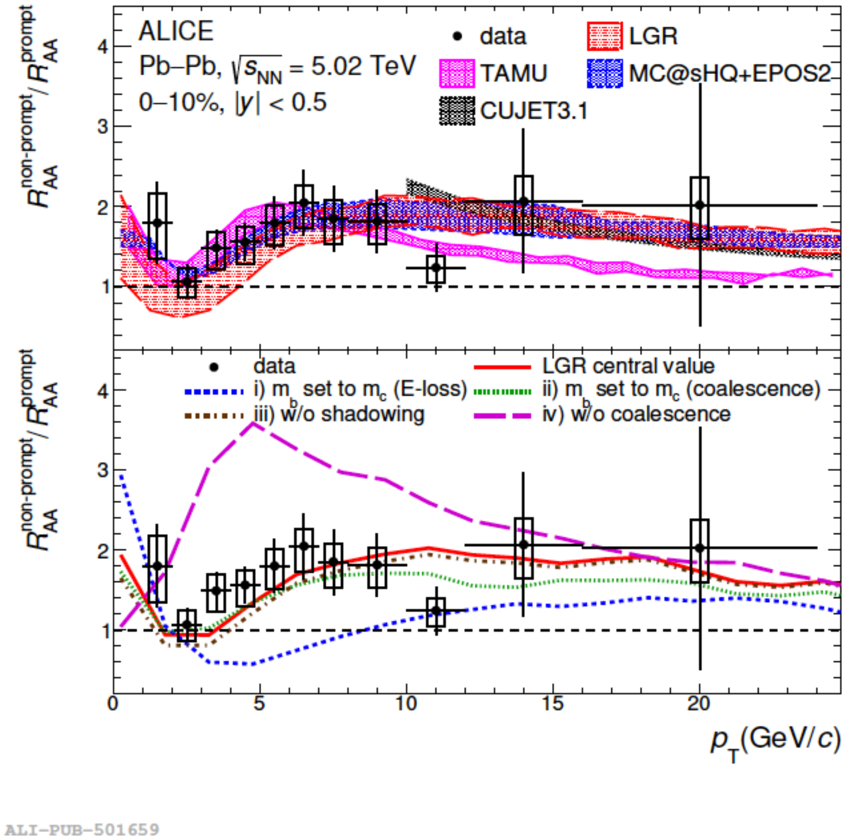

Energy loss predicted to depend on QGP density, but also on quark mass $\Delta E_c > \Delta E_b$

Less suppression for (non-prompt) D mesons from B decays than prompt D mesons

- Data described by models that include collisional and radiative energy loss, and recombination
- Valley structure at low p_T mainly due to formation of D via quark coalescence

Jet quenching: extended reach in p_T and R

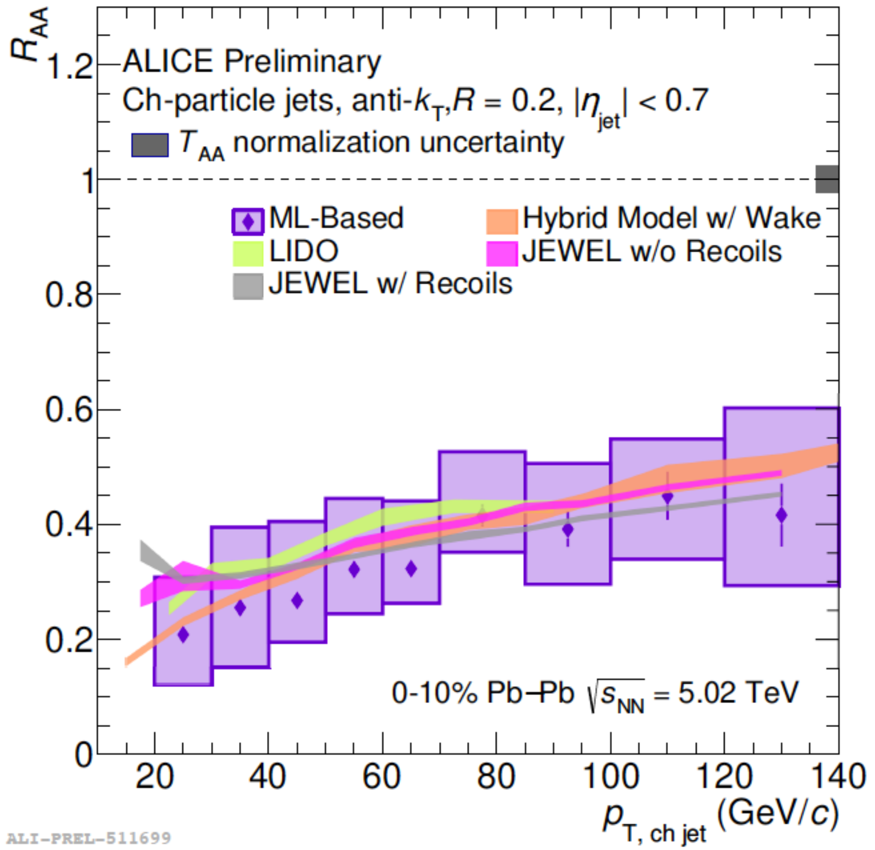

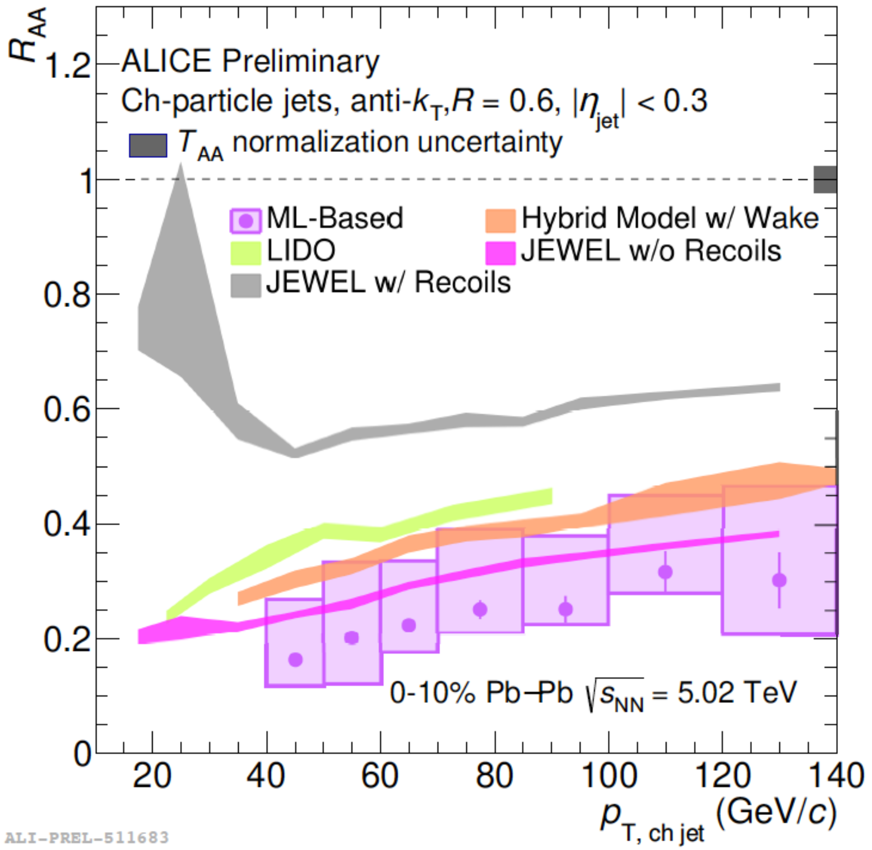

New ML method to subtract underlying Pb-Pb event fluctuations from jet energy: 2x better energy resolution

- Large reduction (factor 3-4) of jet yields, down to p_T = 20 GeV/c
- Lost energy not recovered within the jet "cone"
- Suppression may be even larger for large-cone (R=0.6) low-p_T jets

Microscopic structure of the QGP: acoplanarity

$$\Delta_{\text{recoil}}(p_{\text{T,jet}}, \Delta\varphi) = \frac{1}{N_{\text{trig}}} \frac{d^3 N_{\text{jet}}}{d\eta_{\text{jet}}\, dp_{\text{T,jet}}\, d\Delta\varphi}\Bigg|_{p_{\text{T}}^{\text{trig}} \in \text{TT}_{\text{Sig}}} - c_{\text{Ref}} \cdot \frac{1}{N_{\text{trig}}} \frac{d^3 N_{\text{jet}}}{d\eta_{\text{jet}}\, dp_{\text{T,jet}}\, d\Delta\varphi}\Bigg|_{p_{\text{T}}^{\text{trig}} \in \text{TT}_{\text{Ref}}}$$

$$I_{\text{AA}} = \frac{\Delta_{\text{recoil}}(\text{Pb}-\text{Pb})}{\Delta_{\text{recoil}}(\text{pp})}$$

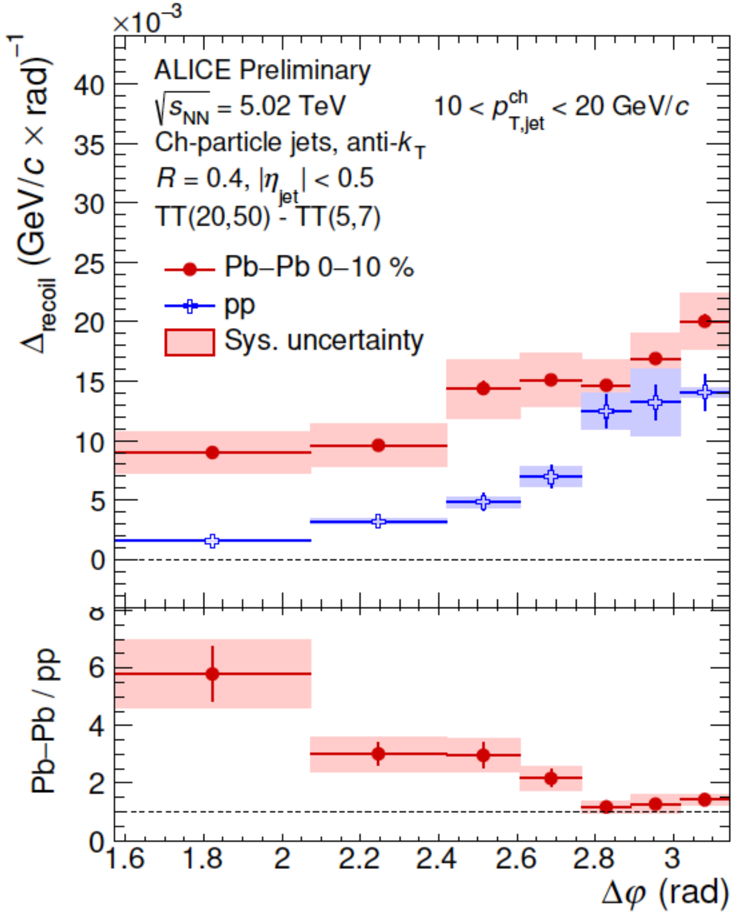

ALI-PREL-524907

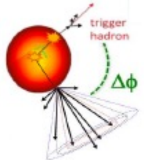

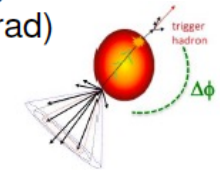

$\Delta\phi$ broadening for larger R and small jet p_T

Scattering on QGP constituents?

Medium response to energy loss ?

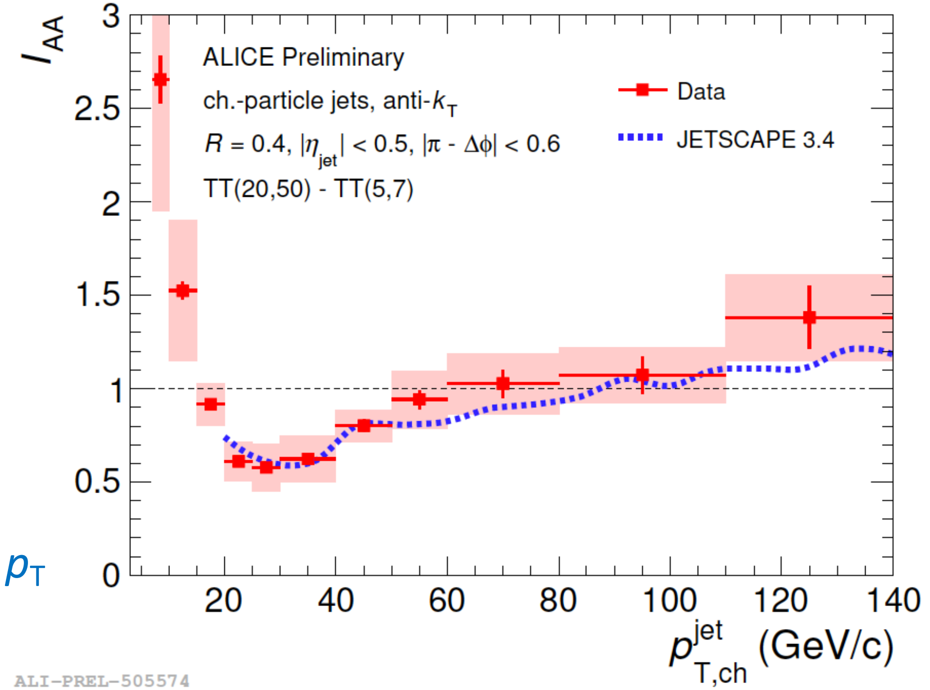

ALI-PREL-505574

Hint of energy recovery at low jet momenta

Exploring angular dependence: groomed jet radius

PRL 128 (2022) 102001

$$z_g \equiv \frac{p_{T,\text{subleading}}}{p_{T,\text{leading}} + p_{T,\text{subleading}}}$$

$$\theta_g = \frac{\sqrt{\Delta y^2 + \Delta\varphi^2}}{R}$$

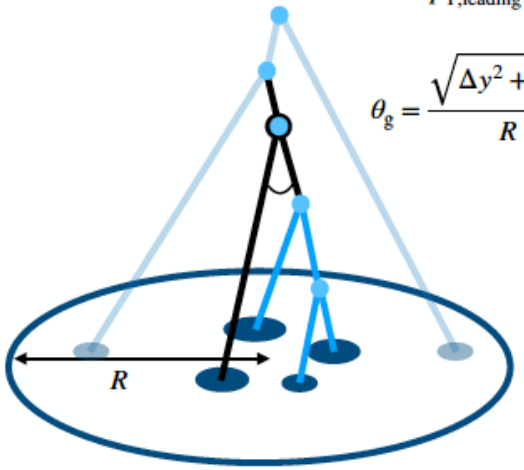

Grooming condition: $z > z_{cut}$

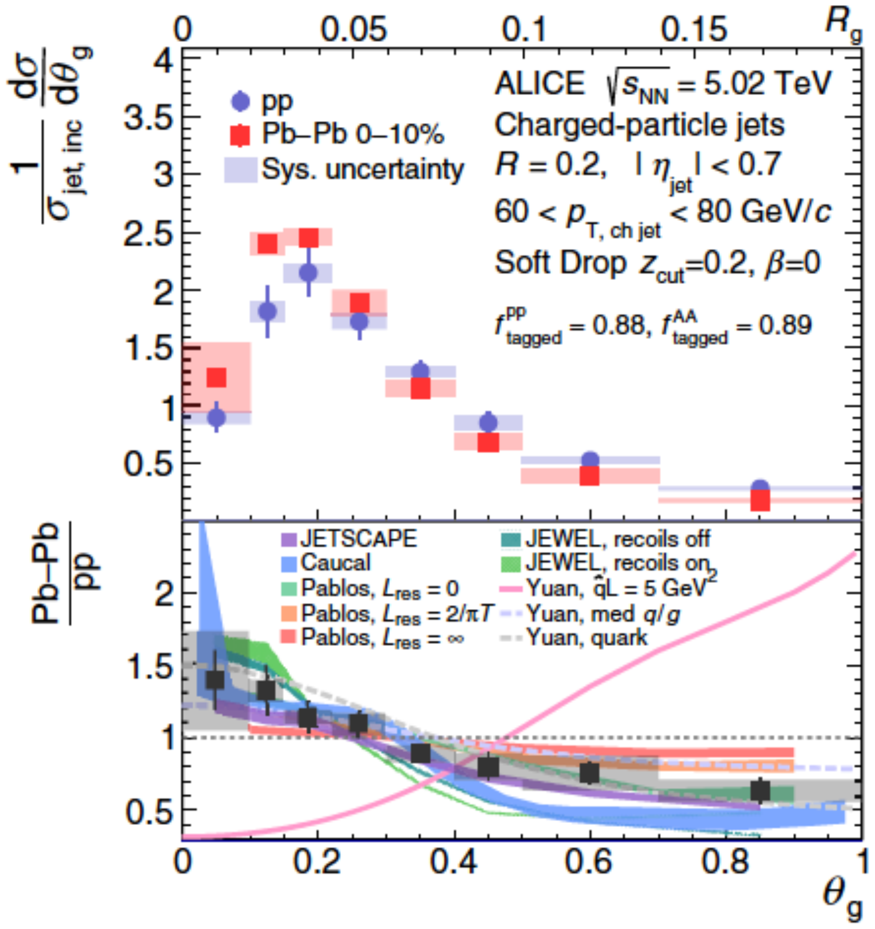

- Suppression of large angles
- Enhancement of small angles

First experimental evidence for modification of angular scale of groomed jets in HIC

Nuclear physics at the LHC

d/p and ^{3}He/p vs multiplicity

JHEP 01 (2022) 106

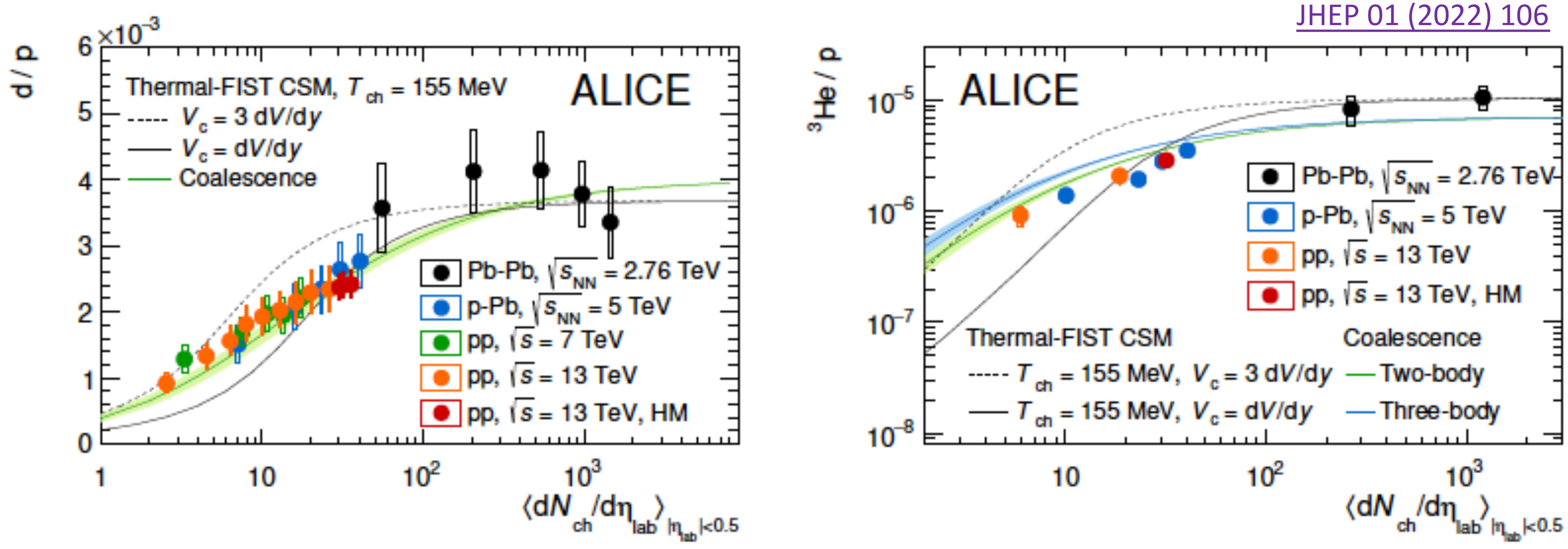

(a) (Anti)deuterons.

(b) (Anti)helions.

Ratios:

- increase with multiplicity and saturation at high multiplicities
- interplay between the evolution of the yields and of the system size with multiplicity

Coalescence model provides a better description of the data

LHC,… also (anti)nuclei factory

- Accessible in Run 2 : d, t, $_{\Lambda}^{3}$H, ^{3}He, ^{4}He
- Production not yet fully understood:

nucleon coalescence vs statistical hadronization

Strong impact on dark matter searches in Space, e.g. $\chi_0\chi_0$ -> $\bar{d}$, $^{3}\overline{He}$ +X (AMS-02, GAPS, BESS)

- Ordinary antinuclei hadroproduction by cosmics is major background
- Antinuclei absorption in space poorly constrained

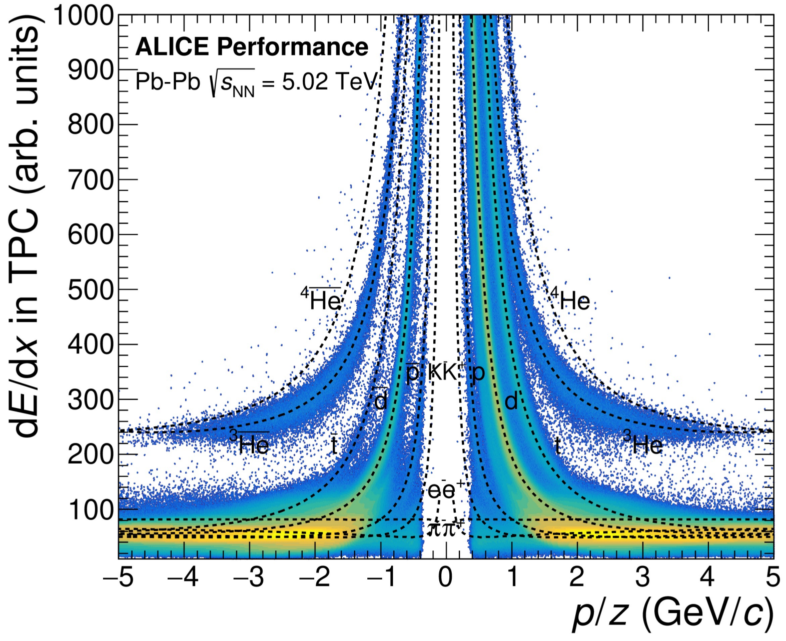

ALI-PERF-341664

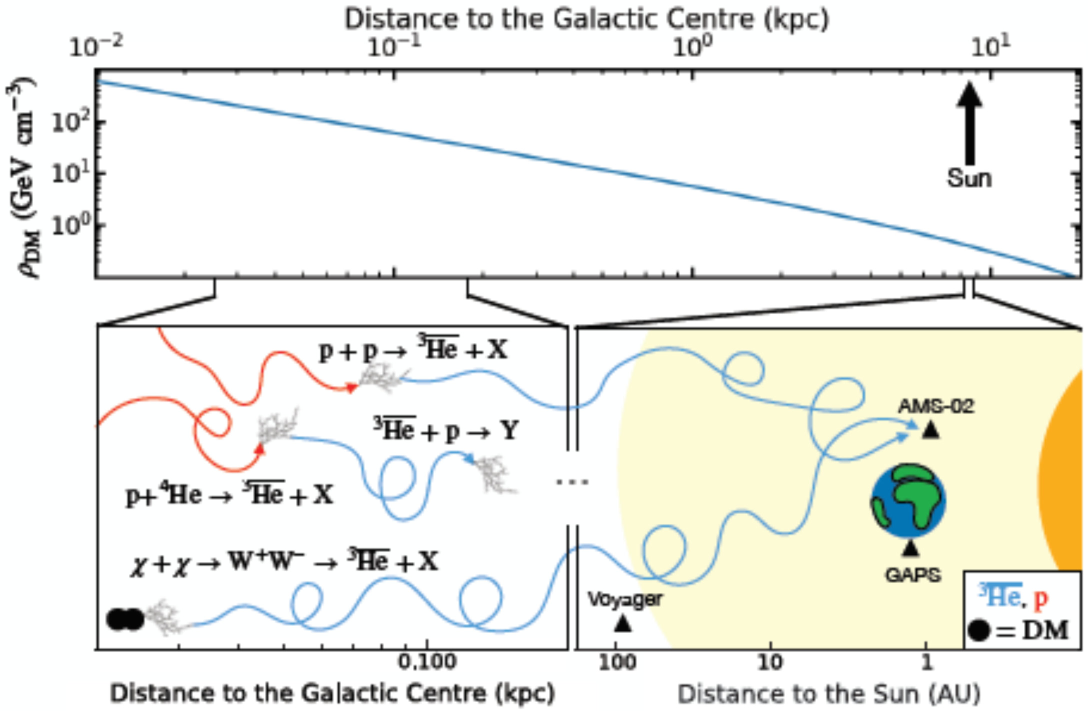

arXiv:2202.01549

$^{3}\overline{\mathrm{He}}$ absorption in ALICE and in the Galaxy

arXiv: 2202.01549

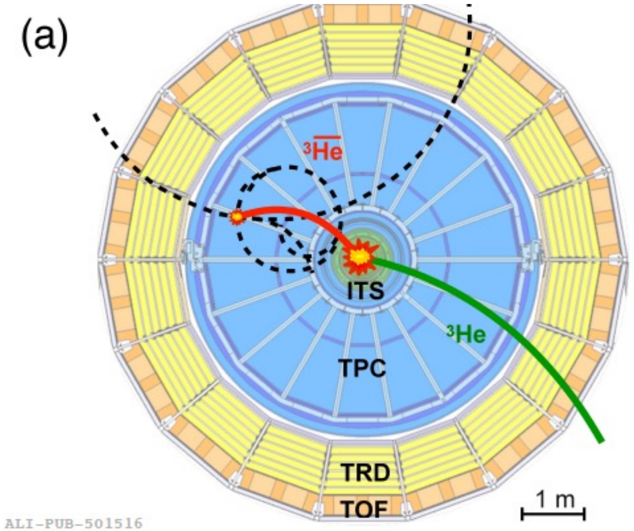

ALI-PUB-501516

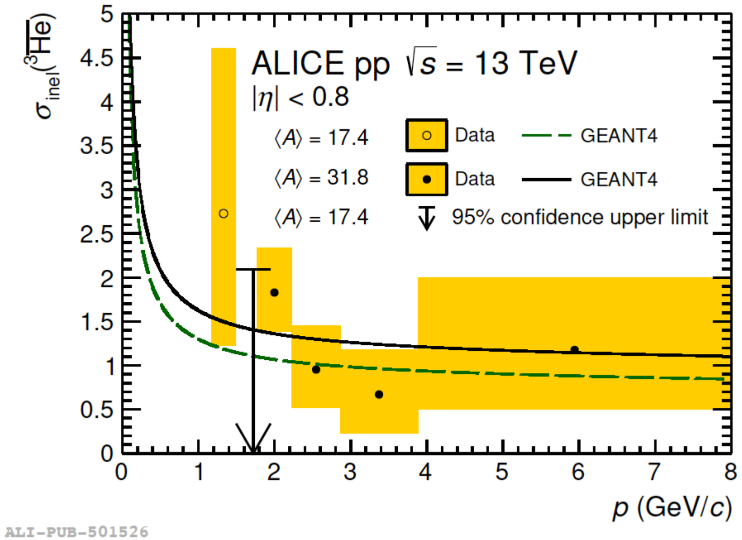

ALI-PUB-501526

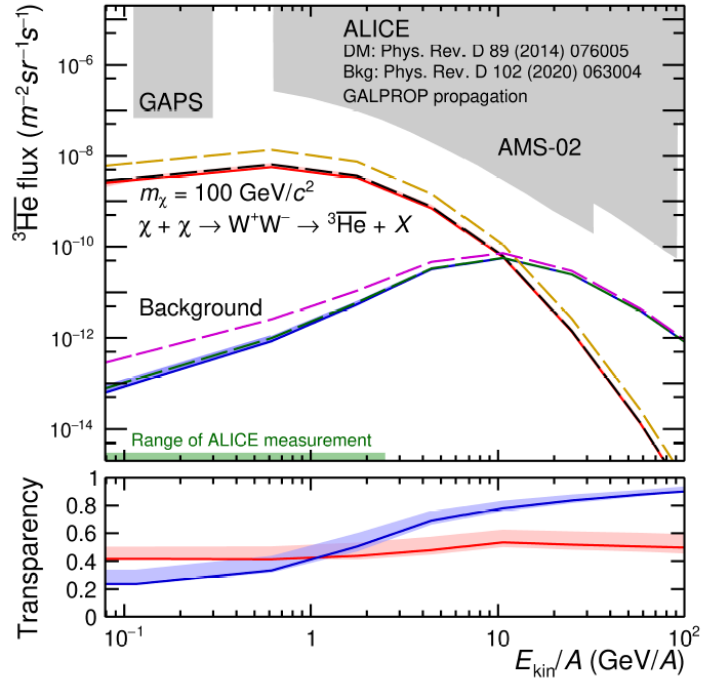

ALI-PUB-501546

Novel technique to use detector material as $\overline{d}$ and $^{3}\overline{\mathrm{He}}$ absorber: measure σ_{inel}

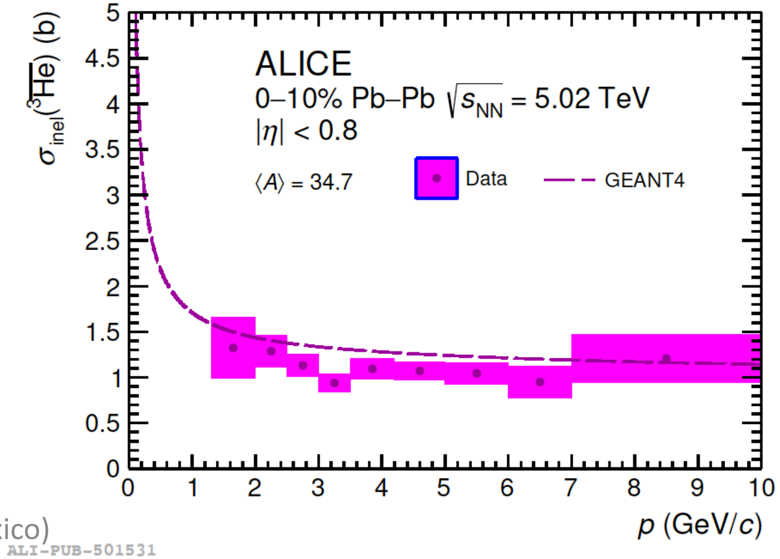

ALI-PUB-501531

Experiment-driven estimate of absorption probability of antinuclei and DM searches and from cosmic-ray background in the Galaxy

Antimatter-matter imbalance at the LHC

Precise μ_B measurement at the LHC

$$\bar{h}/h \propto \exp\left[-2\left(B+\frac{S}{3}\right)\frac{\mu_B}{T} - 2I_3\frac{\mu_{I_3}}{T}\right]$$

where T = 156.2 ± 2 MeV and

	π^+	p	^{3}He	$^3_\Lambda H$
B+S/3	0	1	3	8/3
I_3	1	1/2	1/2	0

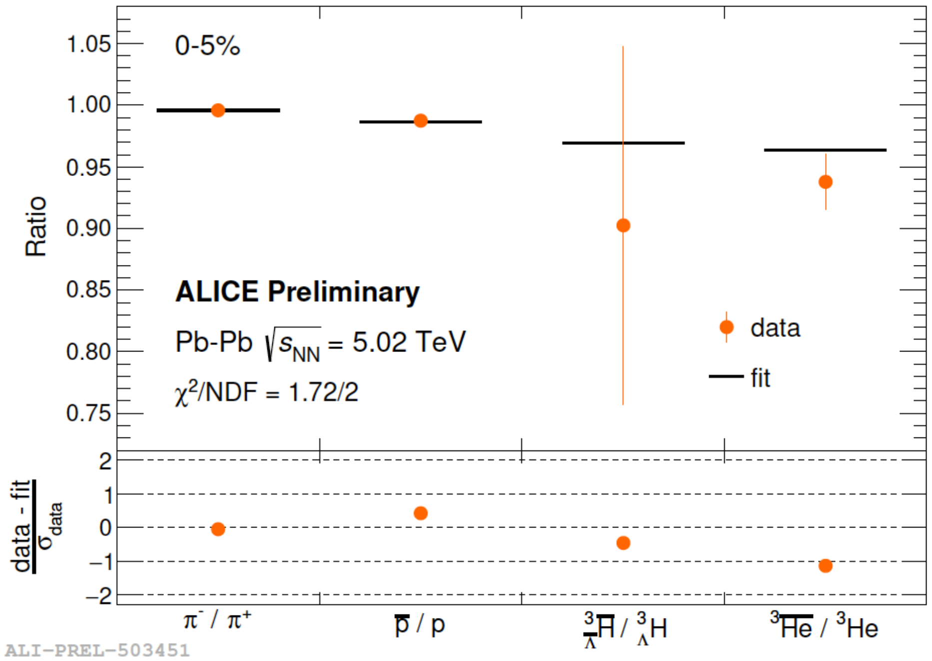

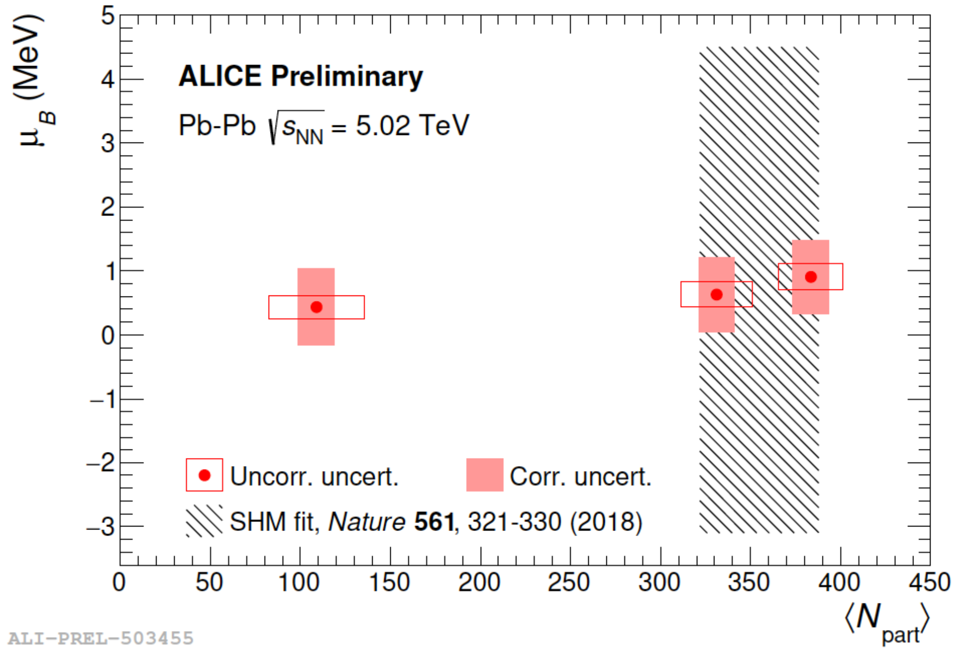

Direct cancellation of correlated uncertainties →Uncertainties reduced wrt thermal model fit by a factor ~6

${}^{3}_{\Lambda}H$ lifetime and B_{Λ}

arXiv: 2209.07360

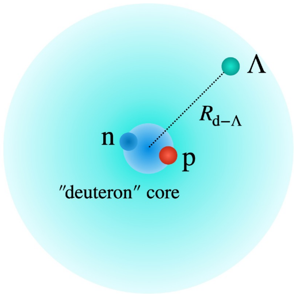

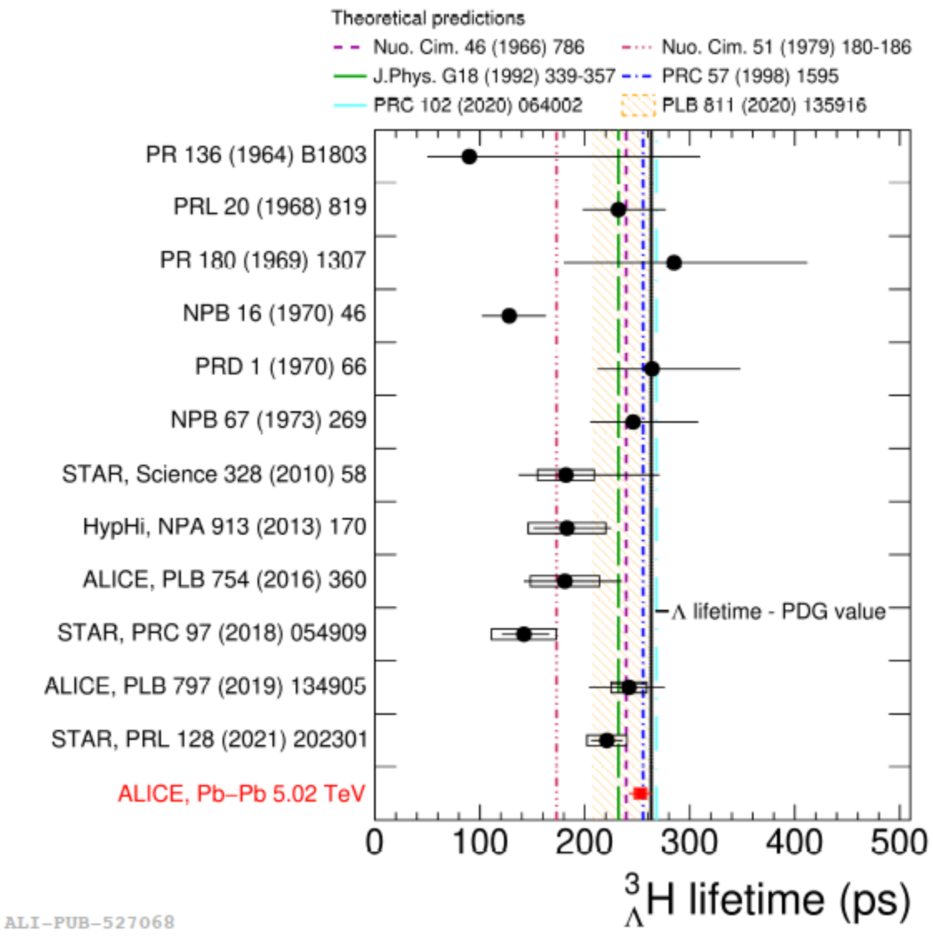

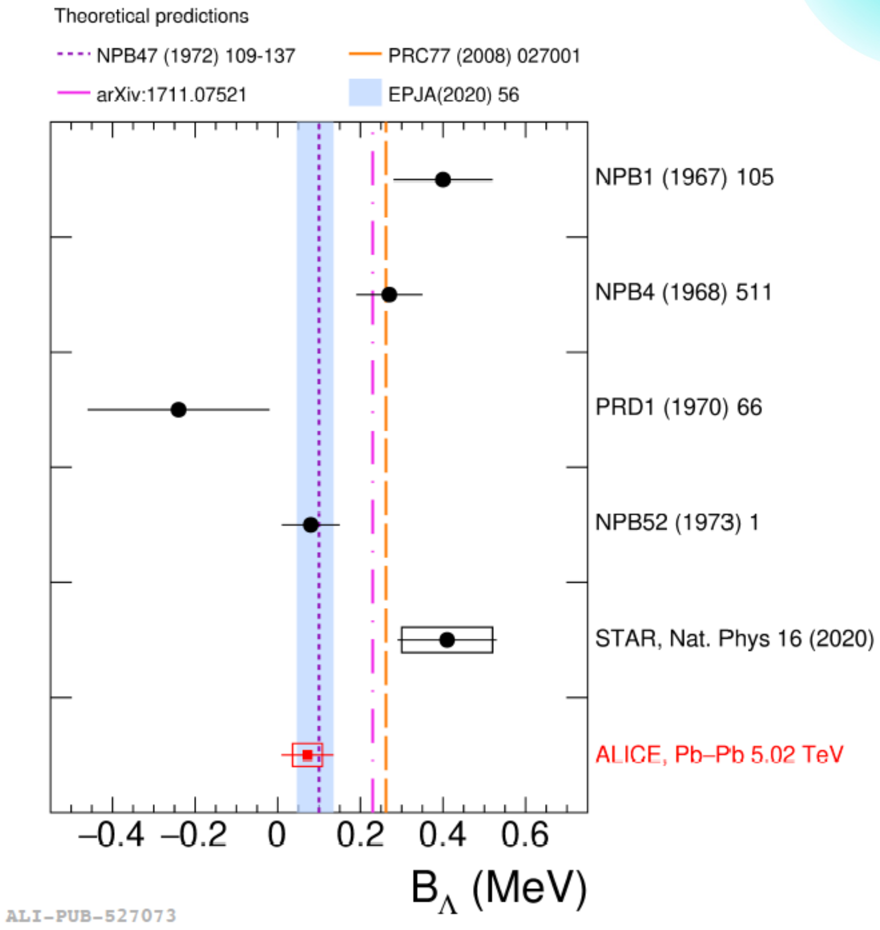

Hypertriton lifetime and Λ binding energy measured with high precision

Weakly bound state

Run 3 and Run 4

ALICE 2 Upgrade

Improve tracking resolution at low p_T

x50 statistics increase for most observables

Run 3+4: 13 nb^{-1} Pb-Pb
50 kHz (Pb-Pb) ~ 1 MHz (pp)
Online reconstruction
all events to storage!

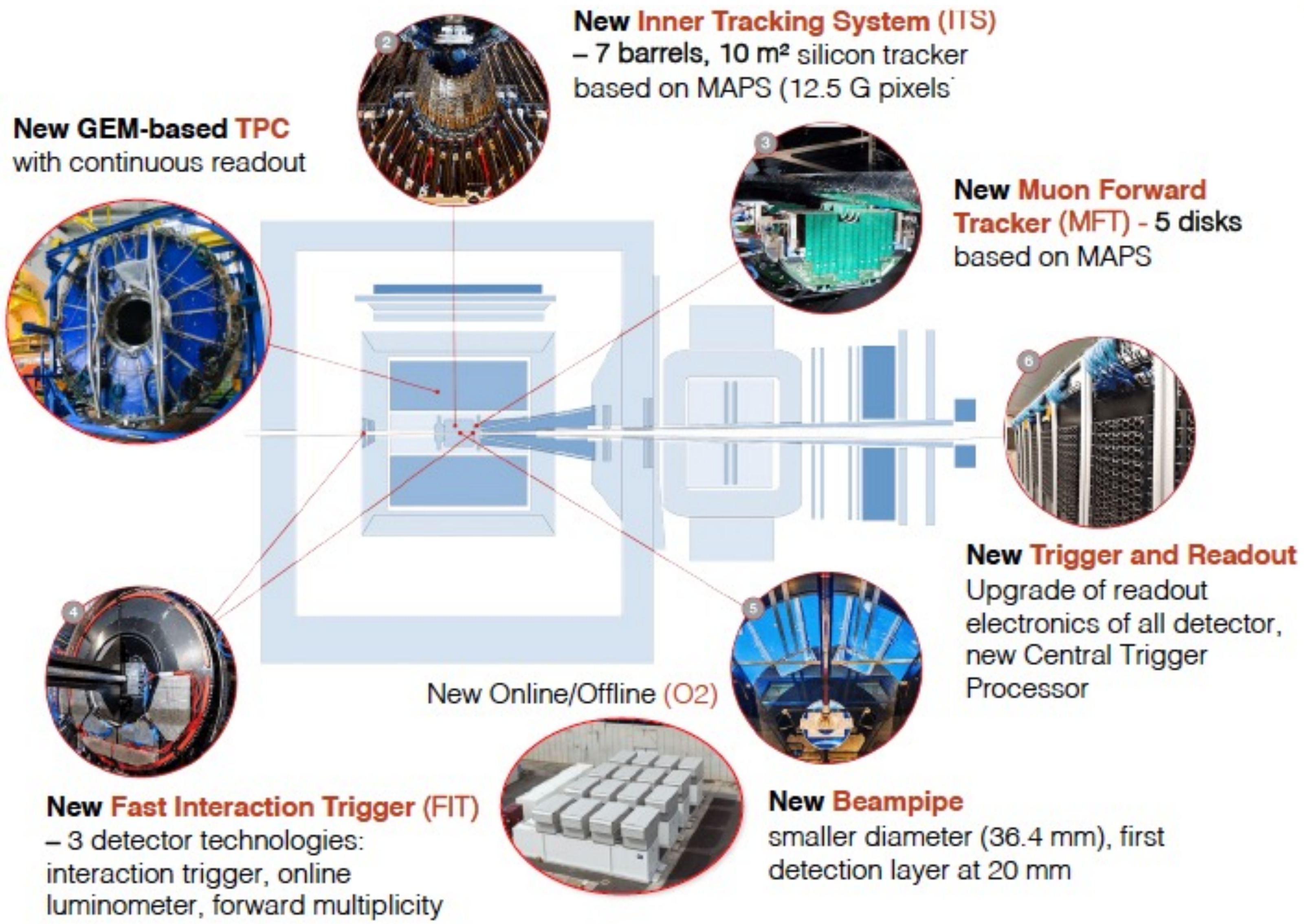

Commissioning with pilot beam and start of Run 3

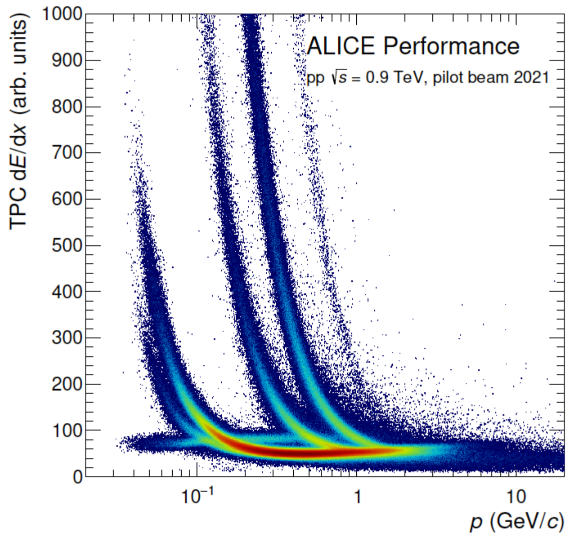

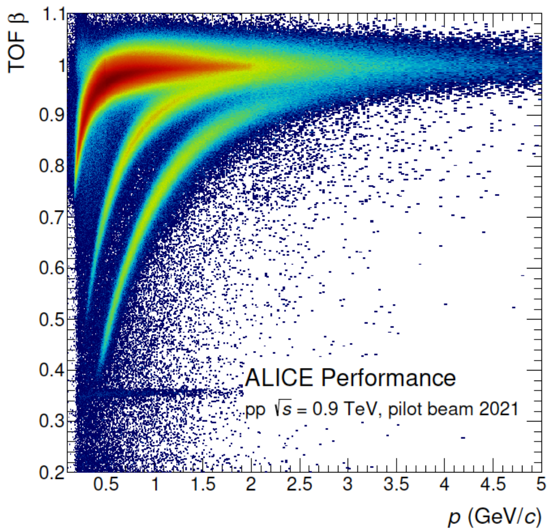

PID capabilities fully available

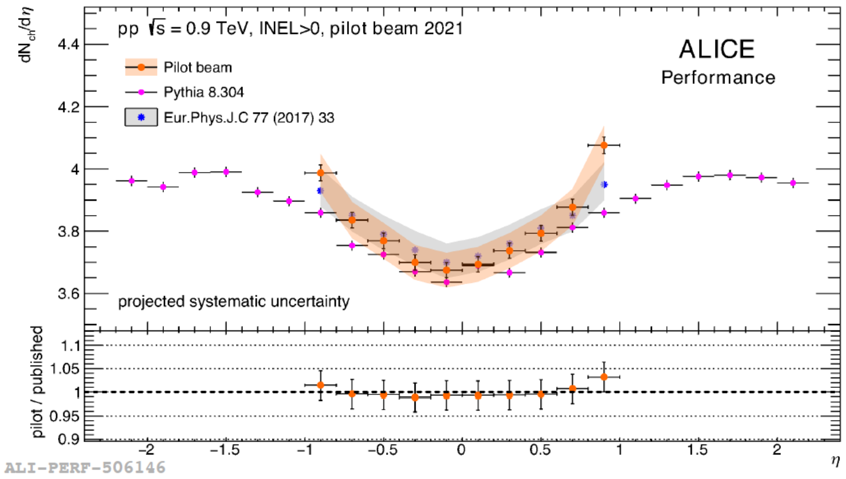

Measured $dN_{ch}/d\eta$ compatible with previous results

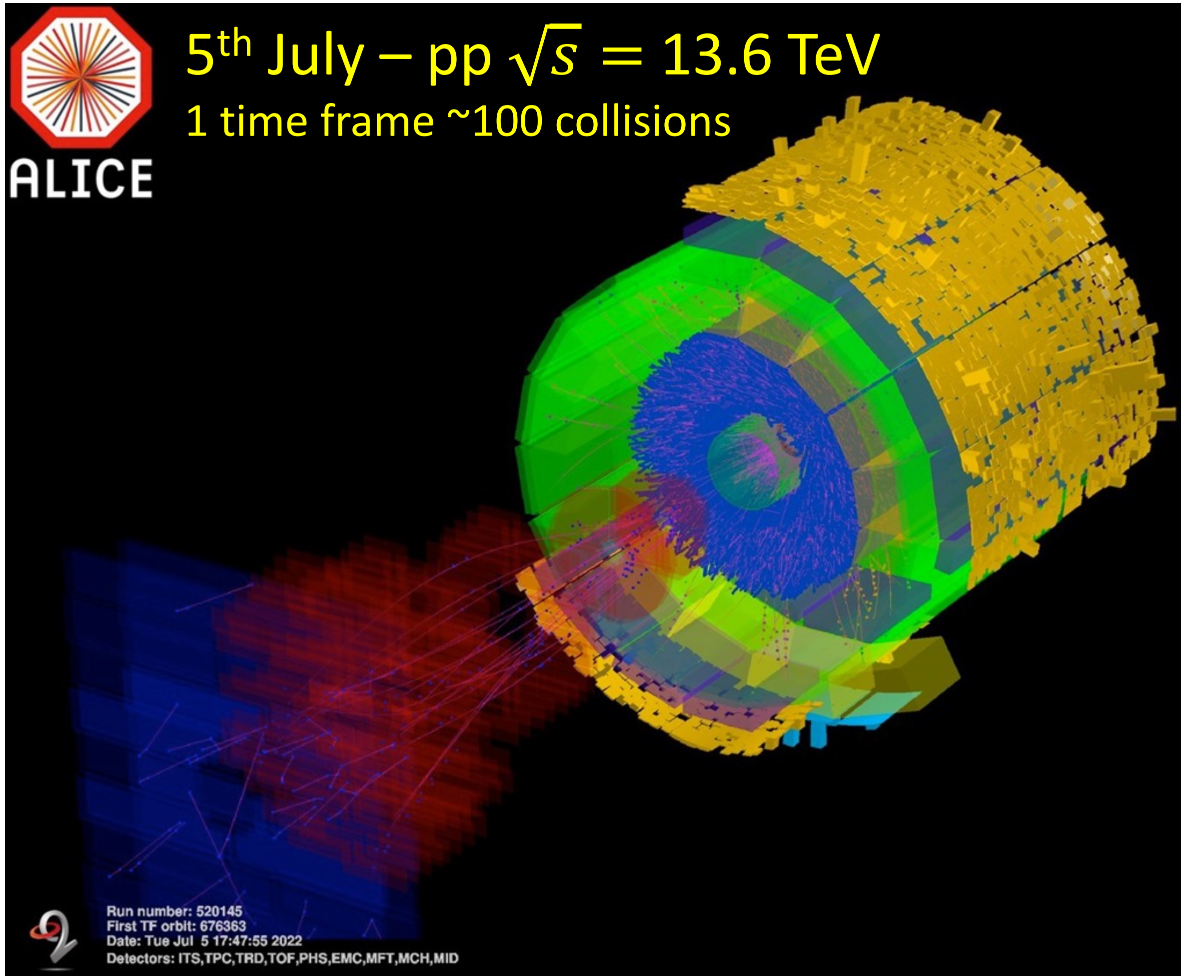

Pb-Pb collisions at the LHC at record energy: 5.36 TeV

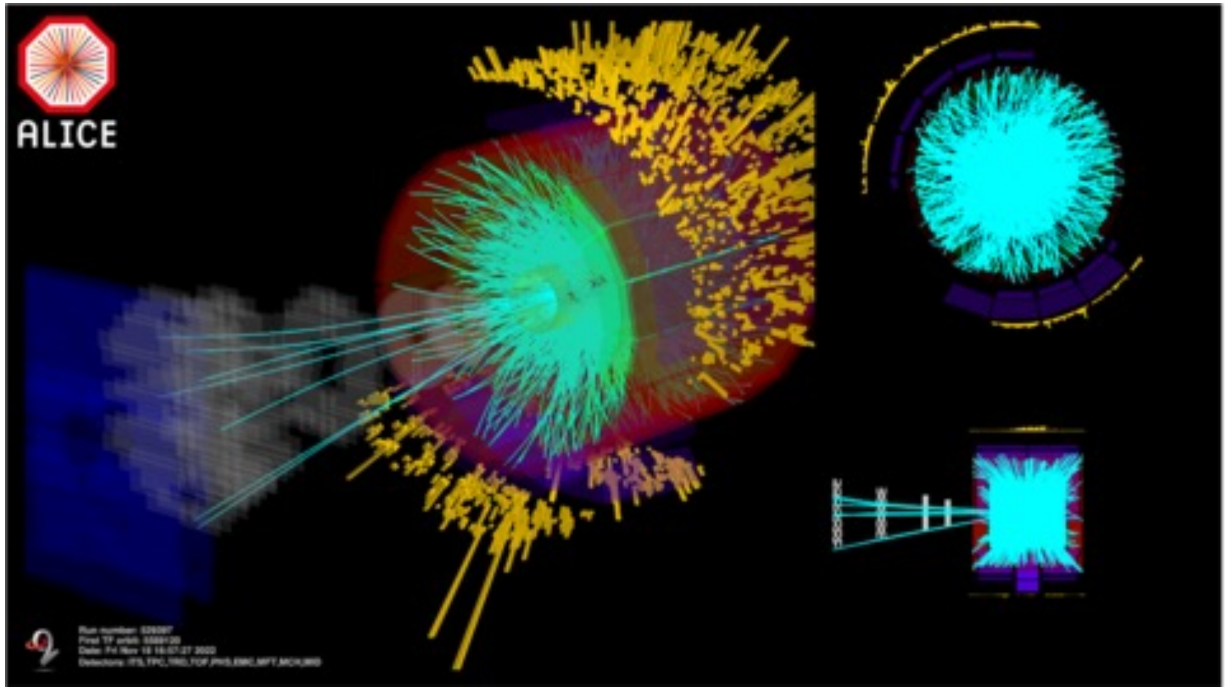

Friday November 18, 5 PM

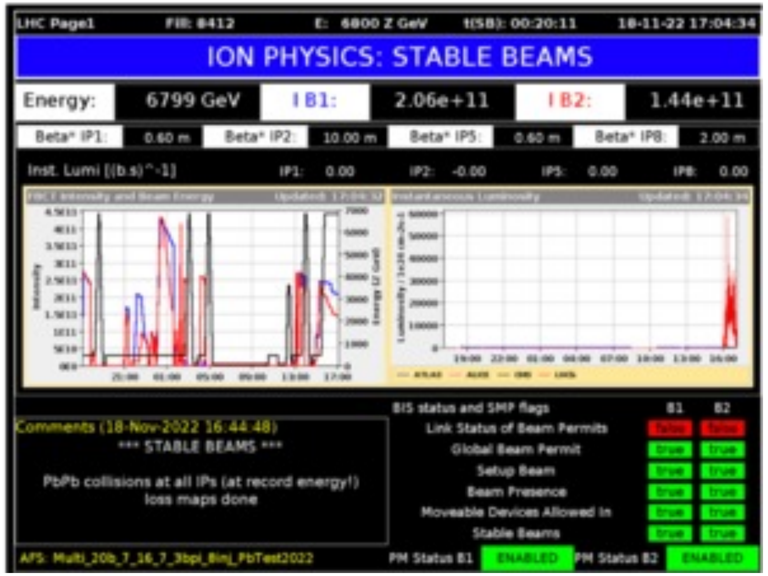

ALICE 2.1: Upgrades in LS3

CERN-LHCC-2019-018

CERN-LHCC-2020-009

ITS3

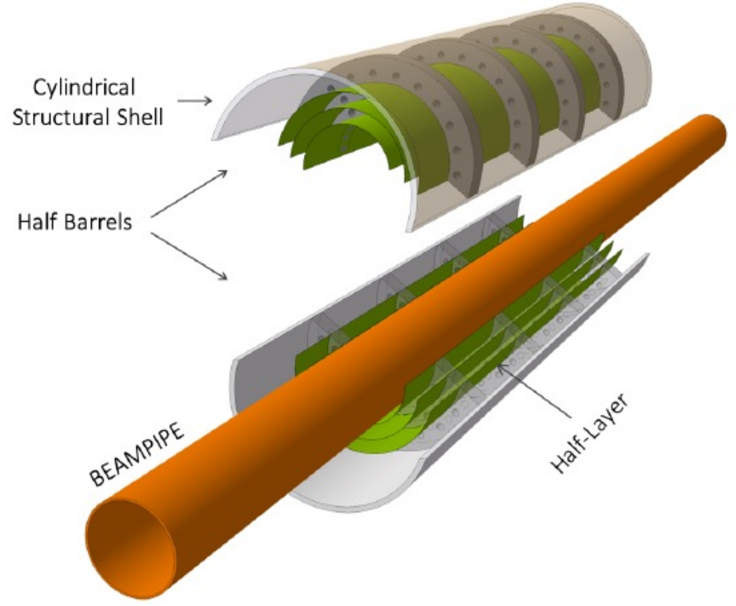

~ 6x less material budget

2x tracking precision and efficiency at low p_T

FoCal

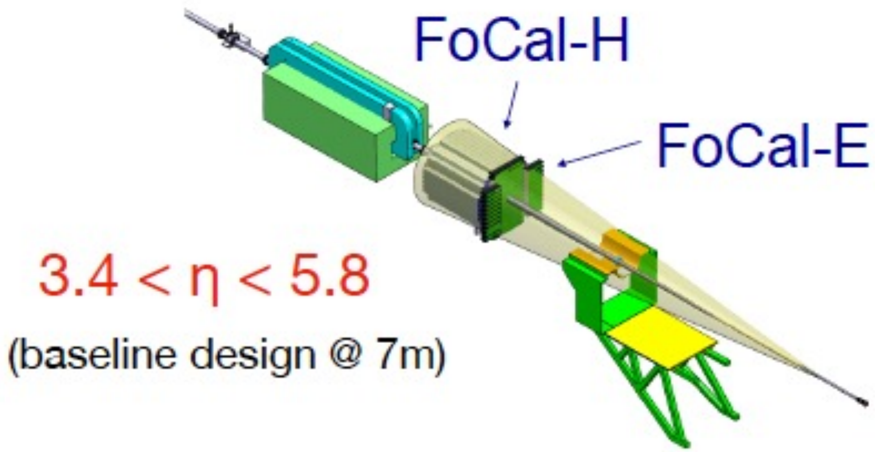

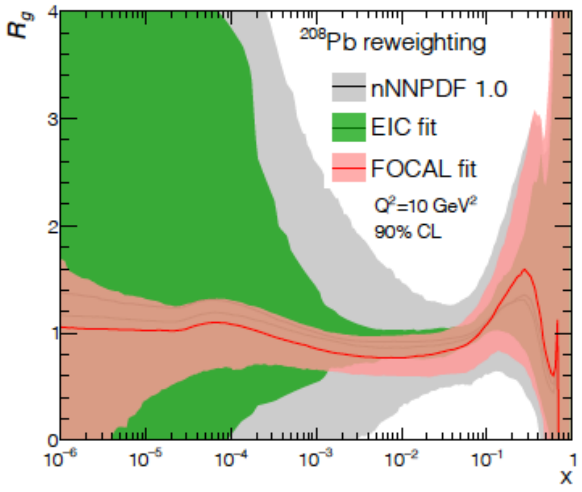

Study saturation/shadowing at low-x with direct photons in pp and p-Pb

Significant constraints to gluon nPDF at $10^{-5} < x < 10^{-2}$

Run 5 and Run 6

ALICE beyond Run 4

2010-2013		2015-2018		2022-2025		2029-2032		2035-2038		
Run1	LS1	Run2	LS2	Run 3	LS3	Run 4	LS4	Run 5	LS5	Run 6
ALICE 1				ALICE 2		ALICE 2.1		ALICE 3		

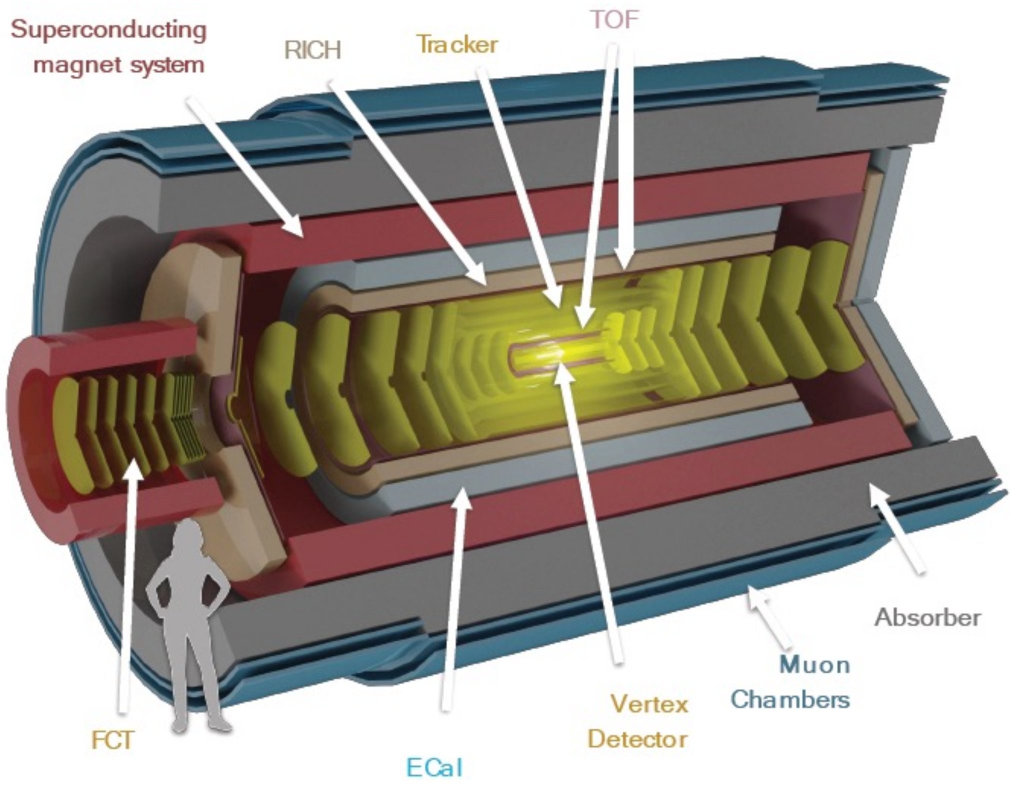

- Heavy-ion Town meeting 2018: "Next-generation heavy-ion experiment" D. Adamova et al. ArXiv: 1902.01211

- Letter of Intent for ALICE 3: CERN-LHCC-2022-009 , arXiv: 2211.02491

Recommendation to proceed with R&D

ALICE 3 detector

CERN-LHCC-2022-009

arXiv 2211.02491

- Compact, ultra-lightweight all-silicon tracker → σ_{p_T}/p_T ~1-2%.
- Vertex detector with unprecedent pointing resolution σ_{DCA} ~ 10 μm (p_T = 0.2 GeV/c)
- Large acceptance $|\eta| < 4$, $p_T > 0.02 GeV/c$
- Particle identification → $\gamma, e^{\pm}, \mu^{\pm}, K^{\pm}, \pi^{\pm}$
- Fast readout and online processing

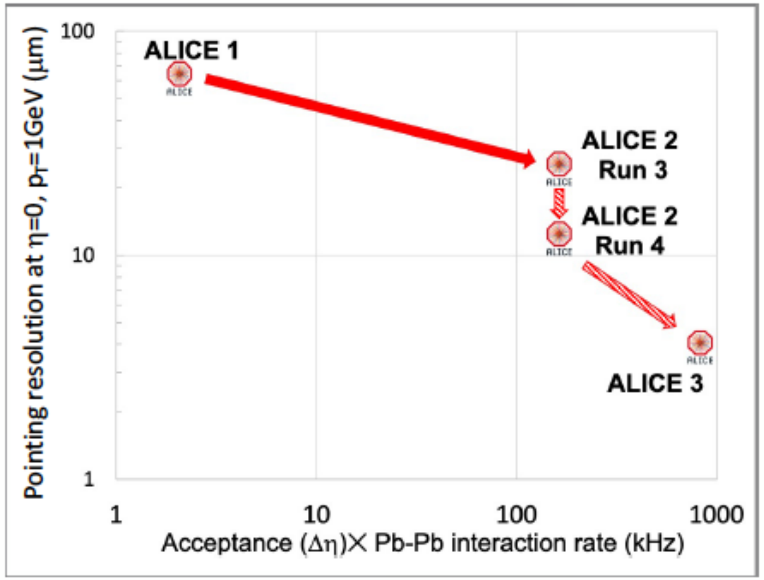

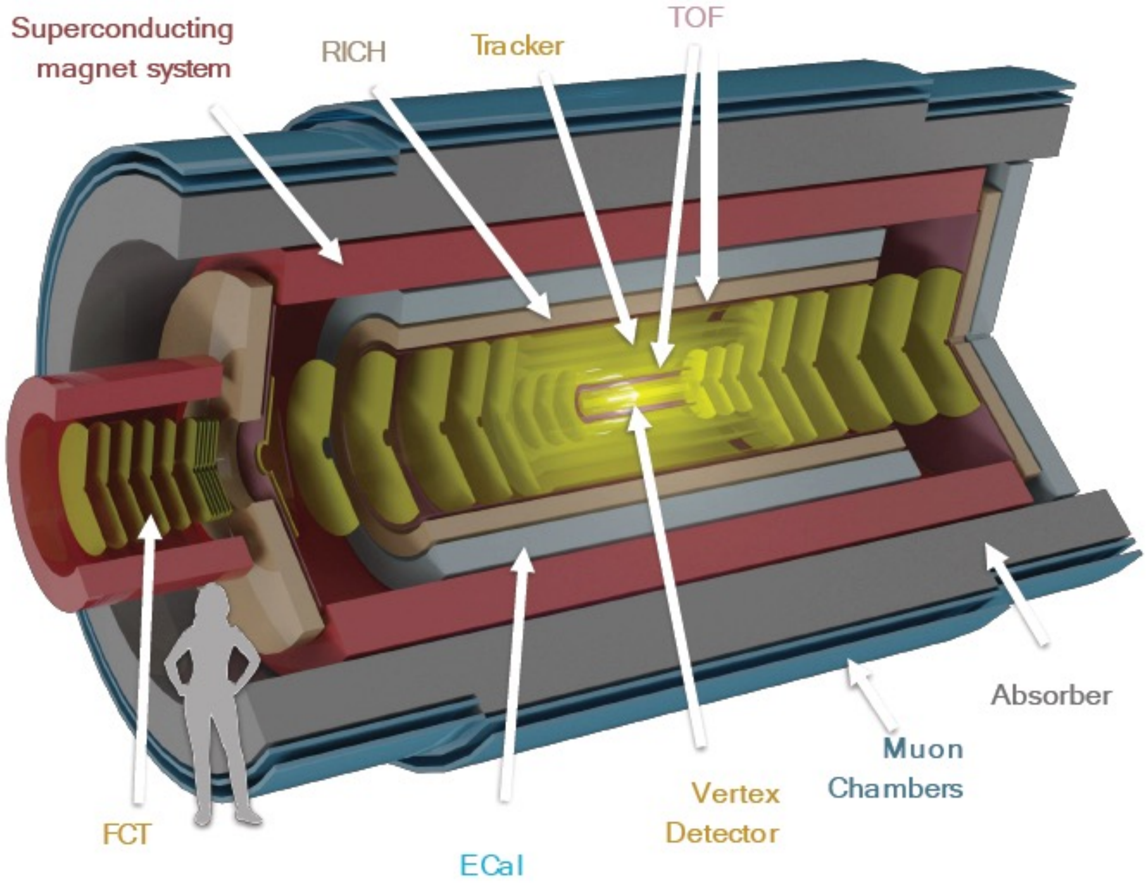

Physics reach improves dramatically!

ALICE 3 : Physics topics

- Precision differential measurements of dileptons
  - Evolution of the quark-gluon plasma
  - Mechanisms of chiral symmetry restoration in the QGP

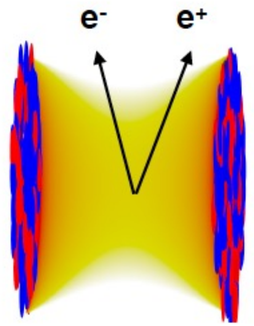

- Systematic measurements of (multi-) heavy-flavoured hadrons down to low p_T
  - Transport properties in the QGP down to thermal scale
  - Mechanisms of hadronization from the QGP

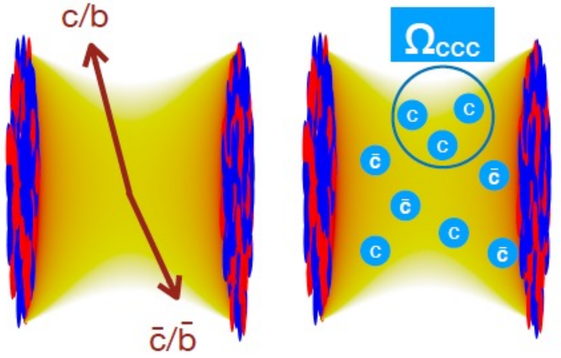

- Hadron interaction and fluctuation measurements
  - Existence and nature of heavy-quark exotic bound states and interaction potential
  - Search for super-nuclei (light nuclei with c)
  - Search for critical behaviour in event-by-event fluctuations of conserved charges

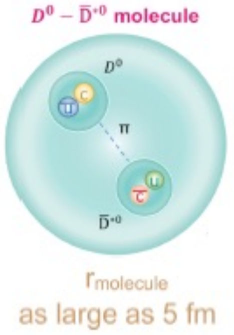

Electromagnetic radiation

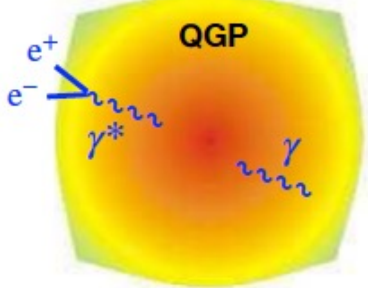

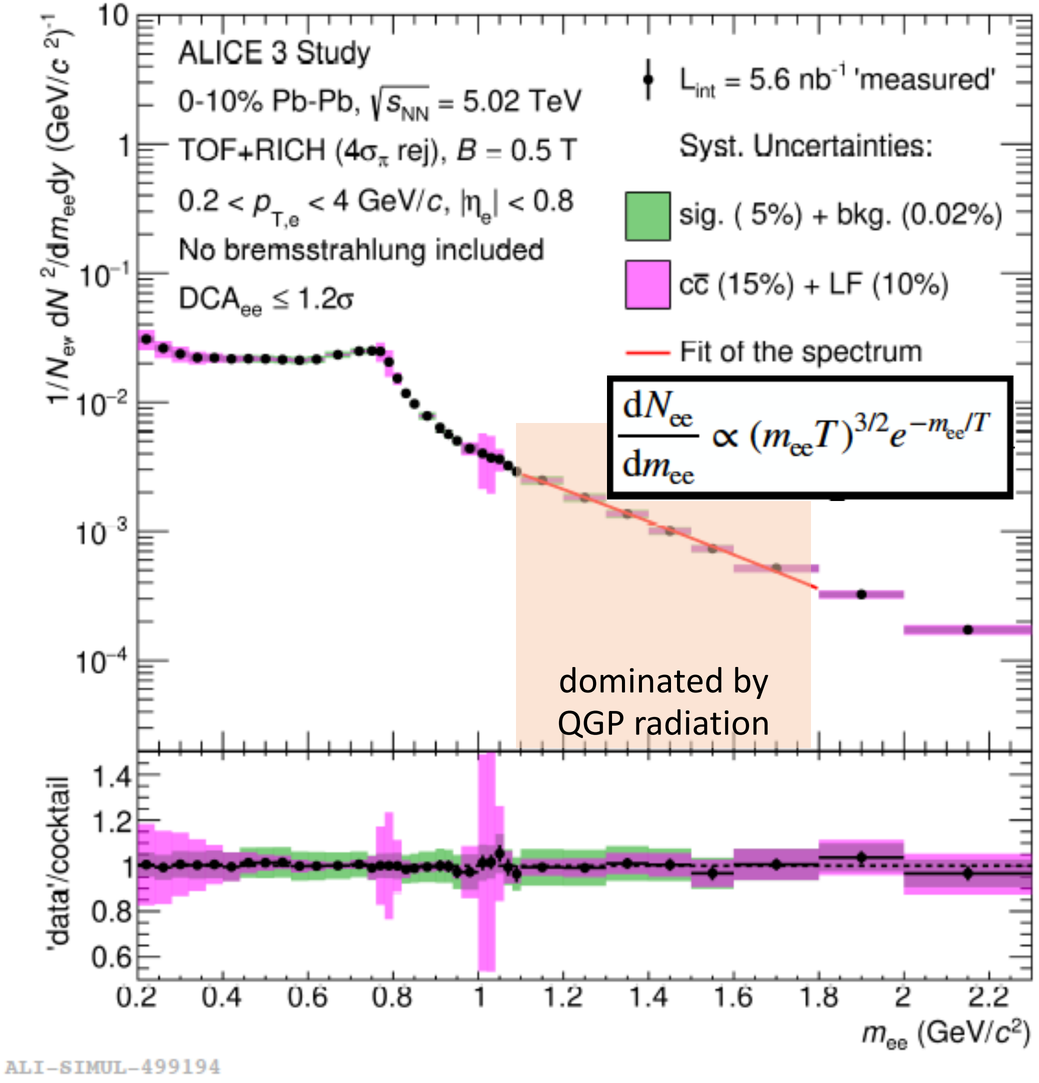

- Average T of the QGP with e^+e^- using thermal dielectron m_{ee} spectrum for $m_{ee} > 1.1$ GeV/c^2 (QGP radiation dominated)

- Requirements:
  - Good e PID down to low p_T
  - Small detector material budget (γ background)
  - Excellent pointing resolution (heavy-flavour decay electrons)

Possible with ALICE 3 due to excellent pointing resolution and small material budget

R. Rapp, Adv. High Energy Phys. 2013 (2013) 148253
P.M Hohler and R. Rapp, Phys. Lett. B 731 (2014) 103
ALICE CERN-LHCC-2022-009

Chiral symmetry restoration

Study chiral symmetry restoration (CSR) mechanisms using thermal dielectron spectrum $m_{ee} < 1.2$ GeV

ALICE 3 access to CSR mechanisms like ρ-a_1 mixing

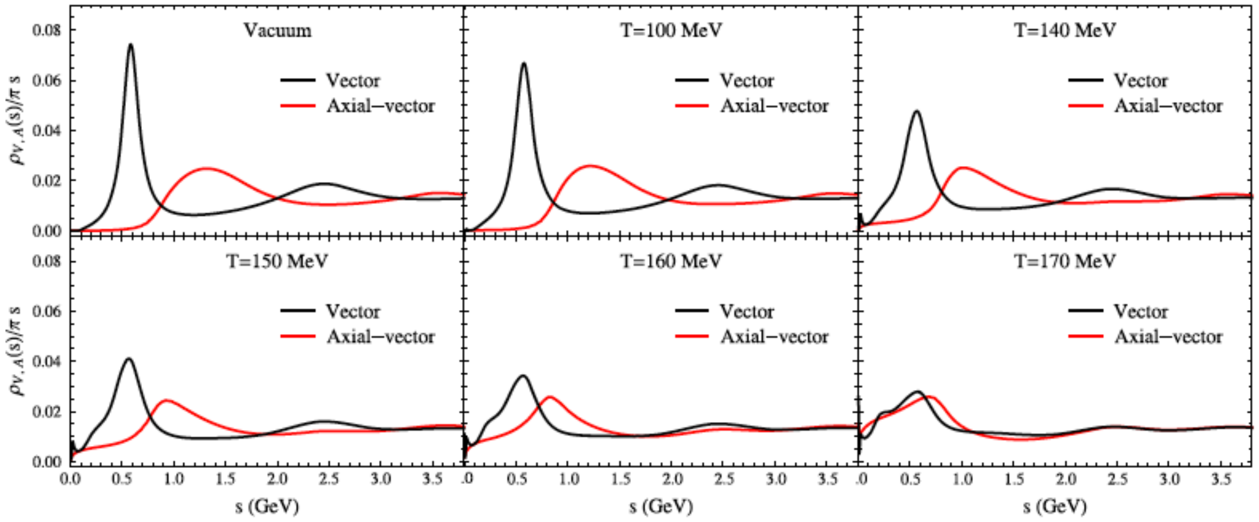

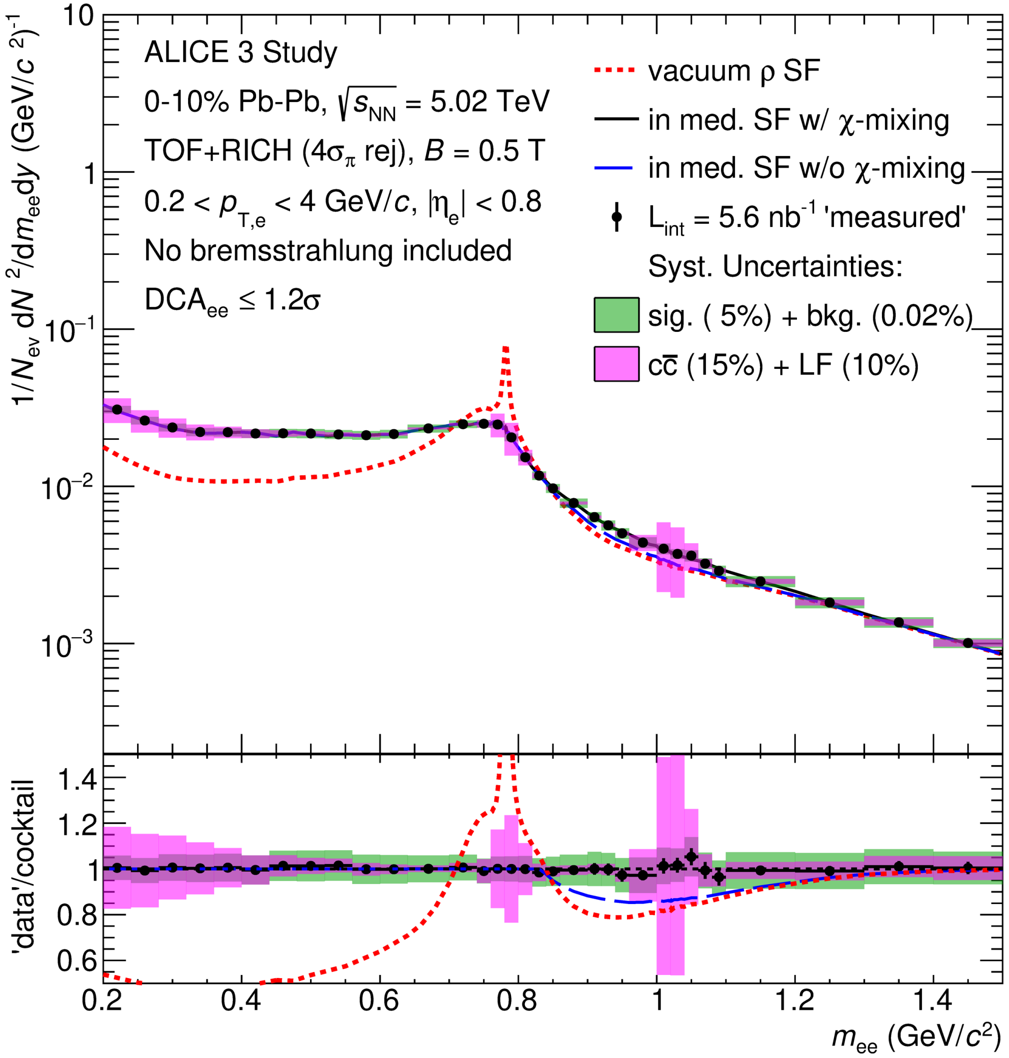

Heavy flavour transport

Extension to beauty

Extension to multi-charm

Λ_c v_2 performance

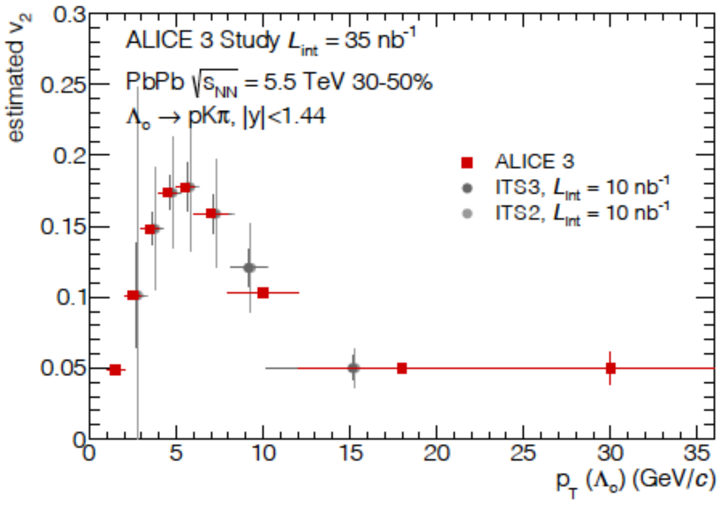

Λ_b v_2 performance

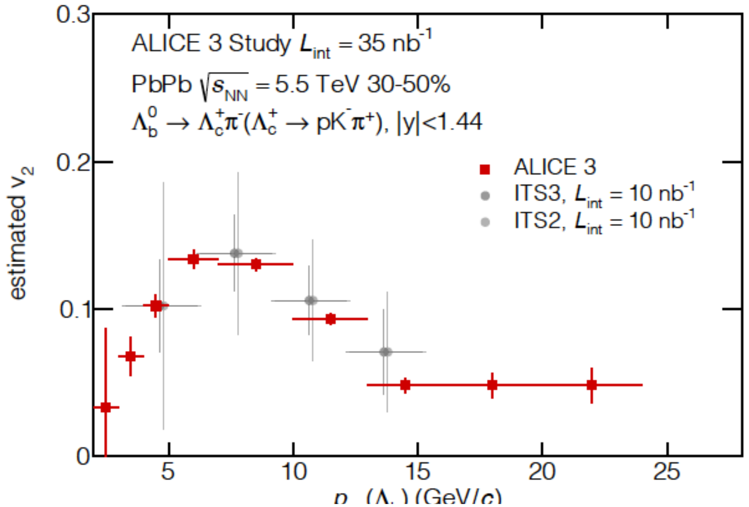

Ξ_{cc}^{++} v_2 performance

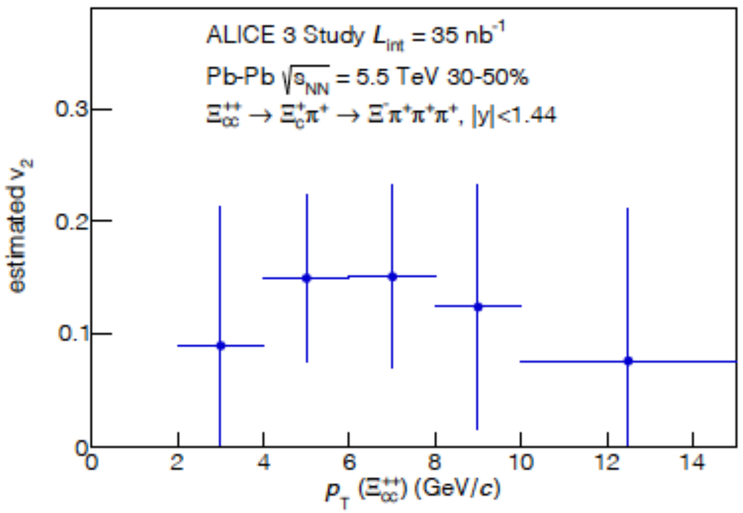

Non-central collision

$$\frac{dN}{d\phi} \propto 1 + 2v_2\cos 2(\varphi - \psi)$$

Interactions with the plasma generate azimuthal anisotropy v2:

Relaxation time

τ_Q = (m_Q /T) D_S

Understanding of transport properties of the QGP requires heavy-flavor probes

Expect beauty thermalization slower than cham→ smaller v_2

Need ALICE 3 performance (pointing resolution , acceptance) for precision measurement of e.g. Λ_c, Λ_b, and multi-charm v_2

Mechanisms of hadron formation

Multi-charm baryons: test how independently produced quarks form hadrons

- Contribution from single parton scattering is very small
- Very large enhancement predicted by Statistical hadronization model in Pb-Pb collisions
- Progress relies on the reconstruction of complex decay chains

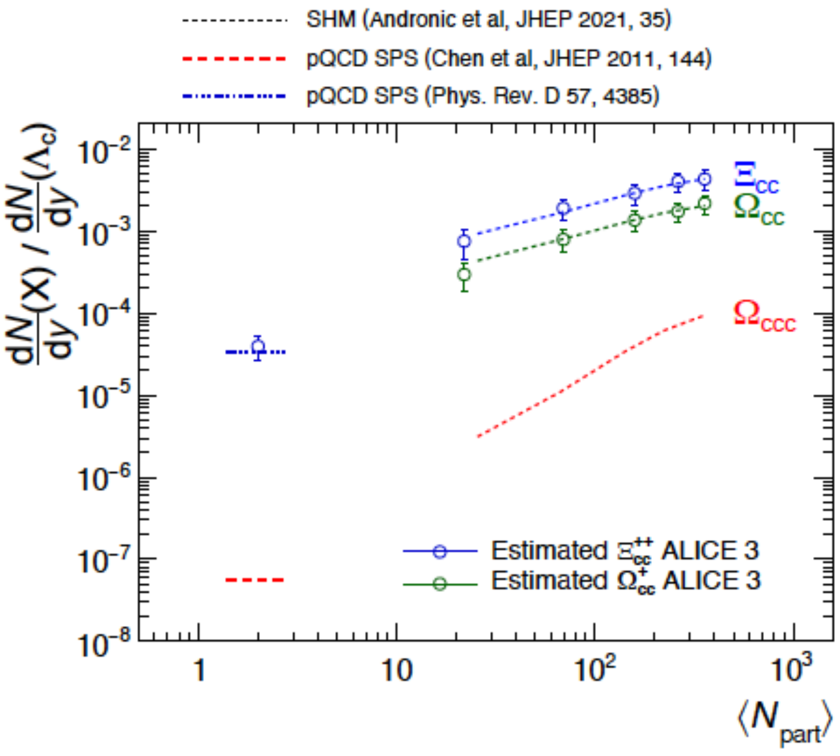

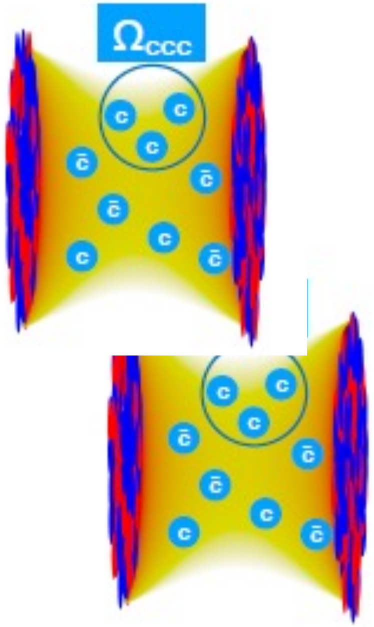

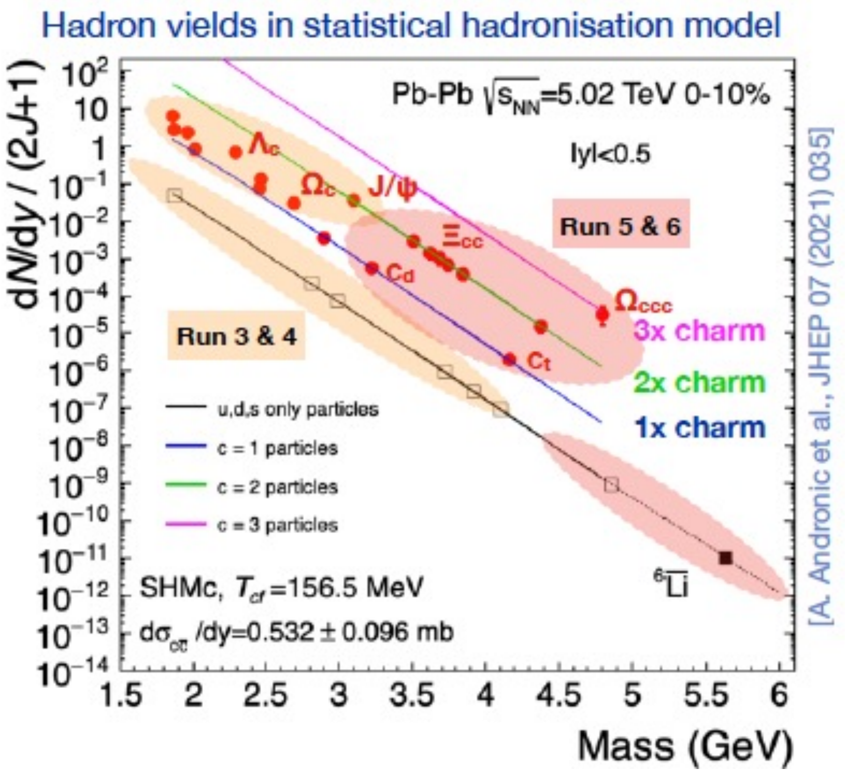

Large enhancements: unique sensitivity to
thermalisation and hadronisation dynamics

Multi-charm baryon reconstruction in ALICE 3

$$\Xi_{cc}^{++} \rightarrow \Xi_c^{+} + \pi^{+} \rightarrow \Xi^{-} + 3\,\pi^{+}$$

First ALICE 3 tracking layer at 5 mm

- Track Ξ^- before it decays, Ξ^- pointing resolution

Unique access with ALICE 3 in Pb-Pb collisions

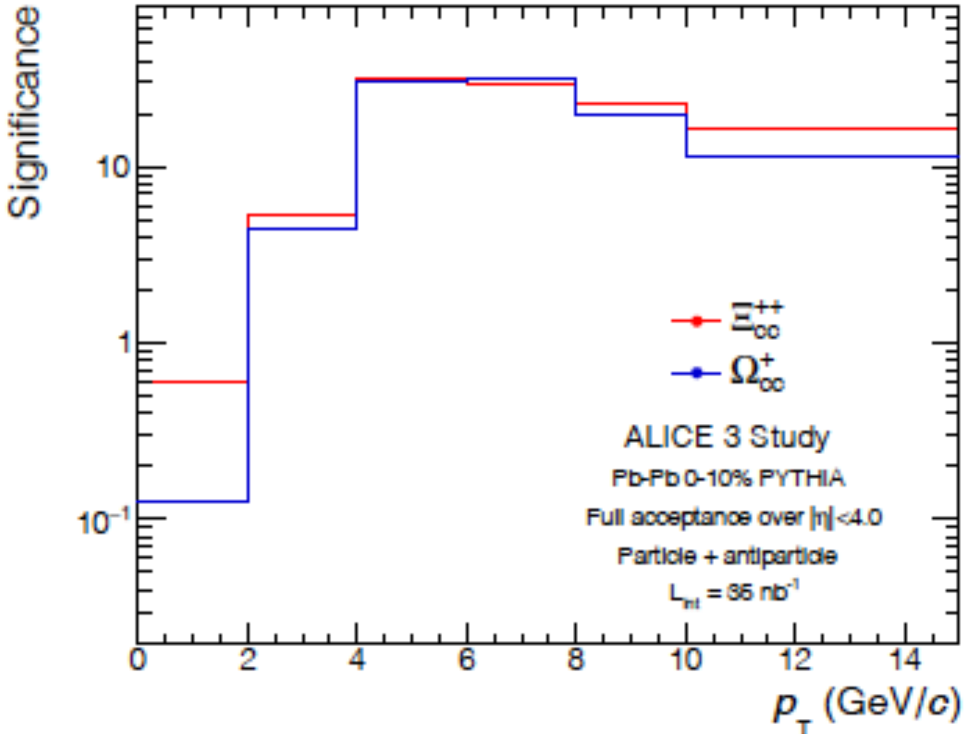

Reconstruction of Ξ_{cc}^{++} decay in the ALICE 3 tracker

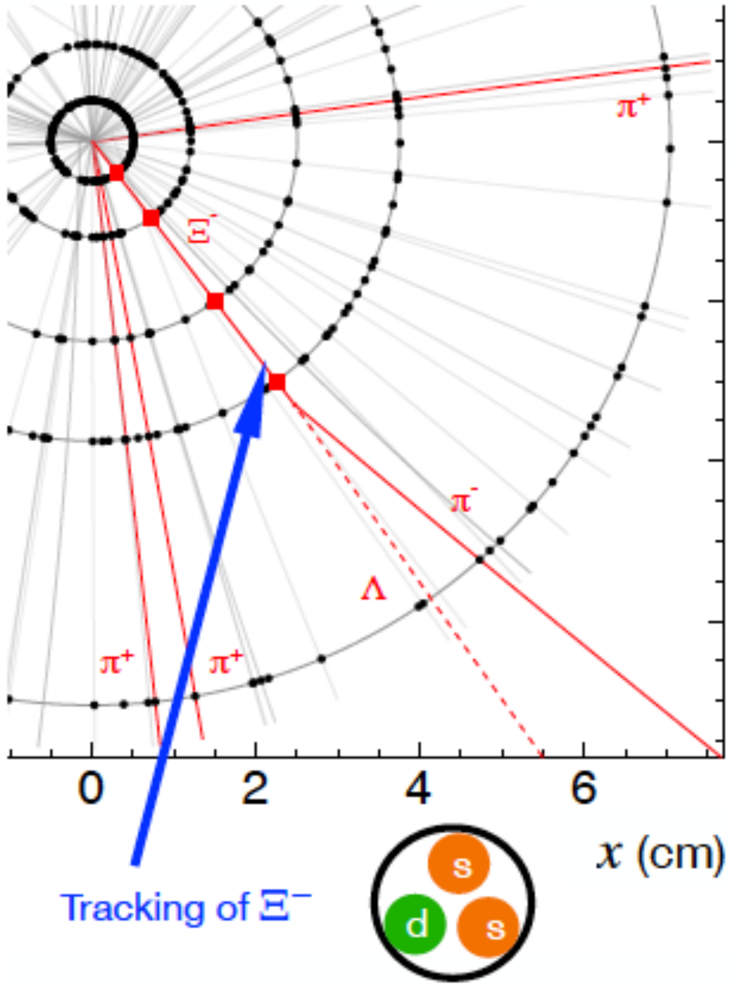

Conclusions

- Immense amount of results obtained in Run 1 and Run 2
  - →detailed insights into QGP properties
- Rich QCD research programme
  - → pQCD, hadron interactions, formation of hadrons and nuclei
- Run 3 started
  - →ALICE 2 detector taking data
- Preparations for Run 4
- ALICE 3 LOI endorsed by LHCC for Run 5 + 6
  - →Moving forward to the R&D phase

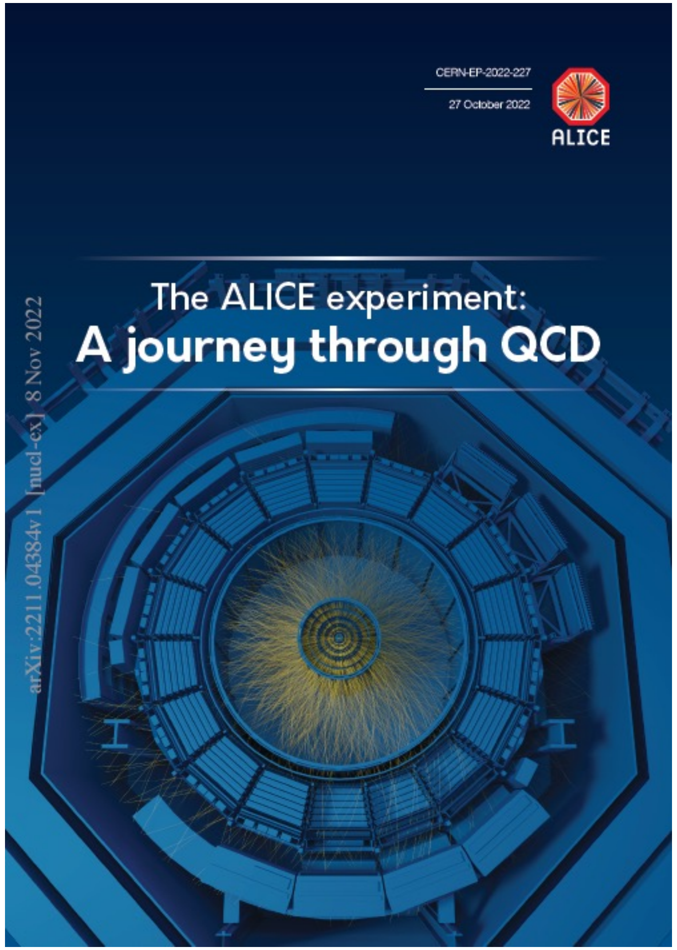

Extra slides

π^0 and η mesons

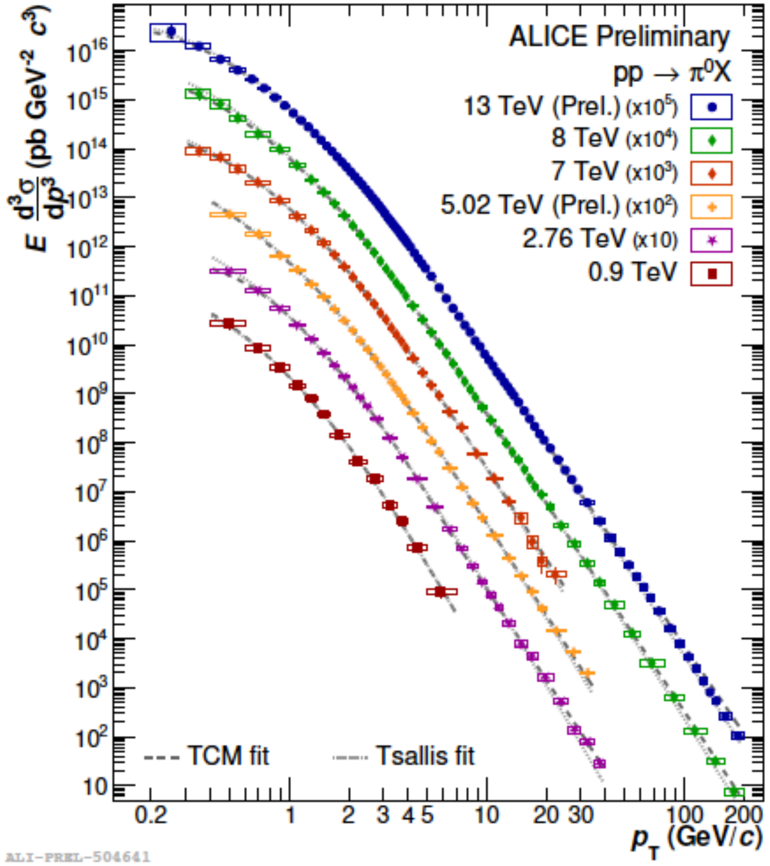

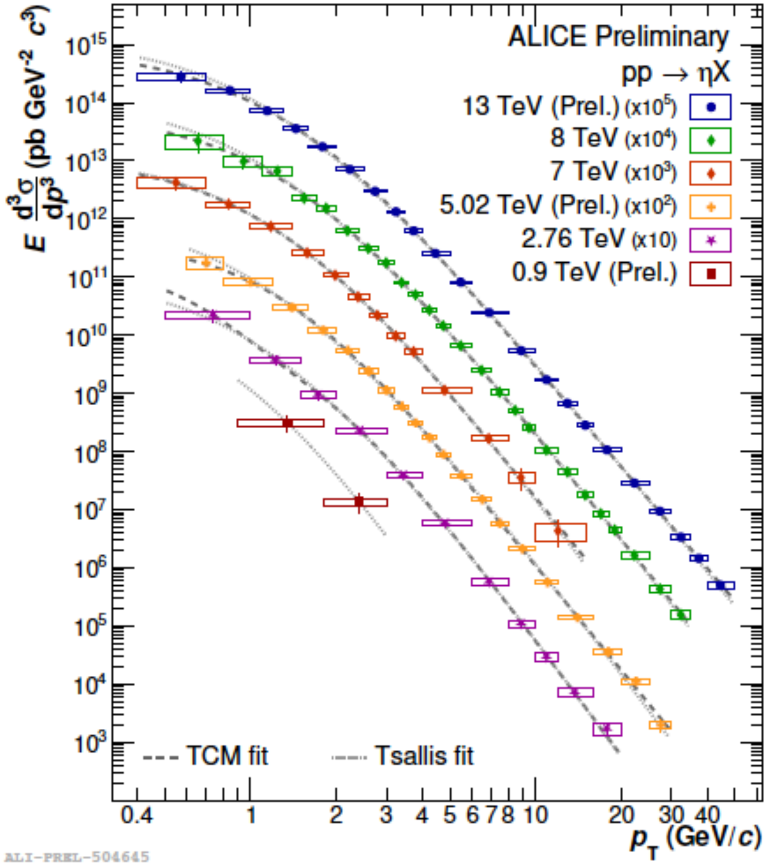

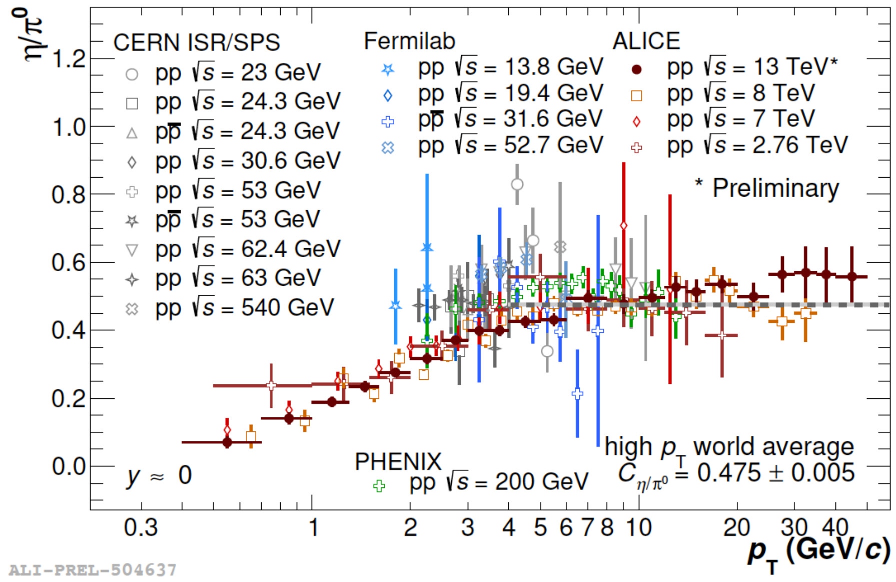

Universal behavior for all collision energies →

World data at high p_T: $\eta/\pi^0 = 0.475 \pm 0.005$

π^0: $0.2 \leq p_T < 200$GeV/c

η: $0.4 \leq p_T < 50$GeV/c

π^0 and η mesons

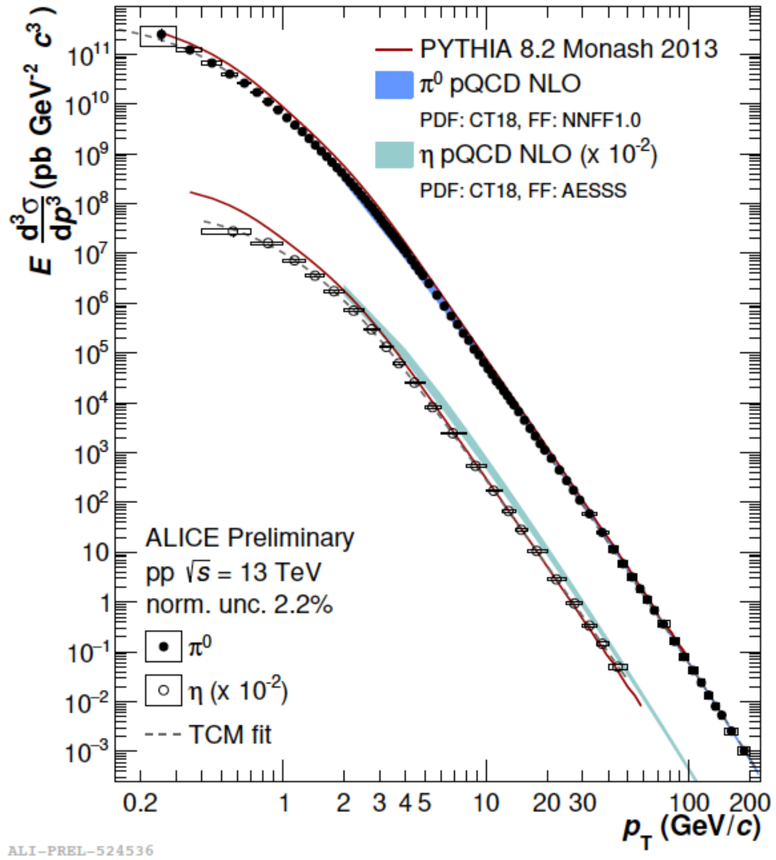

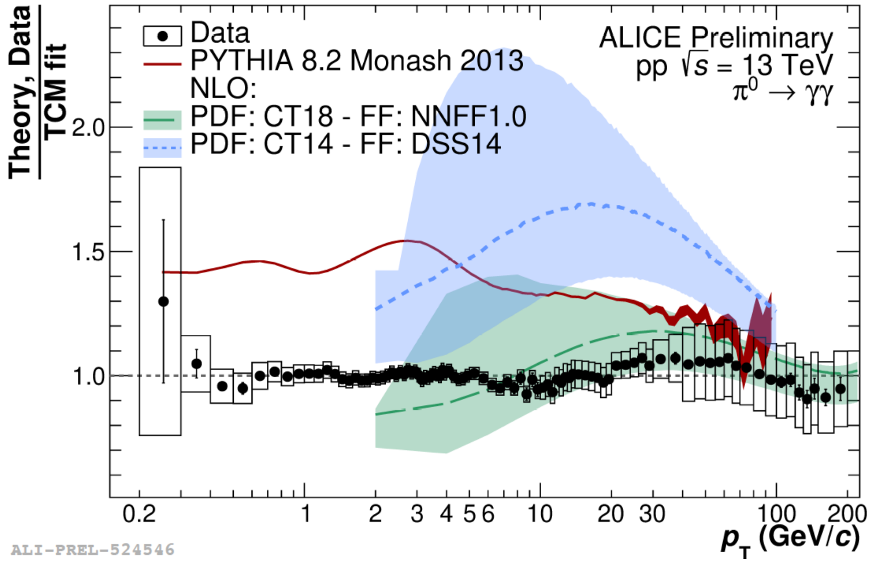

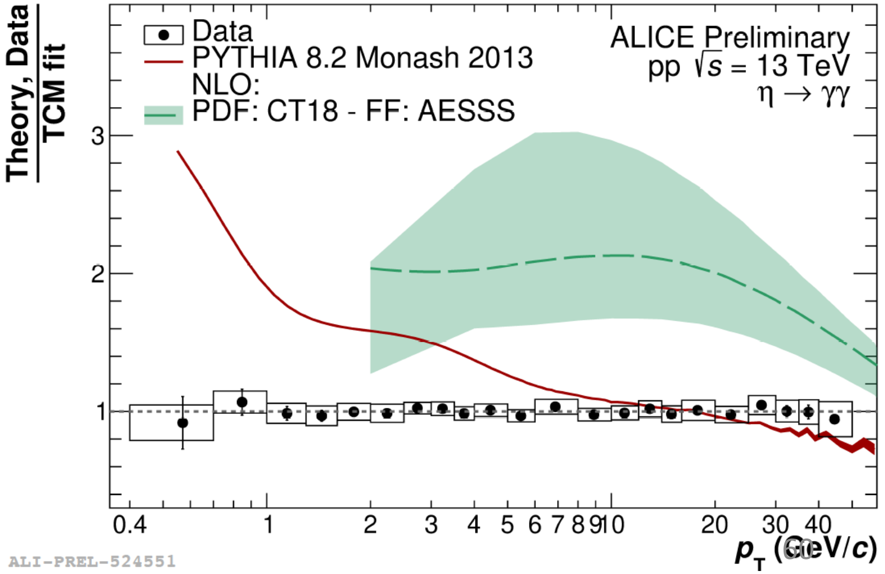

- NLO using NNFF1.0 FF describes the π^0 spectrum
- PYTHIA overshoots data and does not describe shape of spectra
- New FF are needed for the η meson

π^0 and η mesons

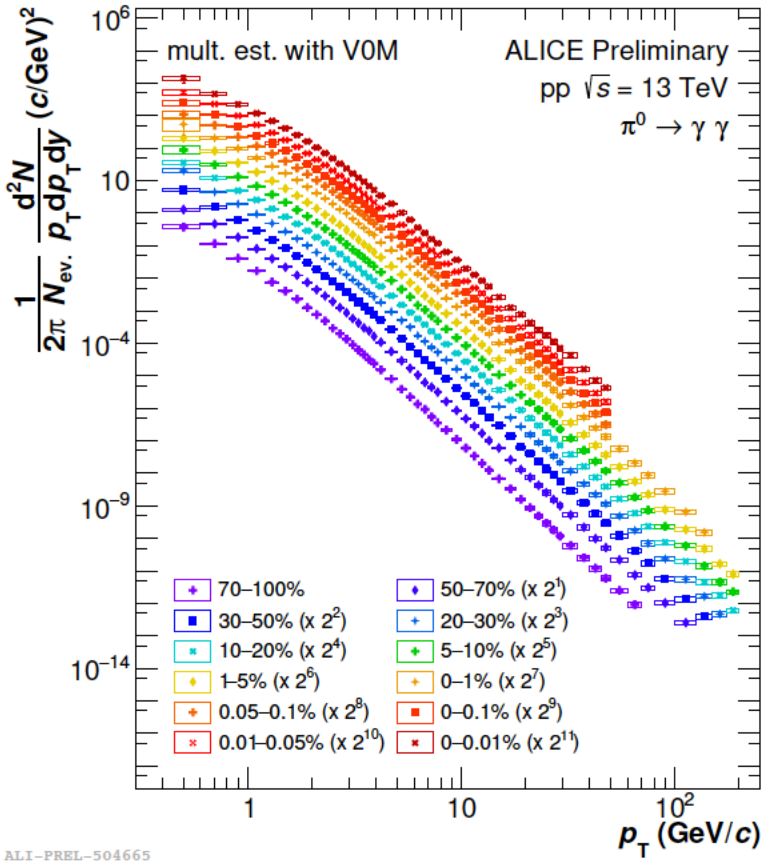

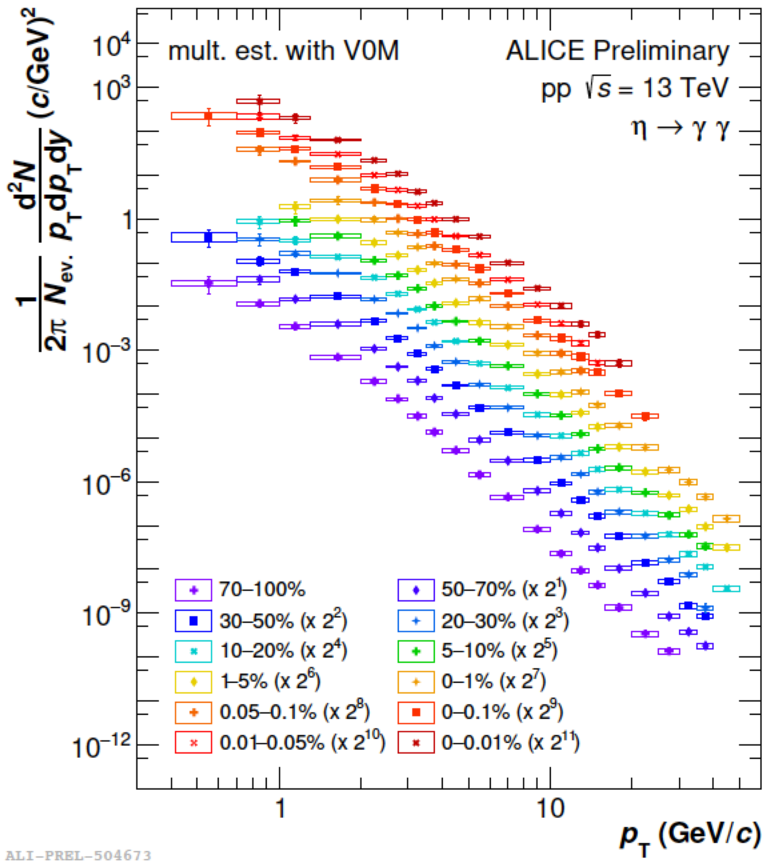

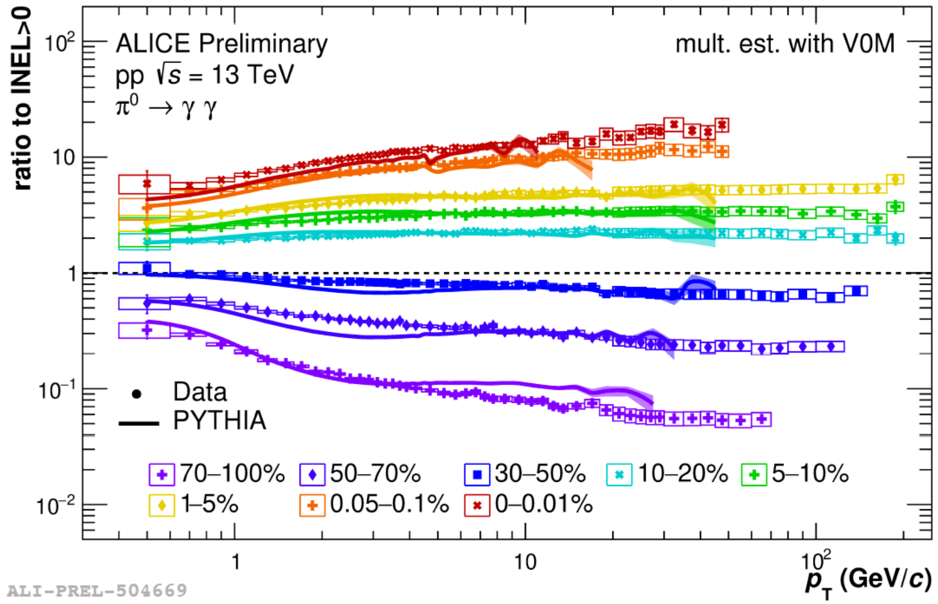

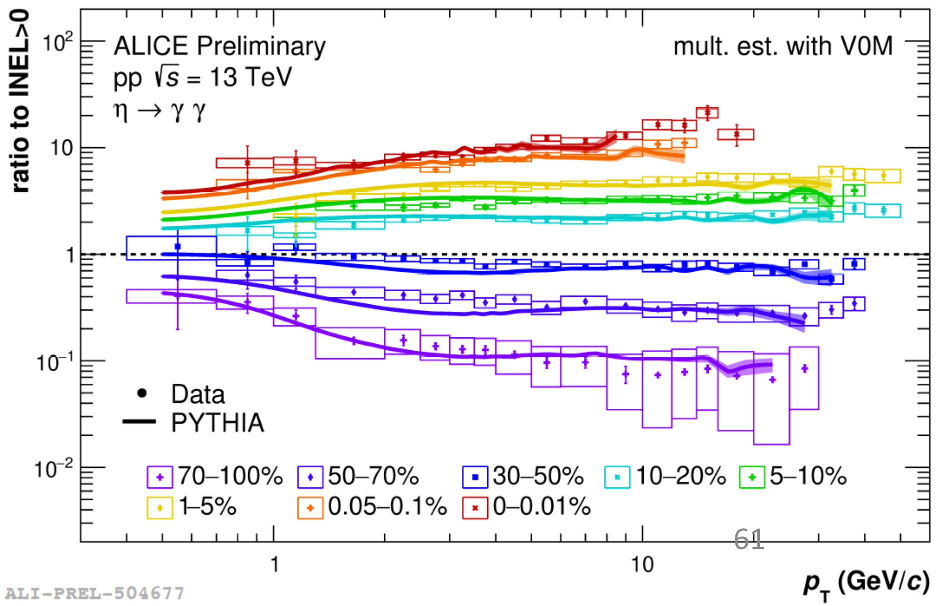

Hardening of p_T spectra with rising multiplicity

- General ordering and magnitude described by PYTHIA
- Slightly different p_T dependence

Mean p_T

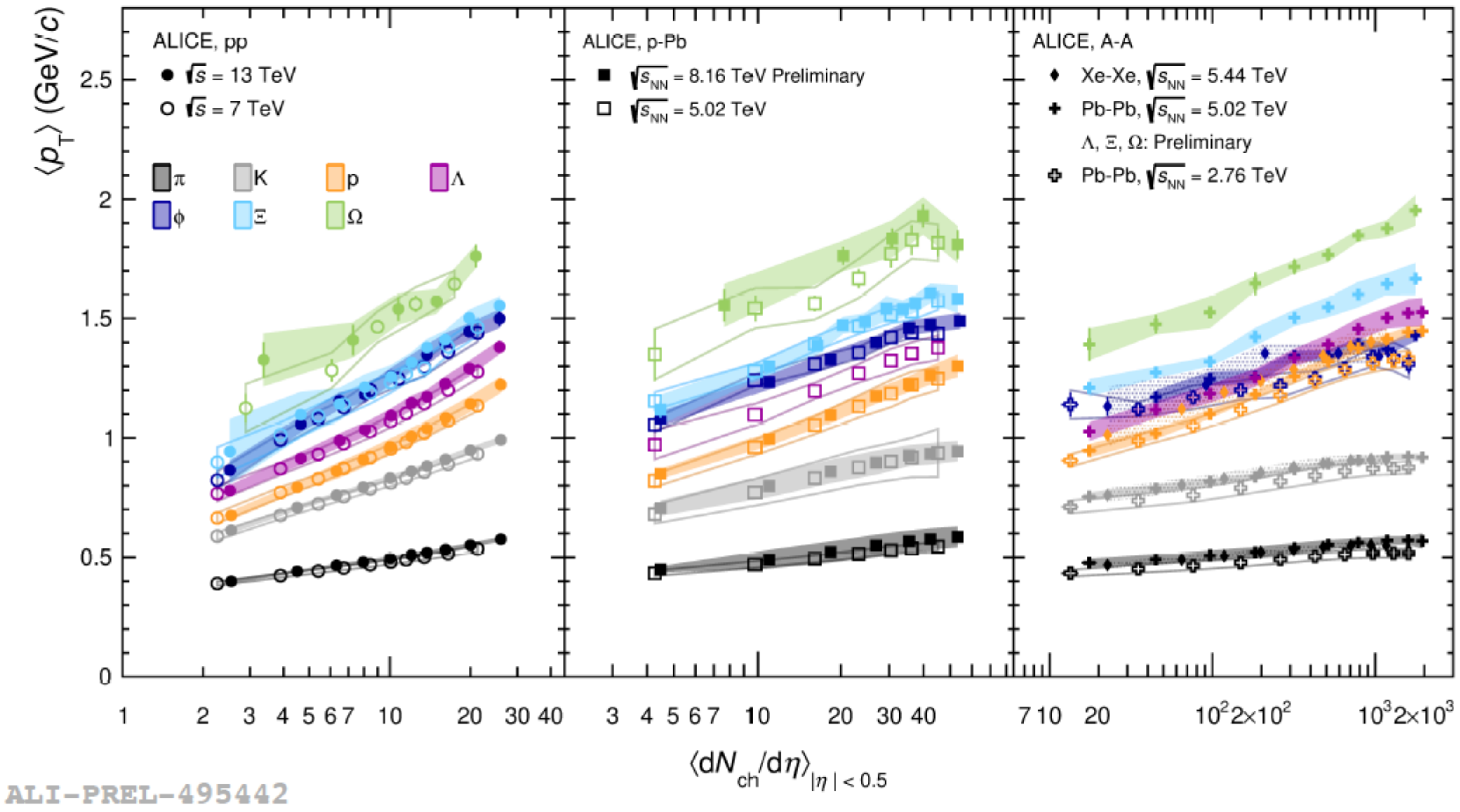

In central heavy-ion collisions particles with similar masses have similar $<p_T>$ (hydrodynamic expansion)

→ ϕ meson ($m_\phi \approx m_p$) mass ordering breaks down for peripheral collisions and in pp and p-Pb

Constraining initial condition and QGP medium properties

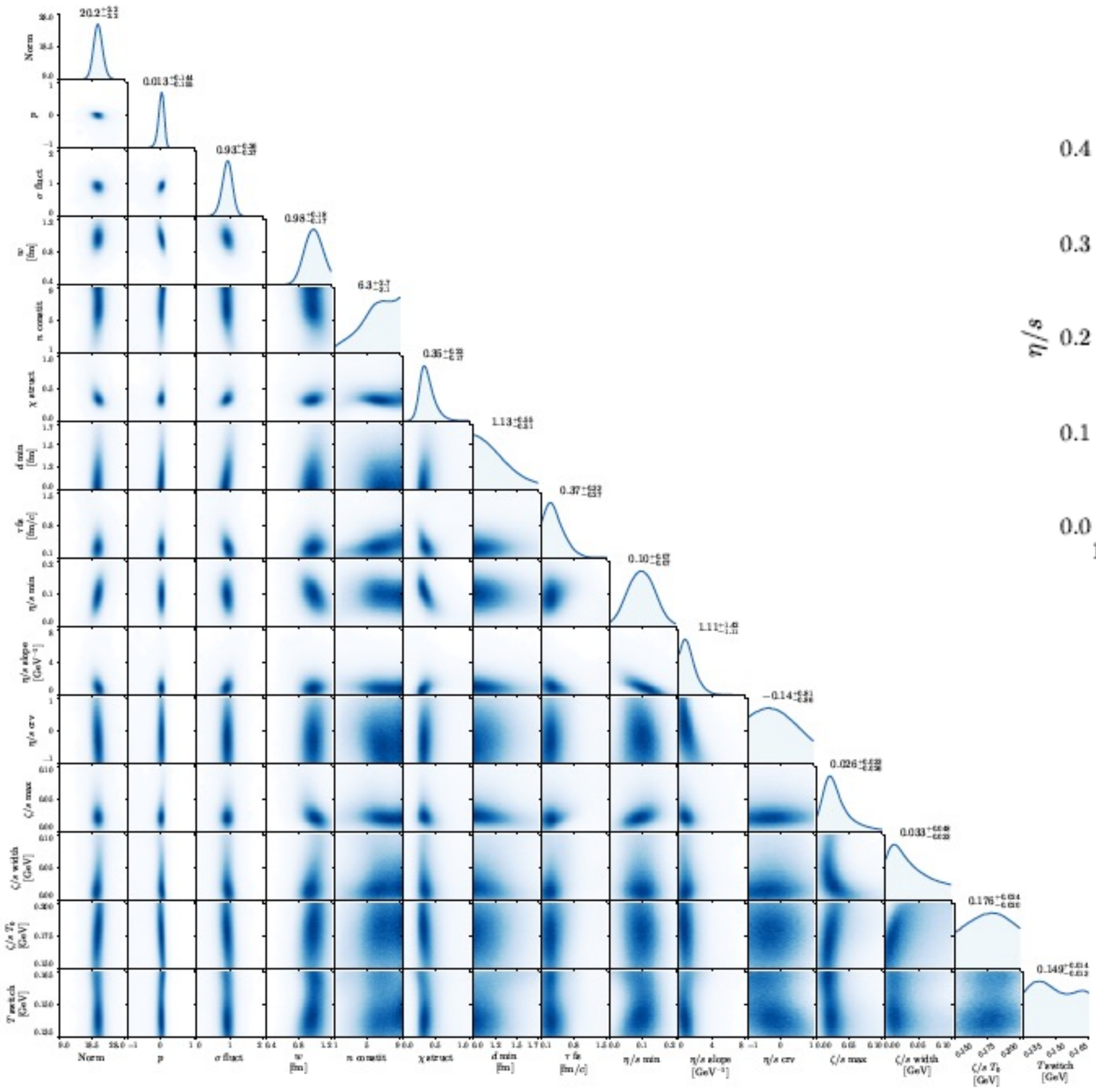

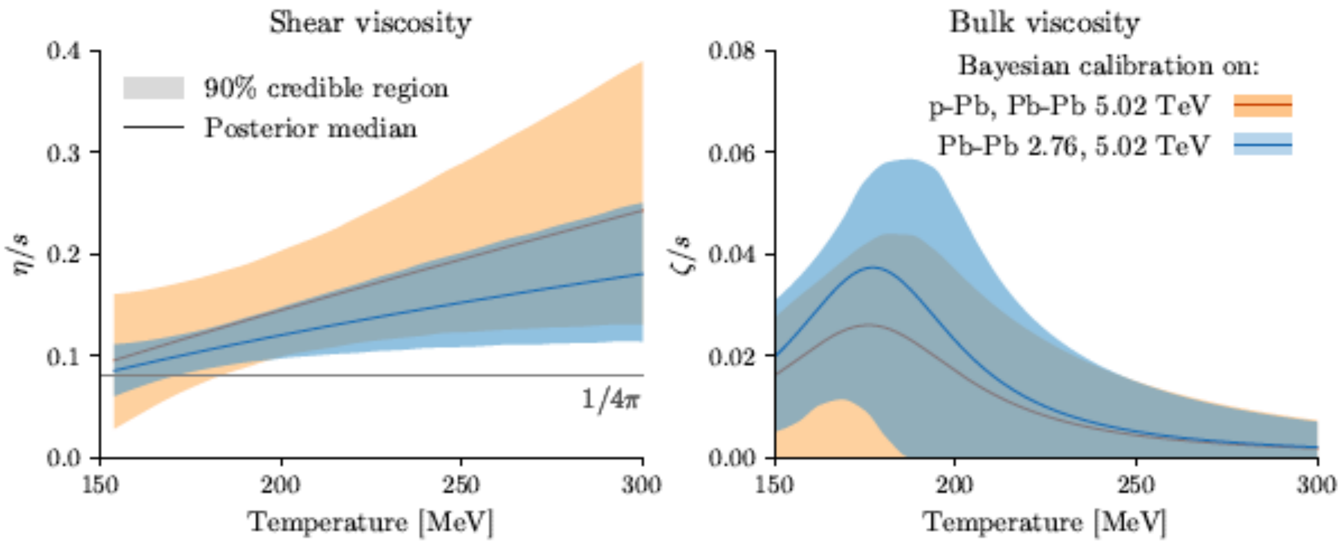

Phys. Rev. C 101, 024911 (2020)

Strong interaction between hadrons

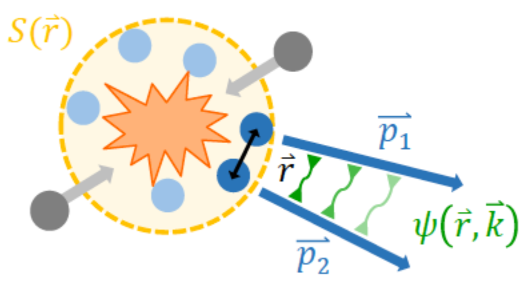

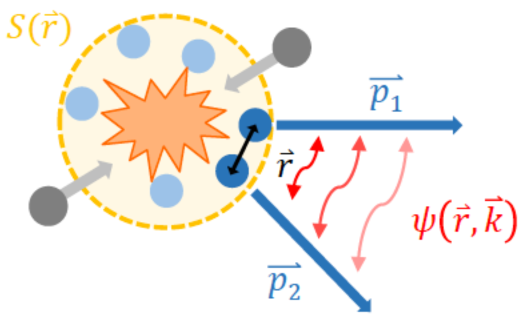

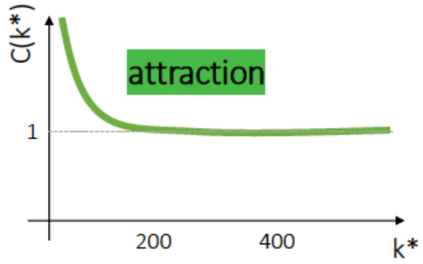

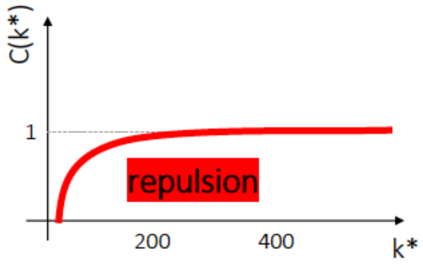

Koonin-Pratt equation, M.Lisa, S. Pratt et al., Ann.Rev.Nucl.Part.Sci. 55 (2005) 357-402

$$C(k^*) = \zeta(k^*) \cdot \frac{N_{same}(k^*)}{N_{mixed}(k^*)} = \int S(r)\ \left|\psi(\vec{k}^*,\vec{r})\right|^2 d^3r$$

Emission source

Two-particle wave function

Schrödinger Equation:

V(r) → $\left|\psi(\vec{k}^*,\vec{r})\right|^2$ relative wave function for the pair

$\bar{p}$ and $\bar{d}$ absorption in ALICE

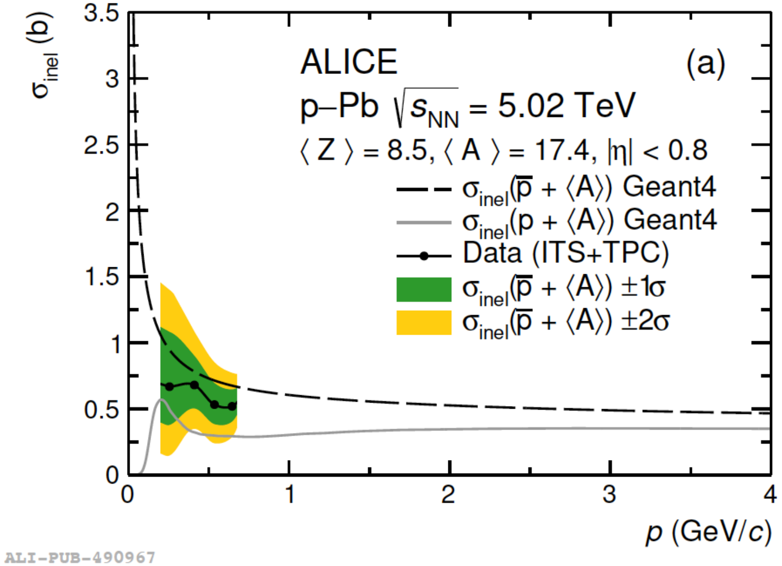

ALI-PUB-490967

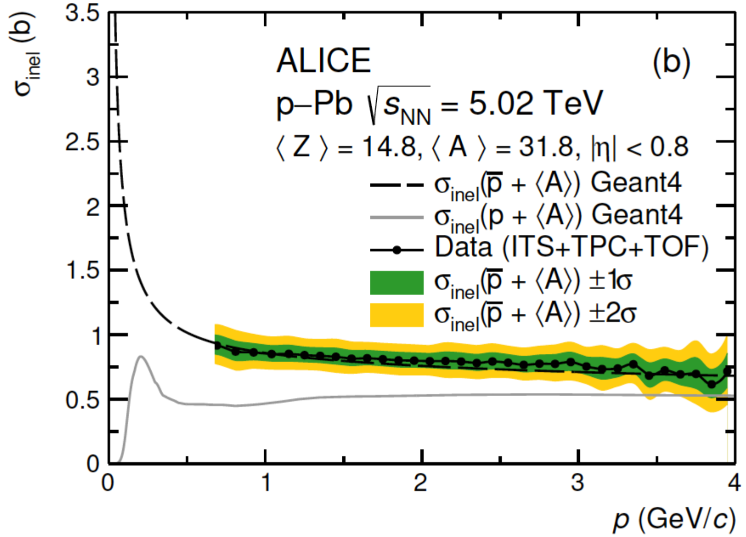

ALI-PUB-490972

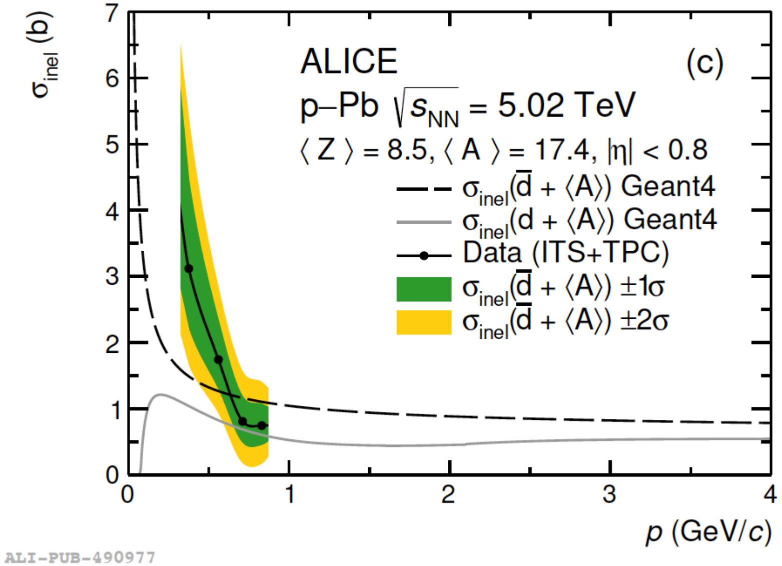

ALI-PUB-490977

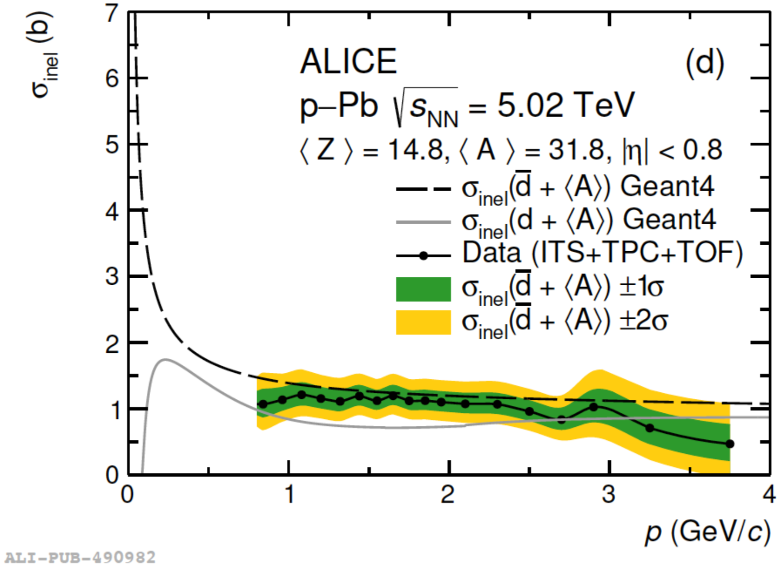

ALI-PUB-490982

PRL 125(2020) 162001

Strong interaction between hadrons

Nature 588 (2020) 232

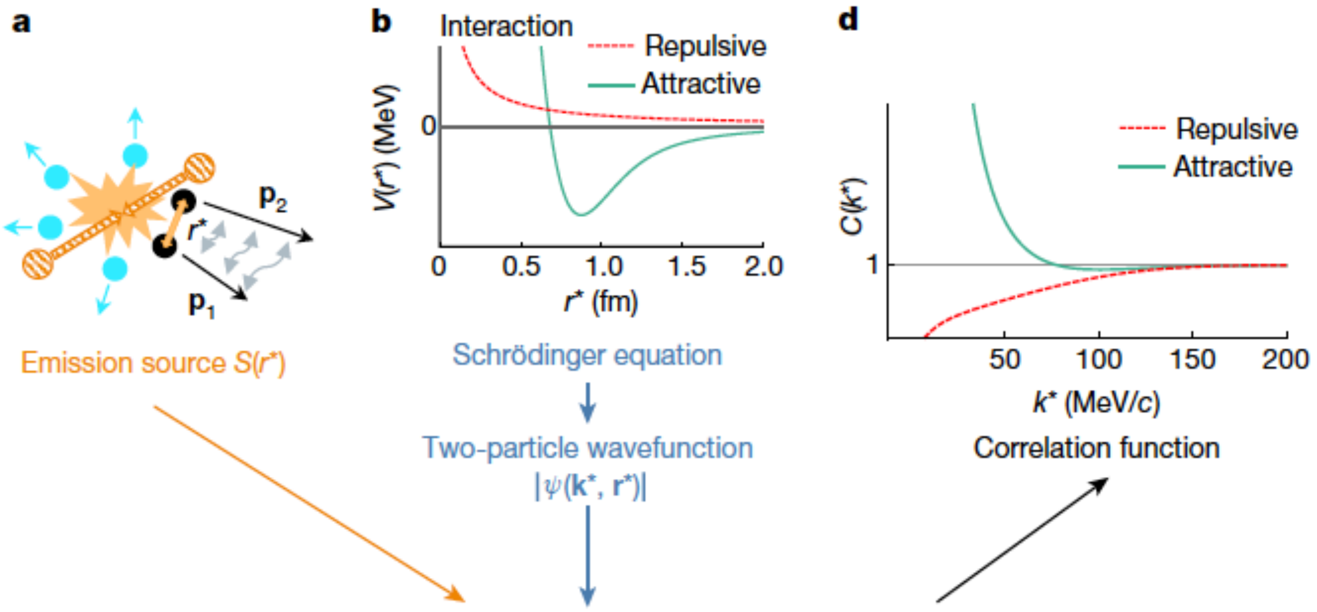

$$C(k^*) = \int S(r^*)\,|\psi(\mathbf{k}^*, \mathbf{r}^*)|^2\, d^3r^* = \xi(k^*)\,\frac{N_{same}(k^*)}{N_{mixed}(k^*)}$$

Koonin-Pratt equation, M.Lisa, S. Pratt et al., Ann. Rev. Nucl. Part. Sci. 55 (2005) 357-402

Strong interaction between hadrons

Test for lattice QCD calculations of strong h-h and h-h-h interactions

Important input for the equation-of-state of neutron stars (which contain hyperon-rich matter)

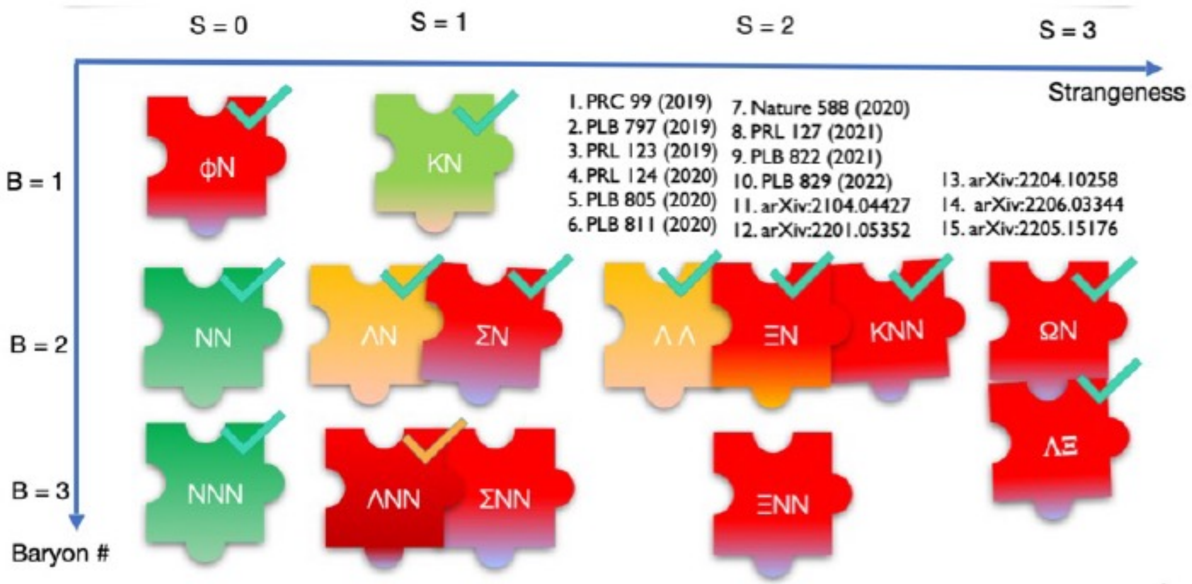

arXiv: 2201.05352

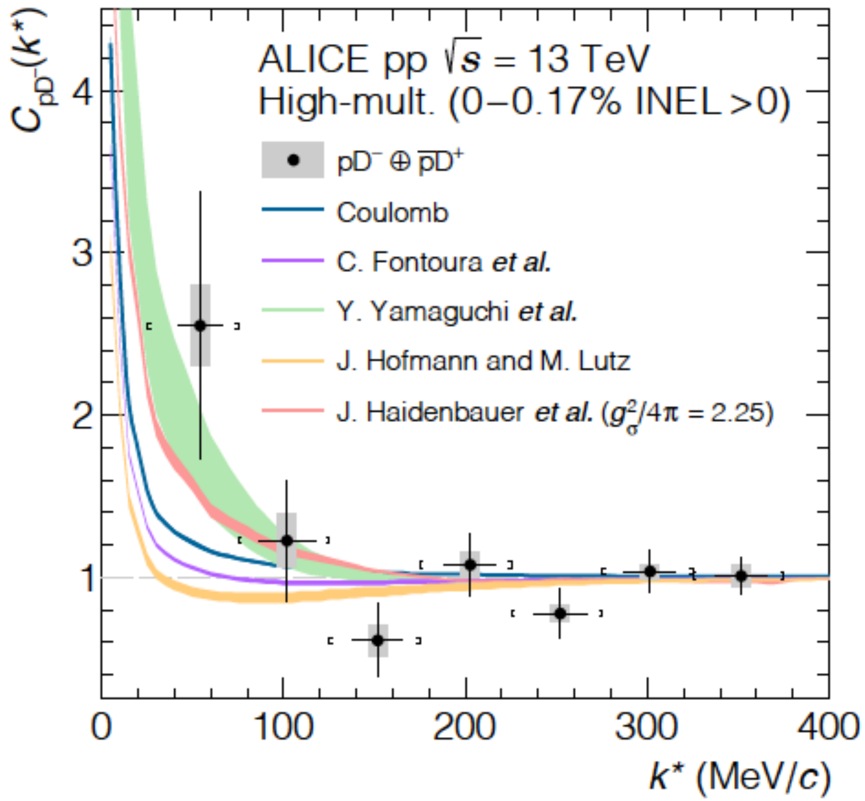

First measurement of p-D correlation function:

- Coulomb+ attractive strong interaction describes data better
- Estimate of QCD scattering parameters

Residual strong interaction between charm and light hadrons

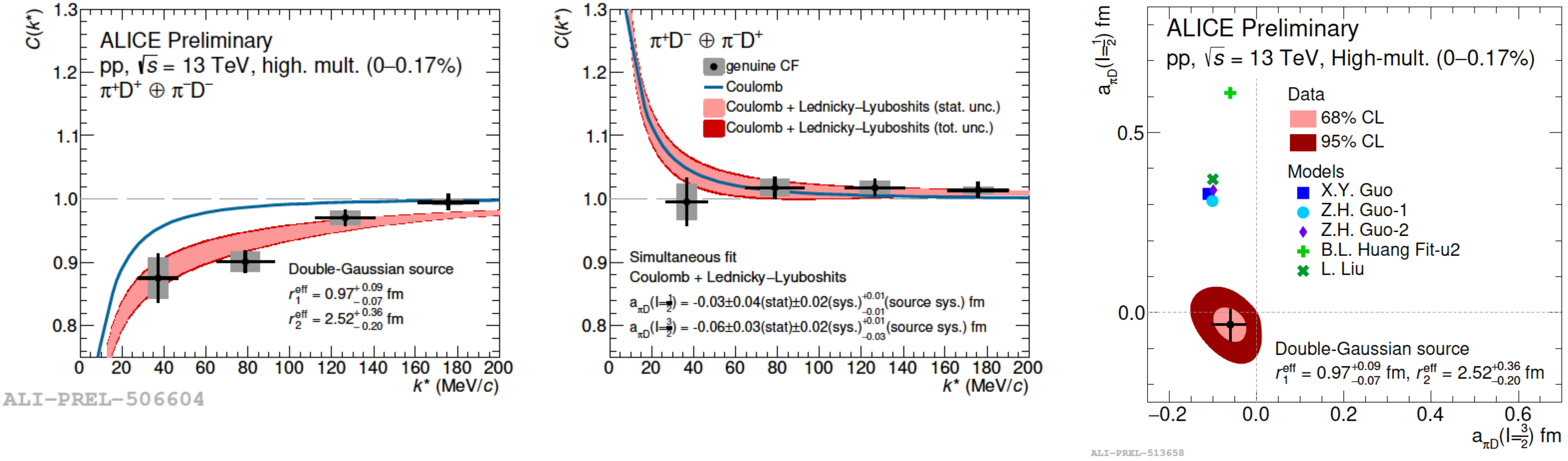

Dπ correlation function suggests deviation from the Coulomb baseline

- Simultaneous fit to same and opposite sign correlations to study the isospin dependence

π^+D^+: I = 3/2 channel

π^+D^-: I = 3/2 (33%), I = 1/2 (66%)

Extracted scattering parameters are lower than lattice QCD expectations

- Suggest a small rescattering of D mesons in the hadronic phase of HI collisions

Hadronization of charm quarks from pp…

PRD 105 (2022) L011103

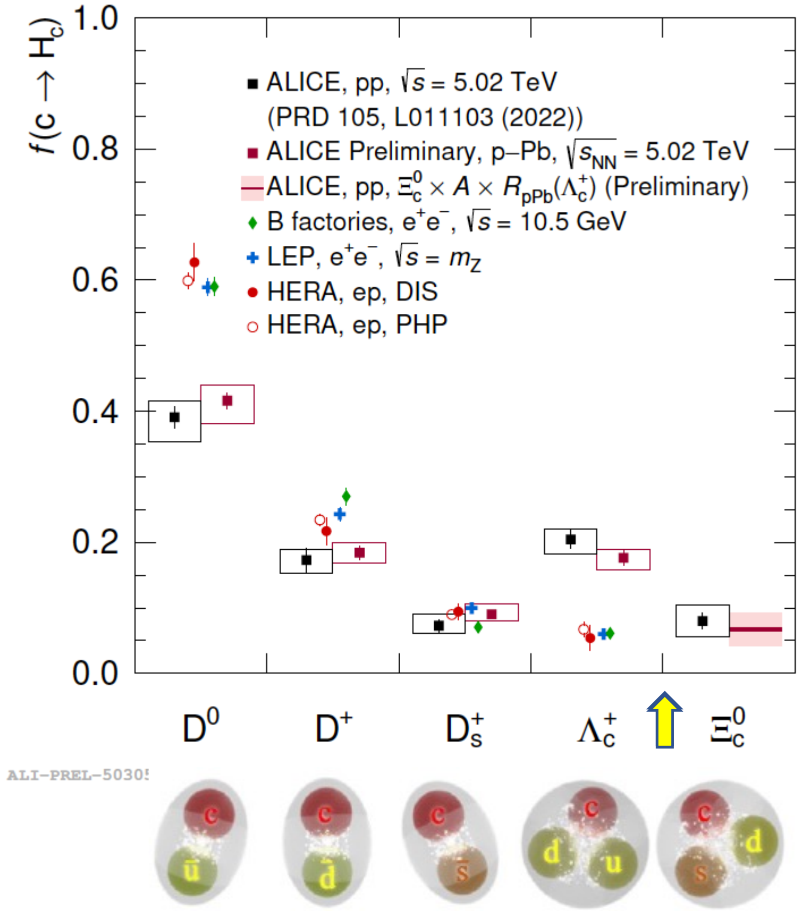

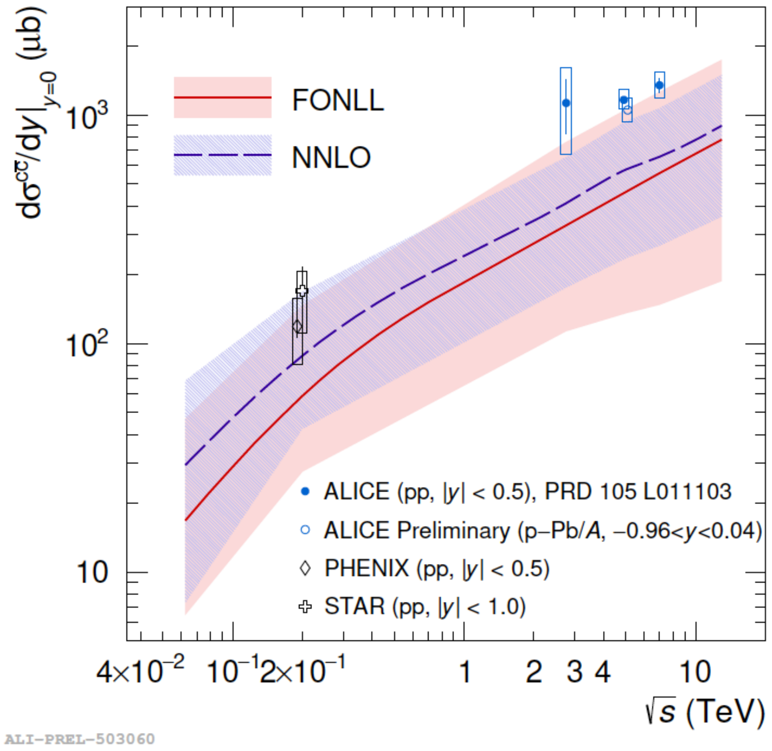

~40% increase driven by observed baryon enhancement
Data on the upper edge of FONLL and NNLO calculations

Significant baryon enhancement with respect to e$^+$e$^-$ or e$^-$p

~30% c --> baryons in pp and pPb

Charm fragmentation functions are not universal

H_c	$f(c \to H_c)[\%]$
D^0	$39.1 \pm 1.7(\mathrm{stat})^{+2.5}_{-3.7}(\mathrm{syst})$
D^+	$17.3 \pm 1.8(\mathrm{stat})^{+1.7}_{-2.1}(\mathrm{syst})$
D_s^+	$7.3 \pm 1.0(\mathrm{stat})^{+1.9}_{-1.1}(\mathrm{syst})$
Λ_c^+	$20.4 \pm 1.3(\mathrm{stat})^{+1.6}_{-2.2}(\mathrm{syst})$
Ξ_c^0	$8.0 \pm 1.2(\mathrm{stat})^{+2.5}_{-2.4}(\mathrm{syst})$
D^{*+}	$15.5 \pm 1.2(\mathrm{stat})^{+4.1}_{-1.9}(\mathrm{syst})$

Charm baryon/meson enhancement: pp→Pb-Pb

arXiv:2112.08156

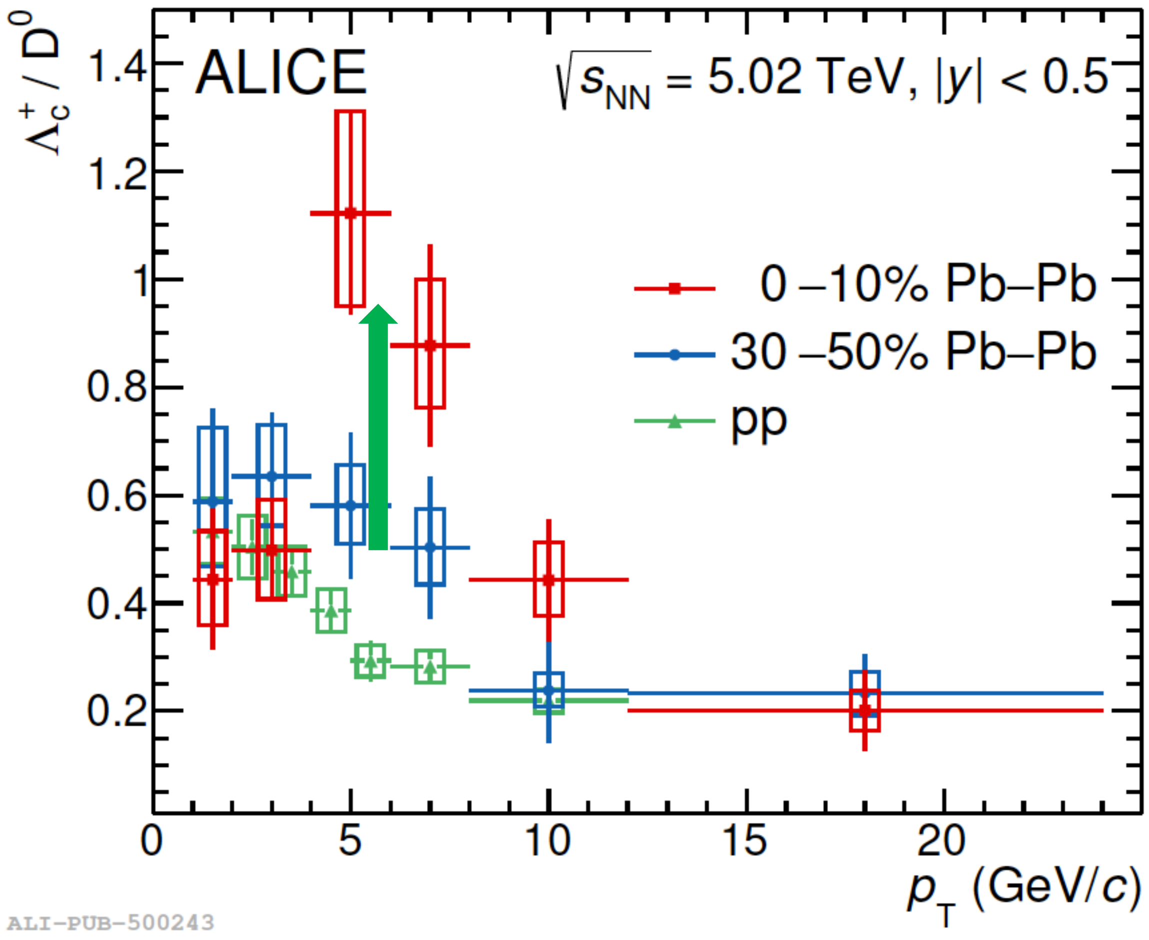

Additional dynamics in QGP

Λ_c / D^0 enhancement at intermediate p_T relative to pp

- similar to light flavor hadrons
- parton recombination at play also for c quarks
- mass-dependent p_T shift from collective flow

Dead- cone effect now exposed by ALICE

Reduction of gluon radiation from heavy quarks at small angles

Dokshitzer, Khoze, Troian, J. Phys. G17 (1991) 1602

$$R(\theta) = \frac{1}{N^{\mathrm{D^0\,jets}}} \frac{dn^{\mathrm{D^0\,jets}}}{d\ln(1/\theta)} \Big/ \frac{1}{N^{\mathrm{inclusive\,jets}}} \frac{dn^{\mathrm{inclusive\,jets}}}{d\ln(1/\theta)} \Bigg|_{k_T, E_{\mathrm{Radiator}}}$$

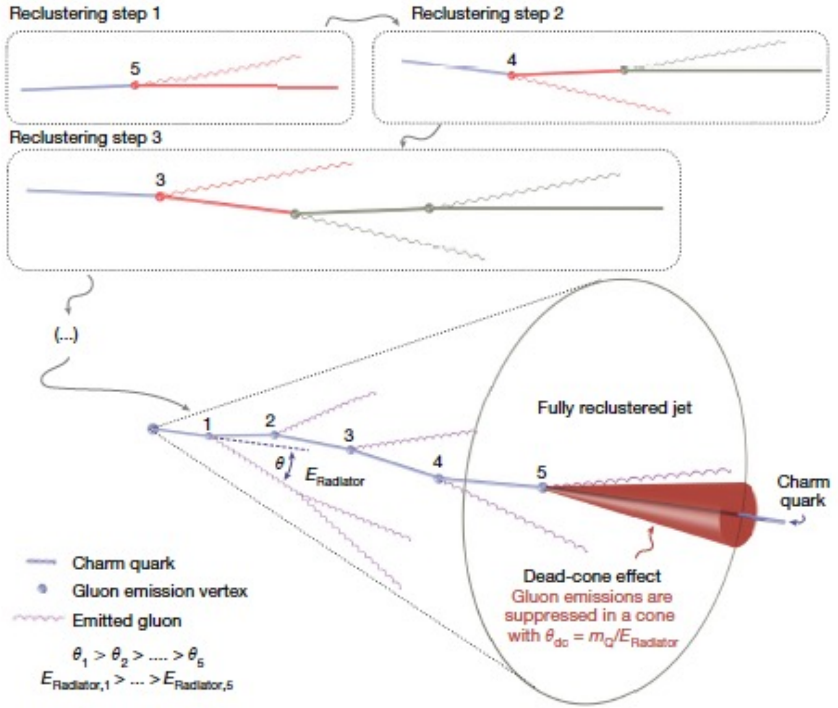

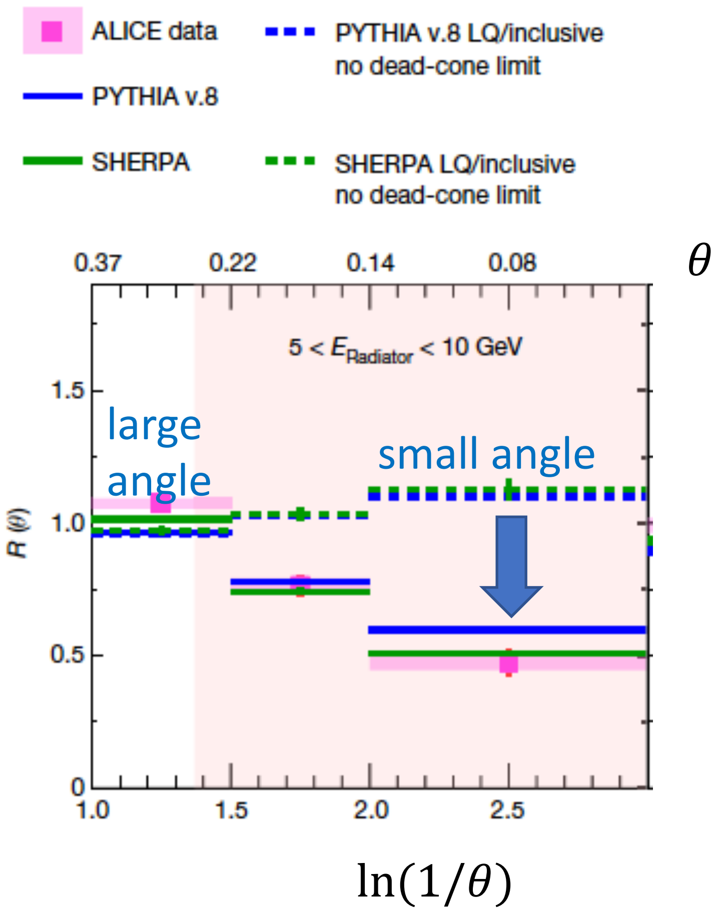

First direct observation using jet iterative declustering and Lund plane analysis of jets that contain a soft D^0 meson

Nature 605 (2022) 7910, 440

Charm splitting function in jets

arXiv: 2208.04857

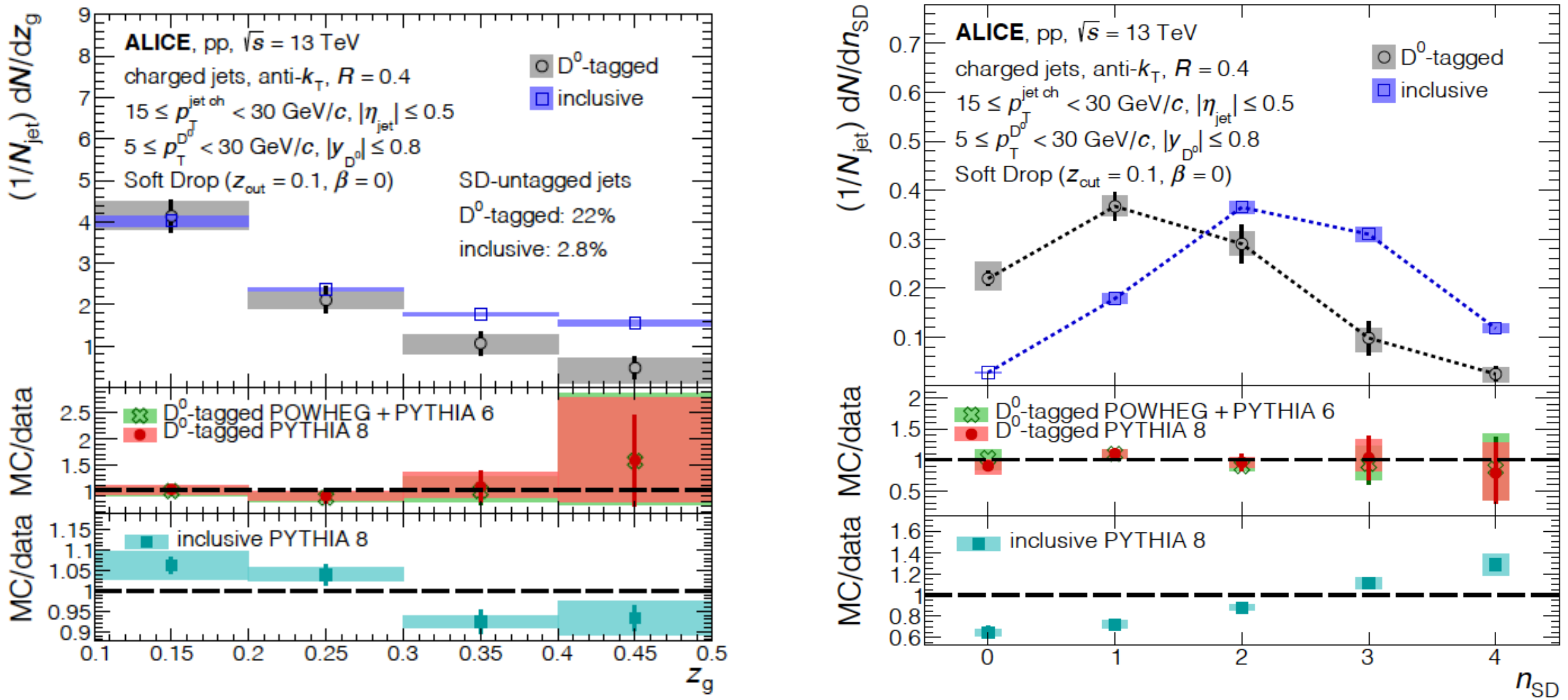

Charm-tagged jets → first direct experimental constraint of the splitting function of heavy-flavour quarks

- z_g distribution appears steeper than that of light quarks and gluons
- heavy-flavour quarks on average have fewer perturbative emissions compared to light quarks and gluons

Electromagnetic radiation

ALICE 3:

- Probe time dependence of T

Double differential spectra: T vs mass, $p_{T,ee}$

- Access time evolution of flow

Dilepton v_2 vs mass and p_{Tee} possible

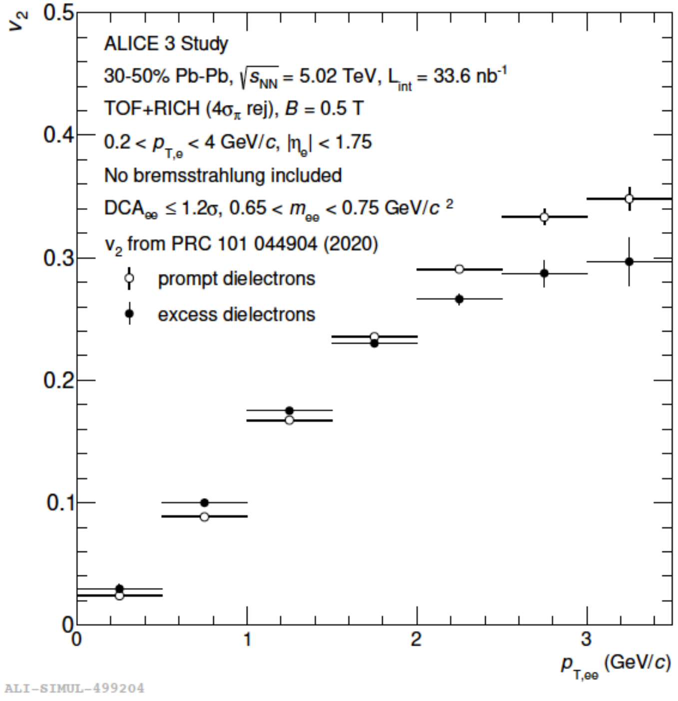

Expected statistical errors of T as a function of $p_{T,ee}$

ALICE 3 projection, one month Pb-Pb

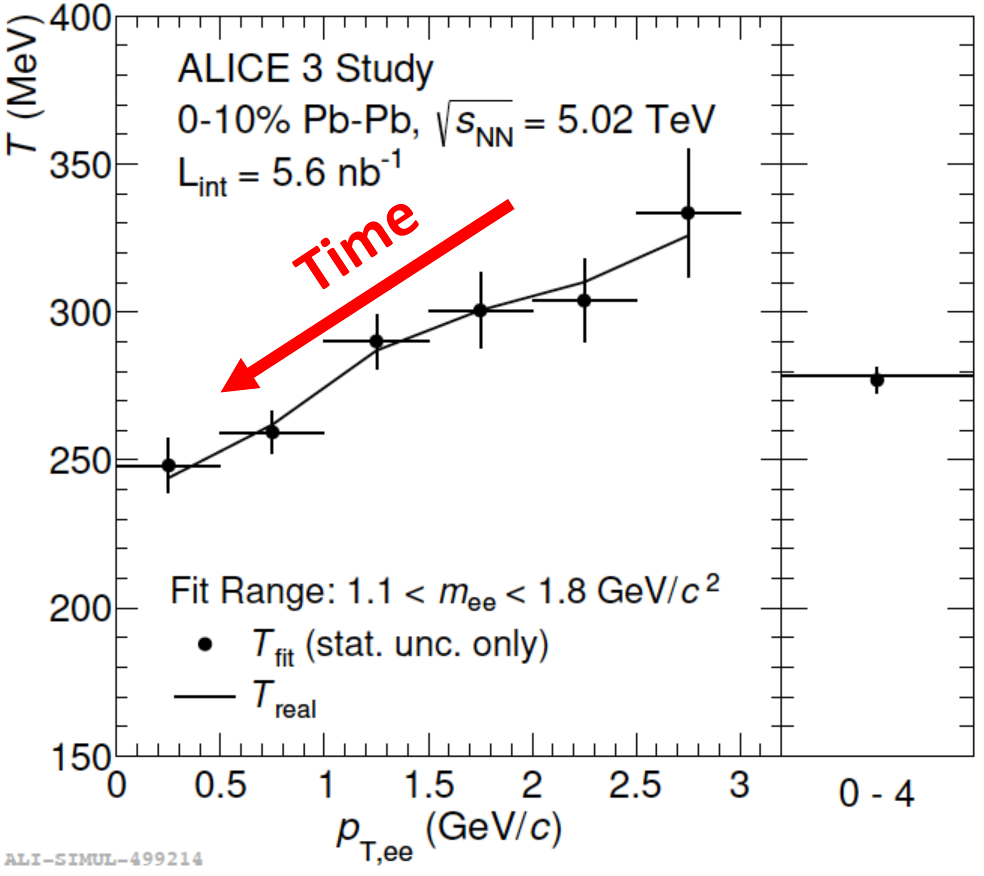

Complementary measurements with real photons.

Different systematic uncertainties → reduce overall uncertainties

R. Rapp, Adv. High Energy Phys. 2013 (2013) 148253
P.M Hohler and R. Rapp, Phys. Lett. B 731 (2014) 103
ALICE CERN-LHCC-2022-009

$D\bar{D}$ azimuthal correlations

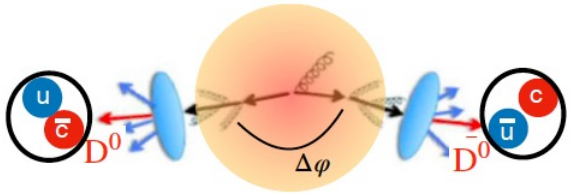

M. Nahrgang et al., PRC90, 024907

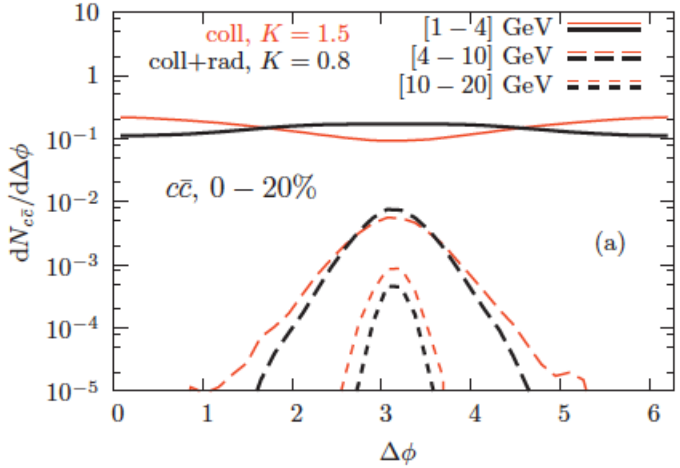

ALICE 3 projection: $D\bar{D}$ correlations

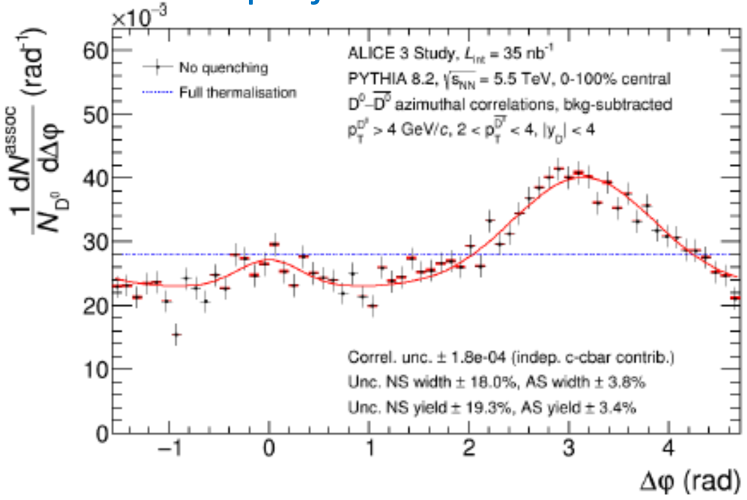

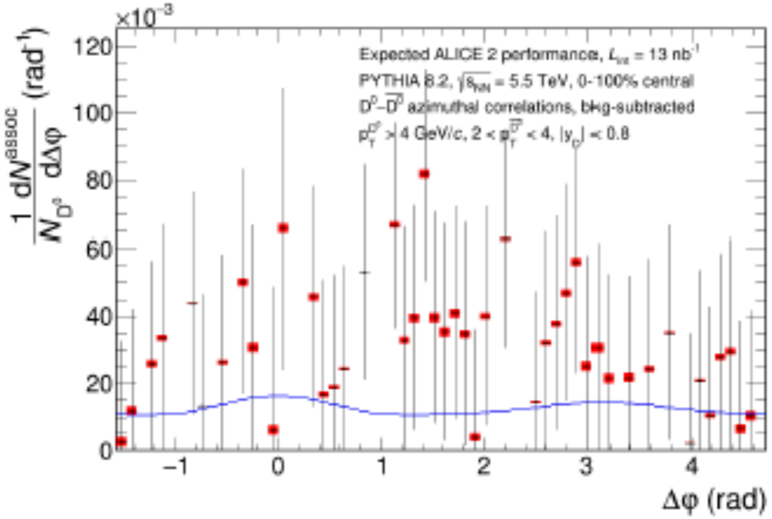

Angular decorrelation directly probes QGP scattering

- Sensitive to energy loss mechanisms, degree of thermalization
- Strongest signal at low p_T

Very challenging measurement: need good purity, efficiency and η coverage

Nature of exotic bound states

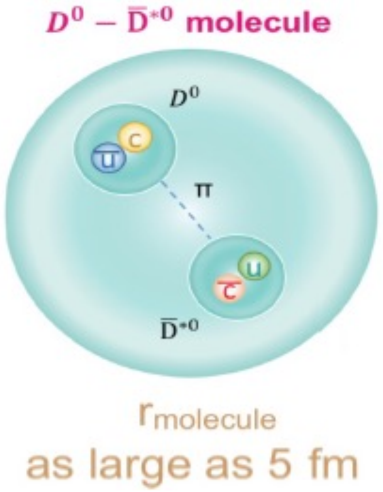

or

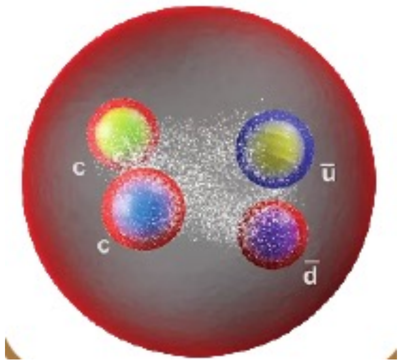

D^0D^{*+}: nature of T_{cc}^{+}

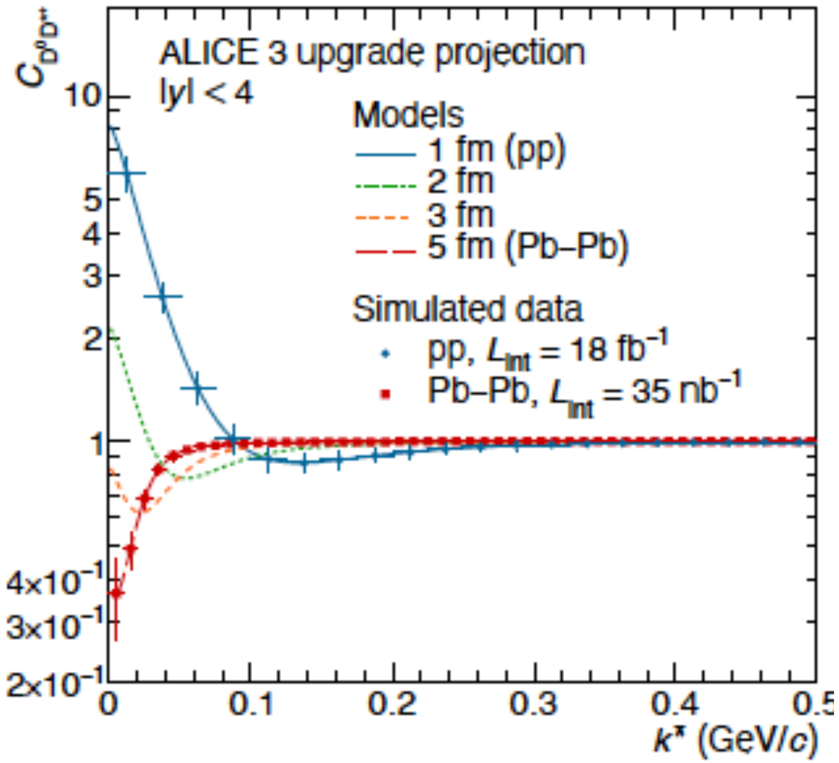

Exotic states: T_{cc}^{+}, $\chi_{c1}(3872)$

- Include double charm states, potentially weakly bound states
- Investigate structure with two particle momentum correlations and yields, arXiv:2203.13814
- Understand dissociation and regeneration in QGP →unique access to low p_T χ_{c1} (3872)

Possible with ALICE 3 thanks to excellent pointing resolution + large acceptance

Electrical conductivity of the medium

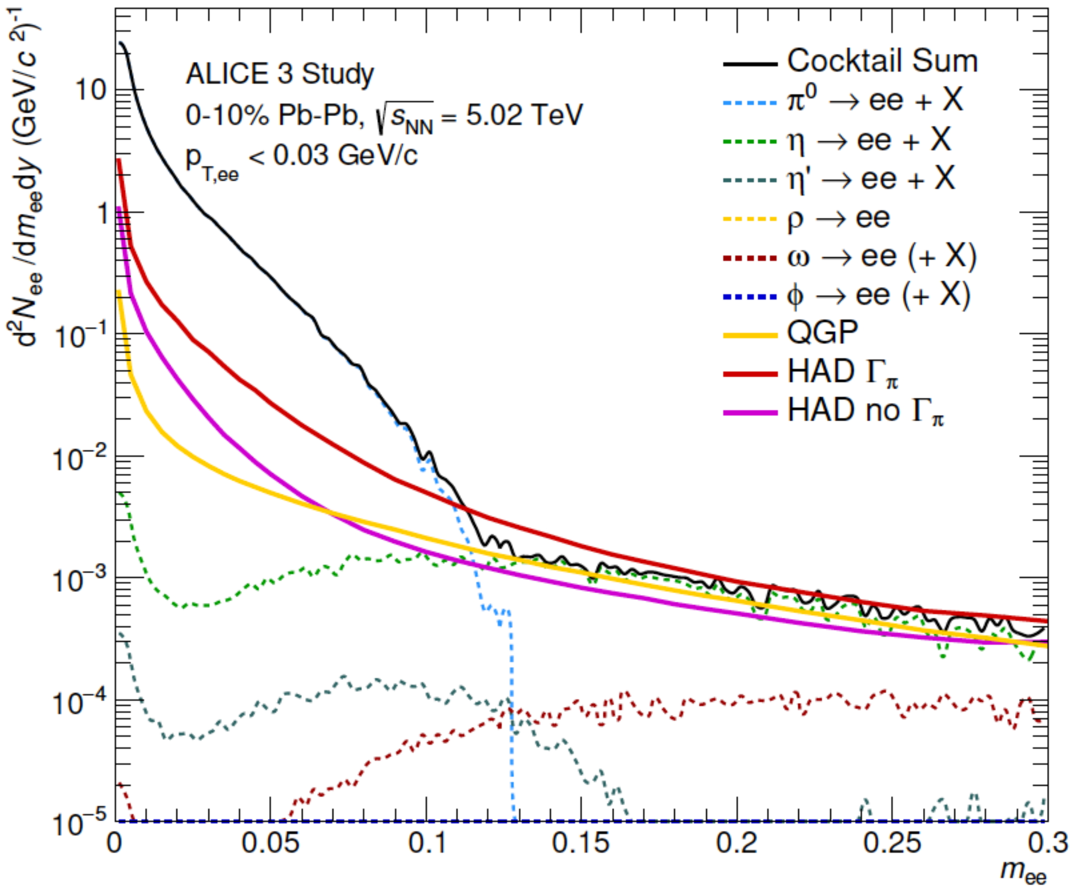

Large acceptance tracker

60 m^2 silicon pixels detector

Based on CMOS Active Pixel sensor technology

9+3 (barrel + disk) tracking layers

- Compact: r_{out}~ 80 cm, z_{out} ~ $\pm$400 cm
- Large coverage : $|\eta| < 4$
- Hight spatial resolution: s pos ~5 μm (req. <10 μm)
- Timing resolution: ~ 100 ns
- Very low material budget
  - 1% X_0 per layer overall → X/X_0 (total) < 10%
- Low power: ~20 mW/cm^2

Relative p_T resolution $\propto \frac{\sqrt{x/X_0}}{B \cdot L}$

- 1% over large acceptance
- Integrated magnetic field crucial (2T)
- Overall material budget critical

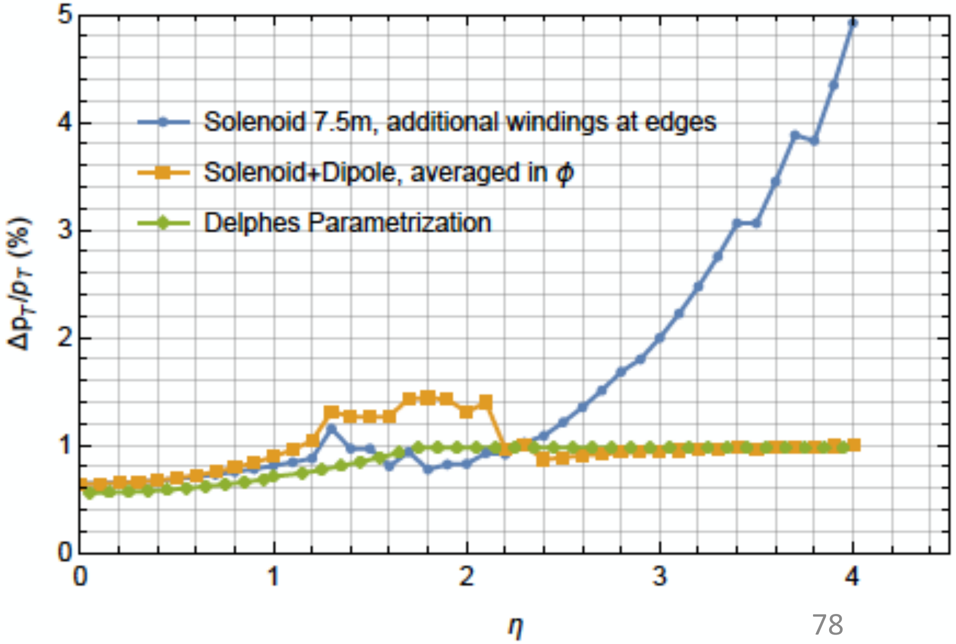

Particle identification

Time-of-flight detector

- 2 barrel + 1 forward TOF layers (R = 19 & 85 cm, z = 405 cm)
- With silicon timing sensors

Ring-imaging Cherenkov detectors

- 1 barrel + 1 forward layer
- Aerogel radiators with continuous coverage from TOF

Large acceptance electromagnetic calorimeter

- Pb-scintillator sampling calorimeter + at η ~ 0 crystal calorimeter
- Photon & high p electron identification

Muon identifier

- Absorber & 2 layers of muon detectors
- Muons down to p_T > 1.5 GeV/c

Forward conversion tracker

- Thin tracking disks in 3 < η < 5 in its own dipole field
- Very low p_T photons (< 10 MeV)